BIOLOGICAL SYNTHESIS OF INORGANIC NANOPARTICLES AND NANO-BIOCONJUGATES

A THESIS
SUBMITTED TO THE
UNIVERSITY OF PUNE

FOR THE DEGREE OF
DOCTOR OF PHILOSOPHY
IN
MICROBIOLOGY

BY

ASAD SAGHIR SYED

UNDER THE GUIDANCE OF
DR. ABSAR AHMAD

DIVISION OF BIOCHEMICAL SCIENCES
NATIONAL CHEMICAL LABORATORY
PUNE - 411008
INDIA.

AUGUST, 2011

Dedication

I dedicate this thesis to my wonderful family. Particularly, to my forbearing and understanding wife Farha and to our precious son Fuzail, who is the joy of our life.

CONTENTS

Chapter 4

Silicate nanoparticles by bioleaching of glass and modification of the glass surface

Chapter 5

Physical manipulation of biological and chemical syntheses for nanoparticle shape and size control

Chapter 6

CERTIFICATE

This is to certify that the work incorporated in the thesis entitled "**Biological synthesis of inorganic nanoparticles and nano-bioconjugates**" submitted by **Asad Saghir Syed** for the degree of Doctor of Philosophy was carried out under my supervision at the Division of Biochemical Sciences, National Chemical Laboratory (NCL), Pune. The materials obtained from other sources have been duly acknowledged in the thesis.

Date: **Dr. Absar Ahmad**
                                                                                    (Research guide)
Place:

DECLARATION

I hereby declare that the thesis entitled, "**Biological synthesis of inorganic nanoparticles and nano-bioconjugates**" has been carried out in the Division of Biochemical Sciences, National Chemical Laboratory (NCL), Pune under the guidance of **Dr. Absar Ahmad.** The work is original and has not been submitted in part or full by me for any other degree or diploma to any other university. I further declare that the materials obtained from other sources have been duly acknowledged in the thesis.

Asad Saghir Syed

Date:

Place:

Acknowledgements

First and foremost, I would like to thank the 'Almighty' who has given me patience, courage and all the things from time to time to complete this thesis. Although only my name will appear on the cover page of this thesis, many people have contributed in its production. I owe my gratitude to all those who have stood by me during tough times and have made this thesis possible. My Ph.D has been one that I will cherish forever. Many may think this thesis is the symbol of an end, however, to me, it marks a new beginning in scientific career.

I express my heartfelt gratitude and sincere thanks to my research guide, Dr. Absar Ahmad for all his guidance, encouragement, support and patience. His sincere interests in science have been a great inspiration to me. I am greatly impressed by his passion, hard work, speed and discipline in research. It has been a great pleasure, being a part of his group and to work under such close association with him. His constant support was invaluable and helped me in the completion of this thesis. I was often lost, puzzled and wondered about the real meaning of this pointless search for the seashore that may or may not even exist. Then, a stream of light, as always, my guide, Dr. Absar Ahmad guided me through the darkest hours and helped me venture past the mazes of uncertainty into the harbour of hope where I can sail once again. I owe him a lot for giving me a stable ground in all his capabilities and for the care he has shown toward me.

My special thanks to Dr. Satish Ogale, for his suggestions, valuable guidance and useful discussions during the course of research work.

I feel a deep sense of gratitude for my late Grandfather, who always wished for my higher education and taught me good things that really matter in life.

I would like to express my sincere respect toward my Grandmother, Mother, Father, Uncle, Aunt and In-laws (Father, Mother and Brother) for their love, blessings and constant extraordinary moral support during hard times in my research work. I express my deep gratitude and affection to my sisters and brother in laws who have always extended their help and love whenever I needed them the most.

I am thankful to Dr. (Mrs). Vidya Gupta, Chairman, Division of Biochemical Sciences, NCL for her support and help during the research work and especially in course work and allowing me to work in Division of Biochemical Sciences, NCL.

Abbreviations

µg	Micro gram
µL	Micro litre
µm	Micro meter
AD	In the Christian era; used before dates after the supposed year Christ was born
AFM	Atomic Force Microscopy
AgNO$_3$	Silver Nitrate
ATP	Adenosine Triphosphate
BC	Before the Christian era; used following dates before the supposed year Christ was born
BE	Binding energy
BLAST	Basic Local Alignment Search Tool
CdS	Cadmium Sulfide
CdSe	Cadmium Selenide
CdTe	Cadmium Telluride
cm	Centimeter
CTAB	Cetyltrimethyl ammonium bromide
CVD	Chemical Vapor Deposition
DNA	Deoxyribonucleic acid
dNTP	Deoxyribonucleotide triphosphate
E.coli	*Escherichia coli*
EDAX	Energy Dispersive Analysis of X-rays
EDC	1-Ethyl-3-(3-methyl amino propyl)-carbodiimide
eV	Electron volt
fcc	Face centered cubic
Fig.	Figure
FRET	Fourier Resonance Energy Transfer
FTIR	Fourier Transformed Infrared
g	Gram
hr	Hour
H$_2$PtCl$_6$	Hexachloroplatinic acid
HAuCl$_4$	Chloroauric acid
HEPES	4-(2-hydroxyethyl)-1-piperazineethanesulfonic acid
HPLC	High Performance Liquid Chromatography
HRTEM	High Resolution Transmission Electron Microscopy
ITS	Internal Transcribes Spacer
K.pneumonia	*Klebsiella pneumonia*
kbp	Kilo base pair
kDa	Kilo Dalton
kV	Kilo volt
LED	Light Emitting Diode
M	Molar
mA	Milliampere
MES	2 (N-morpholino) ethanesulfonic acid
MGYP	Malt extract-Glucose-Yeast extract-Peptone
min	Minute

mL	Mililitre
mM	Milimolar
mm	Milimeter
MRI	Magnetic Resonance Imaging
MTT	3-(4,5-Dimethylthiazol-2-yl)-2,5-diphenyltetrazolium bromide
NADH	Nicotinamide Adenine Dinucleotide (reduced)
nano	Dwarf
NCBI	National Centre for Biotechnology Information
NCIM	National Collection of Industrial Microorganism
NIR	Near Infrared region
nm	Nanometer
PAGE	Polyacrylamide Gel Electrophoresis
PCMS	Percolative Multicavity Synthesis
PCR	Polymerase Chain Reaction
PDA	Potato Dextrose Agar
pH	*Potentia hydrogenia*
PL	Photoluminescence
Qdots	Quantum dots
RNA	Ribonucleic acid
rpm	revolution per minute
RT	Room temperature
SAED	Selected Area Electron Diffraction
SMAD	Solvated metal atom dispersion
SPR	Surface Plasmon Resonance
Taq	*Thermus aquaticus*
TEM	Transmission Electron Microscopy
TGA	Thermogravimetric analysis
TMV	Tobacco mosaic virus
UV-Vis	Ultraviolet-Visible
Viz.	Namely
w/v	Weight by volume
XPS	X-ray Photoelectron Spectroscopy
XRD	X-ray Diffraction

Objective of the thesis

Although enormous research has been done in the field of nanotechnology, many efforts are still being focused on the synthesis mechanism, characterization, applications and toxicity of nanomaterials in order to improve our understanding. The goal of this work is to use fungi to synthesize metallic and semiconductor materials in an efficient and reproducible manner. The motivation behind this work was to find a new route as compared with current methods to fabricate inorganic materials with greater ease, precise control with desirable features and to improve upon available biological methods for synthesis of nanoparticles. The work described in this thesis expands upon initial studies performed in Dr. Absar Ahmad's lab and seeks to gain greater control over, and insight into, biological procedure for synthesis and characterization of nanomaterials. The fungus, *Thermomyces lanuginosus* (*Humicola lanuginosa)* was isolated, identified and further employed for the production of nanomaterials. A biological method was discovered to efficiently synthesize gold and silver nanoparticles by the fungus. These nanoparticles were characterized by different techniques such as UV-visible spectroscopy, Transmission Electron Microscopy (TEM), X-ray Diffraction (XRD), X-ray Photoelectron Spectroscopy (XPS), etc. The biocompatibility and cytotoxicity of gold and silver nanoparticles was assessed by cell viability assay. These gold nanoparticles were radiolabelled with Technitium-99m and biodistribution studies were carried out. Conjugation of gold nanoparticles with anticancer drug (doxorubicin) was achieved by 1-Ethyl-3-(3-dimethylaminopropyl)-carbodiimide (EDC) coupling protocol. Doxorubicin is a very effective drug for liver cancer but this drug causes cardio-toxicity and renal-toxicity with myelosuppression. Asialoglycoprotein receptors are present in abundance in liver and more importantly, known to be over expressed in hepatic cancer. Pullulan is known to have specific affinity for the asialoglycoprotein receptors. Since the gold nanoparticles which we have synthesized using above fungus reach out to liver and pass through urine within forty five minutes and causes no toxicity to NIH3T3 mouse embryonic fibroblast cell line and MDA-MB-231 human breast carcinoma cell line at 50μg/ml. We can use these nanoparticles for drug delivery applications. If we can conjugate Pullulan to gold-doxorubicin conjugate then this system will be very effective for targeted drug delivery of liver cancer without side effects.

Since fungus *Humicola lanuginosa* grows at temperature 50^oC at pH 9, we screened a number of mesophilic fungi in order to synthesize metal and quantum dots (platinum and CdTe) nanoparticles at ambient conditions and pH. Out of several mesophilic fungi screened, only *Fusarium oxysporum* produces protein capped water dispersible extracellular platinum and CdTe (quantum dots) nanoparticles at room temperature. CdTe (quantum dot) nanoparticles were synthesized by the fungus *Fusarium oxysporum* and antibacterial activity was carried out against Gram positive and Gram negative bacteria. The biocompatibility/cytotoxicity of CdTe nanoparticles was assessed by cell viability assay.

Recently, it was discovered that naturally available raw materials (white and zircon sand) as well as agro-industrial by-products (rice husk) can be used for the fungus-mediated bioleaching of oxide nanoparticles of diverse morphologies. To follow up on this way, a method was developed for silicate nanoparticles by bioleaching of borosilicate glass (cover slip). Several approaches already exist in literature for nanoparticle formation but controlling their size, shape and dispersity is the issue of current interest. To address this concern, percolative microcavity synthesis has been developed for gold nanoparticles to achieve such control.

Organization of the thesis

The thesis is presented in six chapters, a brief summary of which is given below.

Chapter 1: General introduction

This chapter presents a general introduction about Nanotechnology and its historical background. Various synthesis methodologies include that of chemical, physical and biological types. Properties of nanomaterials and their potential applications are also discussed in brief.

Chapter 2: Biological synthesis of metal nanoparticles using fungus

This chapter comprises of three parts. The first part deals with isolation and identification of the novel, alkalotolerant, thermophilic fungus, *Humicola lanuginosa*. The second part presents biosynthesis and characterization of nanoparticles. The fungus *Humicola lanuginosa* was employed for the first time in the synthesis of metal nanoparticles. The fungus demonstrates the ability to facilitate synthesis of metal nanoparticles (viz. gold and silver). These particles were characterized using different techniques available for material characterization. The biocompatibility/cytotoxicity of gold and silver nanoparticles was assessed by cell viability assay. Gold nanoparticles were radiolabelled with Tc-99m and biodistribution studies were carried out followed by conjugation with anticancer drug doxorubicin. In the third part, extracellular biosynthesis of platinum nanoparticles was presented using the fungus *Fusarium oxysporum* in ambient conditions.

Chapter 3: Biological synthesis of quantum dots using fungus

As a follow-up to the biosynthesis work of nanomaterials by Dr. Absar Ahmad and colleagues, an effort was extended for the biosynthesis of technologically important quantum dot nanoparticles by the fungus *Fusarium oxysporum*. Cadmium telluride (CdTe) quantum dots for the first time were synthesized by a fungal based process. When the fungus was incubated with an aqueous solution of precursor ($CdCl_2$ and $TeCl_4$), highly stable quantum dots were formed extracellularly. These biogenic CdTe nanoparticles exhibit antibacterial activity against Gram positive and Gram negative bacteria. These CdTe nanoparticles were also assessed for biocompatibility/ cytotoxicity by cell viability assay.

Chapter 4: Silicate nanoparticles by bioleaching of glass and modification of the glass surface

The idea behind this work originated from the recent use of naturally available raw materials (white and zircon sand) as well as agro-industrial by-products (rice husk) for fungus-mediated bioleaching of oxide nanoparticles of diverse morphologies. A bioleaching method for precise synthesis of silicate nanoparticles was developed by bioleaching of borosilicate glass cover slip and is described in this chapter. Characterization of these bioleached silicate nanoparticles was carried out by different techniques such as UV-Visible spectroscopy, XRD, XPS, TEM, etc. It inferred from the results that the processed glass surface also undergoes significant morpho-chemical modifications.

Chapter 5: Physical manipulation of biological and chemical syntheses for nanoparticle shape and size control

A nanosynthesis scheme (percolative microcavity synthesis) has been developed for the shape and size control of the nanoparticles. Gold nanoparticles were synthesized by both biological and chemical methods in order to compare the nanosynthesis scheme. A simple and interesting solution-based process has been developed and can be used for different chemical compositions according to their broader applications.

Chapter 6: General discussions and conclusions

This chapter of the thesis gives summary of the findings and conclusions derived from the work.

Chapter 1

General Introduction

Summary:

This chapter is an introduction to the thesis and presents a brief overview about nanotechnology and the various routes used to synthesize nanomaterials viz, chemical, physical and biological. Biological synthesis methods have developed the interest of many researchers due to their advantages over other methods and their considerable success in the synthesis of nanoparticles of various chemical compositions, sizes and shapes. The properties and various applications of nanomaterials are also discussed in brief.

Introduction:

Nanotechnology is the designing, characterization, production and application of the structures, devices and systems by controlling shape and size at nanometer scale i.e. 1 nm to 100 nm (10^{-9} of a meter) (Fig 1). The unit of nanometer derives its prefix *nano* from the Greek word '*nanos*' meaning extremely small. The small size of nanomaterials provides a large surface area within given space for enabling more functionality with improved performance (1). At nanoscale, properties of the materials are significantly different to their bulk counterparts (2). The change in the materials property is due to increase in surface to volume ratio, which shows surface properties and interaction (3). These properties are optical, catalytic, thermal, electrical, mechanical, etc. These properties are a strong function of the size and shape of the particles in the given composition.
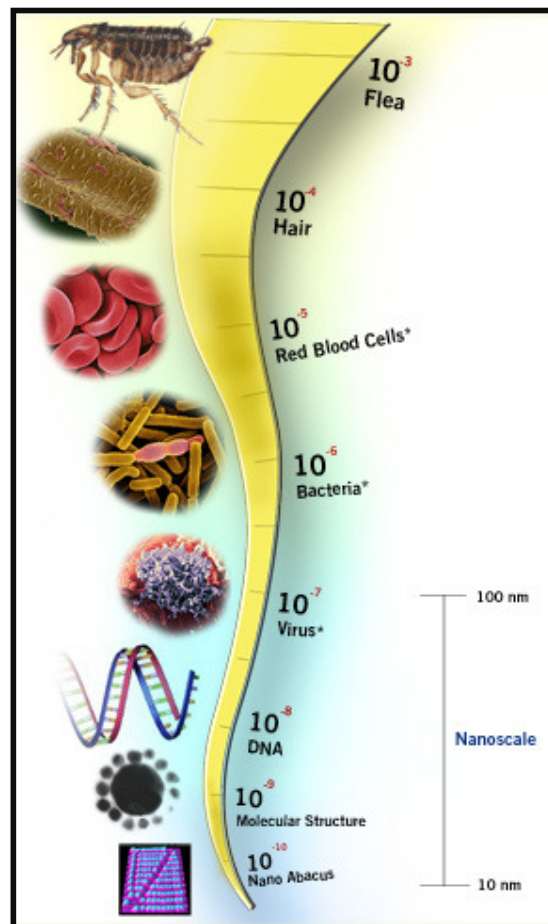

Fig 1: A picture representing the relative sizes of various objects. (Image courtesy: http://images.google.com).

Therefore, design and production of materials with such novel applications resulted by tuning the size and shape at nanoscale. It encompasses contributions from different fields such as biology, chemistry, physics, engineering, medicine, etc. In biology, the cell, a well known example of a machine that works at the nano level and in particular its component DNA, RNA and proteins which are important for life are the best natural bio-nanomaterials (4). The synthesis of nanoparticles in an array for specific applications is an important area of nanoscience and nanotechnology. Generally, the synthesis process comes under two broad categories: Top-down and bottom-up approaches (Fig 2). Both the processes possess advantages and disadvantages.
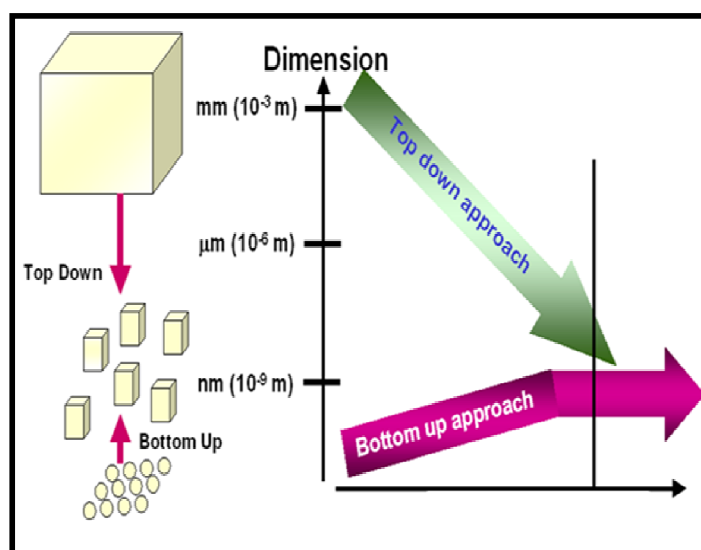
Fig 2: Top-down and bottom-up approach for nanomaterial synthesis (Image courtesy: http://images.google.com).

In top-down approach, bulk materials are chemically or physically designed or milled till a desired shape and size is obtained. After reaching a certain size regime, synthesis of materials becomes laborious and costly as well as introduces internal stress and surface defects which affect properties of nanomaterials. Owing to the above disadvantages the top-down process reaches its practical limits for synthesis. The bottom-up approach refers to building up a material from the bottom, atom by atom, molecule by molecule or cluster by cluster. The process allows synthesizing nanomaterials with less defects, homogenous chemical compositions and better control over size and shape. The bottom-up approach is driven by reduction in Gibbs free energy and therefore the materials are produced closer to a thermodynamic equillibrium state.

Being an important part of our daily life, noble metals have marked an important milestone for our progress. They are being used for numerous applications such as currencies, jewellery, conductors, etc. While making such materials to be used by human beings, care should be taken for its non-toxicity and inert nature. It has become a prime concern in discovering newer materials. Noble metals, in particular gold and silver, associated with humans have their history since 6000 BC and 4000 BC respectively. The use of gold as jewellery continued through different times (civilizations) [tomb of King Tutan Khaman (Egypt, 1300 BC)], the earlier use of gold in jewellery comes from Sumer civilization in southern Iraq around 3000 BC, when Lydian merchants introduced the first coins by using gold-silver alloys. Noble metal in the form of currency was further developed by Roman Empire (100 AD). The medicinal use of gold in the form of *Swarna bhasma* started from the Vedic period (1000 BC-600 BC) in ancient times in India. Chinese literature also supports the findings about the medicinal properties of gold (5). *Aurum potable*, a gold solution preparation was believed to rejuvenate the human body. This work led by Paracelsus, also promotes the use of gold for medicinal purposes. First documented literature on gold colloid and its medical use was described by Antonii in 1618 (6). German chemist, Johann Kunckels also explored the medical properties of the solutions of gold in the year 1676 (7). Some efforts followed by above research also exist in literature which suggests the stable dispersion of gold.

Many researchers were attracted toward metallic gold for its unusual color. Michael Faraday prepared colloidal gold in 1857 by a novel synthetic route, Fig. 3 (8-10). Dark-red solution of gold colloid was synthesized by the reduction of an aqueous solution of chloroauric acid using phosphorus in CS_2. The stability of these gold colloids against aggregation can be achieved using stabilizing agents. Thomas Graham (1861) first coined the term "Colloid" for suspended particles in liquid medium which categorized in the size range of 1 nm to few μm (11). The present development in the field replaces the term "Colloid" by "Nanoparticles" to be describing particles in the size range of 1 nm to 100 nm after the introduction of the term Nanotechnology by Norio Taniguchi (12).
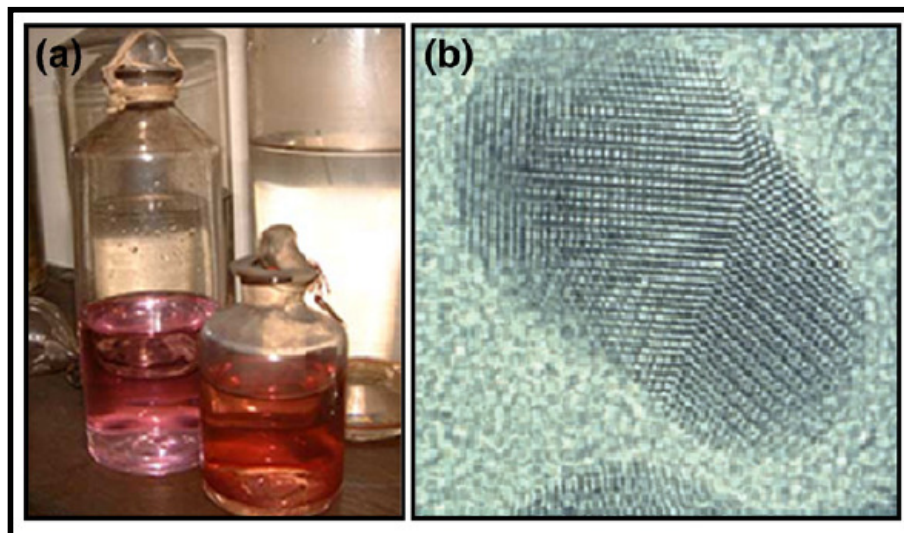
Fig. 3. (a) Faraday's colloidal suspension of gold (9). (b) High resolution transmission electron microscopic image of individual colloidal gold particles (at a magnification of $10^7\times$), prepared according to Faraday's recipe (10). (Image courtesy: http://images.google.com).

Silver, since ancient times have also been equally important for domestic purposes. Household utensils were fabricated by silver linings and these utensils were used for preservation of perishable materials and disinfection of water. The Father of Medicine, Hippocrates, also promoted the use of silver for its rapid healing of wounds (13). Aristotle advised Alexander the Great (335 BC) to store drinking water in silver vessels (14). In the late 13th century, Lanfranc exploited silver for medical purposes (15), after which Paracelsus (1493-1541) did the pioneering work for the use of metals in medical applications. Joseph Lister in the mid 19th century promoted the use of sutures of silver wire in order to reduce the incidences of septic infection. Antibacterial pioneering work was established by Ravelin (1869) and Von Nageli (1893), it was suggested that at even low concentrations it is toxic to *Spirogyra* and *Aspergillus niger* spores (13). Silver colloid was prepared for the first time by the reduction of silver nitrate using ferrous sulfate and protection of these colloidal particles with citrate ions (16, 17).

In ancient times, the applications were restricted only to their medicinal values, but the scenario has changed ever since gold and silver are now being continuously used for numerous applications. Most of the applications of these noble metals have been

based on macroscopic form. While comparing, the first evidence for the existence of non-macroscopic properties of gold appear many centuries ago in staining glasses and a well known example is that of The Lycurgus Cup (18-20). Faraday suggests that the origin of the red color in gold is due to the colloidal nature of the particles that interact differently with light. Mie (1908) for the first time explained the dependence of the color on the particles size (21). The major thrust to explore the properties of nanomaterials in general, came after Richard Feynman's talk (December 29th 1959) - "There is plenty of room at the bottom" (22).

The properties of nanomaterials can be influenced by a number of factors. These factors strongly modulate their properties including their size (23), shape (24), surface composition (25), dielectric environment (26) and interparticle interaction (27). The reasons for such notable variations are due to their dimensions comparable to the de Broglie wavelength of the charge carriers and their high surface to volume ratio (28). Among the various properties, one important property in case of metal nanoparticles is their color. The color originates from the surface plasmons i.e. coherent charge density oscillations (29). The excitation of the surface plasmons by an electromagnetic field at an incident wavelength where resonance occurs results in strong scattering of light, in the appearance of intense surface plasmon resonance (SPR) bands and an enhancement of local electromagnetic fields (30).

Size quantization effect becomes more prominent when the size of the metal nanoparticles reduce to a certain size limit, e.g. < 3 nm for gold nanoparticles, that leads to a discrete energy level in the conduction band and can be understood by making analogy with the case of particle-in-a-box model (31). The SPR band decreases in intensity due to the size of nanoparticles in the nano regime which provides an increase in surface scattering of the delocalized electrons (32). The quantum size effects have been studied in case of semiconducting nanoparticles and the energy level spacing for a spherical particle is predicted to be inversely proportional to R^2 (33). Thus, with decreasing size, the effective bandgap increases and the relevant absorption and emission spectra blue-shifts.

Different methods for the synthesis of nanoparticles:

Various physical and chemical methods have been reported for the synthesis of nanoparticles. Spray pyrolysis (34), photoirradiation (35), radiolysis (36), physical vaporization (37), electrochemical (38), ultrasonication (39), solvated metal atom dispersion (SMAD) (40), electrospinning (41), lithography (42), chemical vapor deposition (43), sputtering (44), laser ablation (45) etc. are most of the physical methods which have been used for the synthesis of various compositions of nanoparticles. Chemical vapor deposition (CVD), electrospinning and lithography methods have been developed preferentially for the synthesis and formation of one dimensional nanostructure materials such as nanowires, nanorods and nanofibres. Similarly, physical vaporization, chemical vapor deposition, electrochemical deposition and sputtering are used for the formation of thin films (two dimensional) on solid supports. However, chemical methods have received an immense attraction for the synthesis of nanoparticles due to better control over size and shape of nanoparticles. Chemical reduction, sol-gel (46), co-precipitation (47), solvothermal (48) and template based methods (49) are generally employed for nanoparticle synthesis of various compositions. Inorganic nanomaterials such as metals, metal oxides and semiconductor nanoparticles can be synthesized by reduction or oxidation and precipitation of corresponding precursor salts. Although solvents can vary from water to highly nonpolar media (50), few reports are also available on the synthesis of nanoparticles in ionic liquids (51) and supercritical fluids (52) depending upon the nature of the precursors used for the reaction. The nature of precursor ions also determines the kind of reducing agents to be applied. The chemical reduction method is a very common route for the synthesis of metal nanoparticles of different sizes and shapes. Recently, size and shape controlled synthesis of metal nanoparticles has attracted researchers due to their fine control over the chemical and physical properties with respect to their applications. The size, shape and stability of metal nanoparticles can be achieved by incorporating different additives, capping agents and templates. Different templates such as micelles (53), reverse micelles (54), DNA (55), tobacco mosaic virus (TMV) (56), polymeric molecules (57), preformed nanoparticles (58) and mesoporous membranes (59) have been employed in order to attain control over size and shape of the nanoparticles. Polymers, surfactants and biomolecules are well known examples of capping agents, which have been extensively used for the shape-controlled synthesis of metal nanoparticles (60).

The physical and chemical methods employed for the synthesis of nanoparticles are available and are extensively used; but are energy intensive, employ toxic chemicals and also require high temperature for reaction. Therefore, alternative processes which are environment friendly are desired for the nanoparticle synthesis. Bio-based approaches are a good choice for nanoparticle synthesis as they occur in ambient conditions and are environment friendly. Following section will highlight on the biological synthesis of nanomaterials in detail.

Bio-based process for nanomaterial synthesis:

An important aspect of research in nanotechnology deals with the synthesis of nanoparticles of different chemical compositions, sizes and dispersity. Many reports exist in literature which are eco-unfriendly, use toxic chemicals, require higher temperature and are expensive. Thus, there is a growing need to develop clean, eco-friendly processes, which do not use toxic chemicals in their synthesis. This led researchers to look toward the biological systems to develop green chemistry and eco-friendly approaches for synthesis of nanomaterials. In nature, microorganisms are associated with bioremediation of toxic metals. However, exploitation of these microbes for the deliberate synthesis of nanoparticles is a relatively new area of scientific research. The potential of organism to produce nanoparticles ranges from simple prokaryote (bacteria) to eukaryote (fungi) and even plants. Viruses, a new addition to the list, are also used for the assembly of nanomaterials.

Bacteria:

Among the different microorganisms, bacteria have received greater attention for the synthesis of nanoparticles (61-66). The potential of these organisms to survive and grow in the presence of high concentrations of metals (stressful conditions) is remarkable. This might be because of a specific resistance mechanism that includes efflux pumps, metal efflux systems, metal inactivation and complexation, alterations in solubility and toxicity by changes in the redox state of the metal ions, extracellular precipitation of metals and volatilization of toxic metals by enzymatic reactions (67, 68).

Biomineralization, bioremediation and bioleaching are well known examples of metal-microbe interactions. Microbial mediated changes in the surface chemistry of carbon steel, stainless steel, copper alloys or the other ones are gaining attention (69).

Mineral precipitation reactions are also intervened by bacteria either directly or indirectly (70). In order to find out the relevance of nanoparticle production and metal reduction, biorecovery of precious metals (e.g. gold) and bioremediation of toxic ones, researchers have investigated the mechanisms of nanoparticle production and bioreduction and focused their attention on the reducing agents in bacteria (e.g. enzymes) and biochemical pathways leading to metal ion reduction. Pollmann *et. al.* (71) have shown bioremediation of uranium-contaminated waters where nanoparticles of some other metals are produced. *Bacillus subtilis* 168 was able to reduce Au^{3+} ions to octahedral gold nanoparticles (5-25 nm) within bacterial cells by incubation of the cells with gold chloride under ambient conditions (61,72). Recently, silver nanoparticles have been obtained by combination synthesis (culture supernatant of *B. subtilis* and microwave irradiation) in water (73).

The silver-resistant bacterial strain *Pseudomonas stutzeri* AG259, isolated from silver mine, intracellularly accumulated silver nanoparticles obtained along with some silver sulfide (63). *P. stutzeri* AG259 challenged with high concentrations of silver ions during culture resulted in intracellular formation of silver nanoparticles ranging in size from a few nm to 200 nm (74, 75). A genetic system was developed in *E.coli* to study the protein-mediated control of crystal growth using the crystallization of the gold as a model system (76). Nair and Pradeep have shown that *Lactobacillus* strain common in buttermilk, when exposed to silver and gold ions resulted in the production of metal nanoparticles within the bacterial cells. They also extended their effort for the preparation of gold-silver alloy nanoparticles (77). *Lactobacillus* sp. also assists the synthesis of titanium nanoparticles at room temperature (78). Konishi *et.al.* reported the deposition of gold nanoparticles by the metal reducing bacterium *Shewanella algae* and was concluded that pH was an important factor in modulating the morphology and location for deposition of biogenic gold nanoparticles (79). A number of metal-reducing bacteria have been isolated and characterized from a variety of habitats and much work has been focused in this direction.

Shahverdi *et. al.* (80) have reported the rapid biosynthesis of metallic nanoparticles of silver using the reduction of aqueous Ag^+ ions by the culture supernatants of *K. pneumonia*, *E. coli* and *Enterobacter cloacae* (Enterobacteriacae). The biosynthetic process was quite fast and silver nanoparticles were formed within 5 min of silver ion coming in contact with the cell filtrate. *Rhodopseudomonas capsulata* showed the

ability to produce gold nanoparticles in different sizes and the shape of gold nanoparticles was controlled by pH. The nanoparticles were quite stable in solution too (81). He *et. al.* also have shown networked gold nanowire formation in the aqueous solution (82) and believed bioreduction and formation of gold nanoparticles might be due to NADH-dependent enzymes which were secreted by *R. capsulata*. Gram negative bacterium, *E.coli* DH5α could produce gold nanoparticles with mostly spherical, triangle and quasi hexagon shapes and showed potential in direct electrochemisty of hemoglobin (83). In another study, biorecovery of gold from jewellery wastes was obtained using *E.coli* MC4100 (nonpathogenic strain) and *Desulfovibrio desulfuricans* ATCC 29577 (84). Lengke, Fleet and Southam have controlled the morphology of gold nanoparticles using filamentous cyanobacteria such as *Plectonema boryanum* UTEX 485 and obtained cubic gold nanoparticles (<10–25 nm) and octahedral gold platelets (~1–10 µm) (85). Moreover, the mechanisms of gold bioaccumulation by cyanobacteria from gold (III)-chloride solutions have shown that the interaction of cyanobacteria with aqueous gold (III)-chloride initially promoted the precipitation of nanoparticles of amorphous gold(I)-sulfide at the cell walls, and finally deposited metallic gold in the form of octahedral (III) platelets   (~10 nm to 6 µm) near cell surfaces and in solutions (86). Diversity of hyperthermophilic and mesophilic dissimilatory microbes was studied and some of these Fe (III)-reducing bacteria and archaea were found capable of precipitating gold by reducing Au(III) to Au(0) (87). The reaction seemed to be enzymatically catalyzed which was dependent on temperature and the presence of a specific electron donor, hydrogen. *Bacillus megatherium* D01 exposed to the aqueous solution of $HAuCl_4$ formed monodispersed spherical gold nanoparticles capped with self-assembled monolayer (SAM) of thiol in an extracellular synthesis process. These gold nanoparticles were stable without any aggregation (88).

Apart from gold and silver nanoparticles, there is great interest in the development of the synthesis process for technologically important semiconductor nanoparticles such as Cadmium sulfide (CdS), Zinc sulfide (ZnS) and Lead sulfide (PbS) for applications such as quantum dot fluorescent biomarkers and cell labeling agents (89). These luminescent quantum dot nanoparticles are emerging as a new class of materials for biological detection and cell imaging. Bacteria have been used with considerable success in the synthesis of semiconductor nanoparticles (90-92). *Clostridium*

thermoaceticum (an acetogenic bacterium) was able to precipitate cadmium extracellularly, the process was energy dependent and required cysteine. CdS was precipitated from $CdCl_2$ in the presence of cysteine hydrochloride at the cell surface and in the medium (93). CdS particles could be produced intracellularly by exposing *Klebsiella aerogenes* to Cd^{2+} ions in the size range of 20-200 nm (94). In another case, *E. coli*, when incubated with cadmium chloride (1mM) and sodium sulfide (1mM) showed the potential to synthesize intracellular semiconductor CdS nanocrystals and the results revealed that nanocrystal formation increased ~20-fold in *E. coli* grown in the stationary phase cells compared to late logarithmic phase cultures (95). *Rhodopseudomonas palustris* was found to produce CdS nanoparticles when it was incubated with 1 mM $CdSO_4$ at 30°C for 72 h (96). It is believed that C-S-lyase (an intracellular enzyme located in the cytoplasm) was responsible for the synthesis of nanoparticles and interestingly these particles are found to be transported out of the cell. ZnS nanoparticles are formed with spherical morphology by sulfate reducing bacteria (family Desulfobacteriaceae) (97). *Rhodobacter sphaeroides* was found to synthesize ZnS (98) and PbS (99) nanoparticles with an average diameter of 8nm and 10.5 ± 0.15 nm respectively. It was found that the culture time could modulate the size of PbS nanoparticles.

Nanosized magnetic particles are common bacterial products during iron reduction which enable early disease detection, efficacy in therapy, cellular interaction study in biology (100,101). These particles may have some varied applications in drug delivery, magnetic resonance imaging (MRI), diagnostics, immunoassays, molecular biology, DNA and RNA purification, cell separation and purification, hyperthermia (102,103) etc. Bacteria-based processes for the growth of the magnetic nanoparticles have been achieved by iron reducing bacterium *Thermoanaerobacter ethanolicus* (104,105) and particles formed of octahedral morphology in large quantities. A more fundamental study was performed for the assembly of single-domain magnetite particles (Fe_3O_4) into folded-chain and flux-closure ring morphologies by harvested magnetotactic bacterium, *Magnetospirillum magnetotacticum* (106). Many mesophilic microorganisms which own the ability to use Fe(III) as a terminal electron acceptor could also reduce a variety of metals and metalloids other than Fe(III). Many Fe(III)-reducing microorganisms could reduce forms of oxidized metals, including radionuclides such as uranium(VI) and technetium(VII) and trace metals including

arsenic(V), chromium(VI), manganese(IV), and selenium(VI). Many of these metals and metalloids are environmental contaminants. Therefore, Fe(III)-reducing microorganisms could be used for the removal of contaminant metals from waters and waste streams and immobilization of metals in subsurface environments. Microbial reduction of some of these metals may also play an important role in the formation of metal deposits, which may be especially important in hot environments containing metal-rich waters. The sulfate-reducing bacterium, *D. desulfuricans* (107, 108) and metal ion-reducing bacterium, *S. oneidensis* were capable of reducing soluble palladium (II) into insoluble palladium (0) with formate, lactate, pyruvate, or H_2 as the electron donor (109). In another study, *S. algae* were able to deposit platinum nanoparticles by reducing $PtCl_6{}^{2-}$ ions where by the nanoparticles were found to be present in periplasmic space (110).

Actinomycetes:

Thermomonospora sp., an alkalothermophilic actinomycete when exposed to $AuCl_4{}^-$ ions, reduces the metal ions extracellulary by enzymatic process. More research exploration is needed for the exact mechanism of these enzymatic processes. Complete reduction of $AuCl_4{}^-$ ions resulted in spherical monodispersed nanoparticles (with average dimension of 8 nm) at pH 9.0 and 50°C (111).

In addition, intracellular synthesis of monodispersed gold nanoparticles (5–15 nm) occurred in alkalotolerant actinomycete *Rhodococcus* sp. (65), where particles were more concentrated on the cytoplasmic membrane than on the cell wall. It is believed that the reduction of gold ions occurred on the surface of the mycelia and cytoplasmic membranes. As a result, the production of nanoparticles with good monodispersity and desired morphologies and compositions might be achieved by using actinomycetes.

Yeasts:

Yeast has received much attention for the biosynthesis of nanoparticles. Dameron *et. al.* (112) has demonstrated that the yeasts such as *S. pombe* and *C. glabrata* produced intracellular CdS nanoparticles when challenged with cadmium salt in solution. Yeast cells produce metal chelating peptides (glutathiones) accompanied by an increase in sulfide concentration which leads to the formation of CdS nanocrystalline particles. These biogenic CdS particles are capped and stabilized by the secreted peptide,

glutathione and its derivative phytochelatins. Synthesis of zinc phosphate $(Zn_3(PO_4)_2)$ nanoparticles was achieved by chemical precipitation using yeast cells (113). The yeast, *Torulopsis* sp. was capable of intracellular synthesis of semiconductor PbS nanocrystallites when exposed to aqueous Pb^{2+} ions. These crystallites were recovered from the biomass by freeze-thawing (114). They have also shown that the synthesis of CdS nanocrystals intracellularly in *S. pombe* yeast cells exhibit ideal diode characteristics (115). MKY3 (silver-tolerant yeast strain) when challenged with 1 mM soluble silver in the log phase of growth led to extracellular synthesis of silver nanoparticles (2–5 nm size) (116a). Lead resistant marine yeast *Rhodosporidium diobovatum*, was successfully employed for the green synthesis of lead sulfide nanoparticles (116b). In an effort to synthesize nanoparticles by green chemistry, low cost and more reproducible way, Bakers yeast (*Saccharomyces cerevisiae*) was found to produce spherical antimony trioxide (Sb_2O_3) nanoparticles (117). Sb_2O_3 could be used in a variety of applications. In another study, biosynthesis of gold nanoparticles was also achieved by *Yarrowia lipolytica* NCIM 3589 (118).

Fungi:

Among the other microorganisms, fungi are more advantageous in many ways. Usually they grow on simple media and are easy to handle in laboratory. They secrete large amount of enzymes and can be easy for downstream processing. These features make them a novel candidate for the fabrication of nanomaterials synthesis.

The fungus *Verticillium* sp. (intracellular synthesis) and *Fusarium oxysporum* (extracellular synthesis) were found capable to synthesize nanomaterials, when exposed to aqueous gold and silver ions. In the case of *Verticillium* sp. reduction of the metal ions occurred intracellularly leading to the formation of gold (119) and silver (120) nanoparticles. A considerable difference appears in case of *Fusarium oxysporum*, the reduction of metal ions occurring extracellularly resulting in the formation of gold (121) and silver (122) nanoparticles. Apart from metal nanoparticles, the fungus *Fusarium oxysporum* when exposed to the aqueous solution of equimolar mixture of gold and silver led to the formation of gold-silver alloy nanoparticles. The results suggested the secreted cofactor NADH plays an important role and nanoparticles of different chemical compositions could be synthesized by controlling this factor that depends on the amount of fungal biomass (123). Even more interesting, the fungus *Fusarium oxysporum* when challenged with an aqueous

solution of $CdSO_4$ resulted in the formation of highly stable quantum dots of CdS nanocrystals by a purely enzymatic process (124). The CdS quantum dots are formed by reaction of Cd^{2+} ions with sulphide ions formed by the enzymatic reduction of sulphate ions. These enzymes are secreted into the solution by the fungus *F. oxysporum.*

Gericke and Pinches studied many organisms in order to synthesize metal nanoparticles. Obtained results show that the yeast, *P. jadinii*, and the fungus, *V. luteoalbum*, show the most intracellular nanoparticle synthesis of variable shapes such as hexagons, triangles, rods, and spheres (125). Platinum nanoparticles were obtained by reducing H_2PtCl_6 by the fungus (126). Recently, the fungus *F. semitectum* employed to synthesize highly stable crystalline silver nanoparticles extracellularly with 10-60 nm in dimension and mostly spherical in shape (127). Stable silver nanoparticles could be achieved by using *Aspergillus flavus*; the fungus treated solution turned dark red after 72 hr due to extracellular deposition of silver nanoparticles (128). In another study with *Aspergillus fumigatus* for the extracellular silver nanoparticles synthesis, particles with 5-25 nm dimensions with variable shapes were obtained (129). It is believed that handling of *Aspergillus* is somewhat difficult as they produce toxins, thus it is recommended to be more cautious while handling these fungi in laboratory. *Phaenerochaete chrysosporium* (a white rot fungus), when reacted with silver nitrate solution, silver nanoparticles were produced in 24 h extracellularly. It is believed that stabilization of these particles occurs due to protein. The morphology was mostly dominated by pyramidal shape in different sizes, but hexagonal structures are also observed (130). The culture filtrate of *Cladosporium cladosporioides* was used to synthesize crystalline silver nanoparticles; results suggest that proteins, organic acids and polysaccharides released were responsible for spherical nanoparticles (131). Even though, the culture filtrate of *Penicillium fellutanum* (isolated from mangrove root soil) was incubated with silver ion and maintained under dark conditions, spherical silver nanoparticles could be produced. They also changed crucial factors such as pH, incubation time, temperature, silver nitrate concentration and sodium chloride to achieve the maximum nanoparticle production. Results revealed that the highest optical density (at 430 nm) was observed 24 hr after the start of incubation time (1mM concentration of silver nitrate, pH 6.0, 5°C temperature and 0.3% sodium chloride was used) (132). Sadowski *et. al.* reported that *Penicillium* genus could be used for the biosynthesis of silver nanoparticles.

Polydispersed silver nanoparticles obtained might be formed by an extracellular mechanism (133). In addition, *Penicillium* sp. J3 isolated from soil was able to produce silver nanoparticles. Reduction of silver ions occurred on the surface of the cells and proteins might have a crucial role in the formation and stabilization of the synthesized nanoparticles (134). *Coriolus versicolor* was investigated for the ability for the formation of monodispersed and spherical silver nanoparticles. It was also observed that reduction reaction of metallic ions was pH sensitive. For the reduction of silver nanoparticles, glucose was necessary in the case of growth medium, and in the case of fungal mycelium, S-H of the protein played an important role (135). Cell extracts of *Fusarium acuminatum* Ell. and Ev. (USM-3793) isolated from infected ginger (*Zingiber officinale*) was demonstrated for the production of silver nanoparticles. The morphology of the synthesized nanoparticles was found to be spherical with size dimensions of 5-40 nm. The extracellular extract contained enzymes which might be acting as reducing agent in the nanoparticle formation (136). Extracellular synthesis process was developed for the production of Au, Ag and Au-Ag alloy nanoparticles using the extract of *Volvariella volvacea* (a naturally edible mushroom). Size and shape of nanoparticle could be tuned by the two important parameters viz. temperature and amount of extract. The study provides a controlled and scalable synthetic process for the stable nanoparticles (137). An endophytic fungus, *Colletotrichum* sp. was found to produce stable gold nanoparticles with variable morphology (138a). *Trichothecium* sp. when reacted with gold ions produces extracellular gold nanoparticles under stationary conditions, in contrast to intracellular gold nanoparticles formed in shaking conditions (138b). Very recently, different fungi have been successfully employed for the synthesis of nanomaterials (139).

Fusarium oxysporum, is one of the various fungi, which have been explored completely for the production of various nanomaterials. Various nanoparticles have been synthesized extracellularly such as gold, silver, gold-silver alloy, quantum dots, silica, titania, zirconia, magnetite, carbonate biominerals ($CaCO_3$, $SrCO_3$), barium titanate, etc using fungi.

Mukherjee *et. al.* (121) reported gold nanoparticles with spherical and triangular morphology. FTIR spectrum suggested carbonyl and amine stretch vibration from the protein and electrophoresis revealed proteins of molecular mass between 66 kDa and

10 kDa were involved in nanoparticle stabilization. Bimetallic nanoparticles (Au-Ag alloy) are also formed extracellularly. These alloy nanoparticles could be used in biomedical applications due to their unique electronic and structural properties. Anil *et. al.* have also synthesized highly luminescent water dispersible CdSe quantum dot at room temperature using fungus *Fusarium oxysporum* (140). Zirconia nanoparticles were also produced by cationic proteins secreted by *F. oxysporum* when incubated with ZrF_6^{2-} anions. The proteins of molecular weights 24-28 kDa were found to be responsible for the formation of zirconia nanoparticles (141). Similarly, it also produced silica and titania nanoparticles with SiF_6^{2-} and TiF_6^{2-} anionic complexes respectively, which resulted in the synthesis of silica and titania nanoparticles (142). Biosynthesis of carbonate crystals by the fungus was achieved, $CaCO_3$ (143a) and $SrCO_3$ (143b) were synthesized by "total biological synthesis". Recently it was discovered that naturally available raw materials [(white sand (144a) and zircon sand) (144b)] as well as agro-industrial by-products (rice husk) (144c) can be used for the fungus-mediated bioleaching of oxide (silica) nanoparticles of diverse morphologies. In addition, it also produced binary oxide, bismuth oxide (Bi_2O_3) (145a) and ternary oxide, barium titanate nanoparticles ($BaTiO_3$) of irregular quasi-spherical morphology at room temperature (145b). Magnetic nanoparticles with single domain characteristics were also produced when incubated with the mixture of salts $K_3[Fe(CN)_6]$ and $K_4[Fe(CN)_6]$. These biosynthesized nanoparticles which were quasi-spherical in shape with 20-50 nm size (146). Although *Fusarium* sp. can produce various nanoparticles widely, it is not applicable to all *Fusarium* sp. *F. moniliforme*, which produces reducing components was not able to form silver nanoparticles upon incubation with silver ions (147).

In another study, fungus-based approach provides an easy nanosynthesis for inorganic compounds such as $CuAlO_2$, where it is difficult with chemical synthesis, especially under technologically desirable low-temperature condition (148). The use of fungal biomass was discovered to break down chemically synthesized BiOCl nanoplates (size 150-200 nm) into very small particles (<10 nm) while maintaining their crystalline structure and the phase purity (149).

The fungus *Fusarium oxysporum* has been reported to secrete NADH-dependent reductase into the solution. The enzymatic routes for *in vitro* synthesis of gold, silver and CdS nanoparticles have been developed. *In vitro* gold (150a) and silver (150b)

nanoparticles were achieved by sulfite and nitrate reductase respectively. The *in vitro* synthesis of technologically important and highly stable semiconductor CdS nanoparticles capped by photochelatin was also observed by the use of sulphite reductase enzyme purified from the fungus (150c). The use of enzyme for *in vitro* synthesis of nanoparticles showed interesting advantages by eliminating downstream processing for different applications. This approach can be employed for the synthesis of nanoparticles with different chemical compositions.

Plants:

Biosynthesis of nanomaterials using plant based processes has received great attention as simple and viable alternative approach to chemical and physical methods. Gardea-Torresdey *et. al.* have reported the formation of gold and silver nanoparticles inside living plants *Medicago sativa* (Alfalfa) (151,152), even different morphologies were obtained when alfalfa biomass reacted with gold ions (153). In a related investigation, Cr(VI) ions were reduced to Cr(III) ions by agricultural biomass, indicating its efficiency in decontaminating polluted water and soil polluted with heavy metal ions (154). Alfalfa biomass also exploited for the synthesis of iron oxide nanoparticles, at alkaline pH, produced smaller particles within dimension range of 1-4 nm with greater proportion of Fe_2O_3 (155).

Recently, the biosynthesis of metal nanoparticles by plant based processes and their potential applications has been reported (156,164). The bioreduction of gold and silver ions was studied in *Pelargonium graveolens* leaf (156,157) or *Azadirachta indica* leaf (158). Moreover, formation mechanism of triangular gold nanoprisms by *Cymbopogon flexuosus* (lemongrass) extracts was explored, the process involved rapid reduction, assembly and room temperature sintering of "liquid-like" spherical gold nanoparticles (159). Gold nanotriangles and silver nanoparticle synthesis was achieved by *Aloe vera* plant extract, as well (163). *P. graveolens* leaves when exposed to chloroaurate ions resulted in rapid reduction of the metal ions and formation of stable gold nanoparticles of variable sizes. In the case of *P. graveolens* leaves, the reduction of the $AuCl^{4-}$ ions was nearly complete after 60 min of reaction, the particles were of larger dimensions (20-40 nm) (157). In another study, *P. graveolens* leaf broth, when exposed to aqueous silver nitrate solution, resulted in extracellular synthesis of stable crystalline silver nanoparticles (16-40 nm diameters) (156). Very

recently, different plant extracts were used for synthesis of nanomaterials (165). More elaborate studies are needed to show the mechanism of nanoparticle biosynthesis.

Microorganisms such as algae, yeast, fungi and plants were capable of producing glutathione related peptides for detoxification and sequestration of metal ions. These glutathione oligomers [Phytochelatins (PC)] used as a chelator for heavy metal ions such as Cd, Pb, Zn and Cu reduces the intracellular concentration. PC related reports exist in literature (166, 167). In several plants and yeasts, two main groups of cadmium–PC complexes have been resolved, one in which Cd is bound to thiol groups and the other in which inorganic sulfide ions (S^{2-}) were incorporated into these complexes to form nanometer-sized PC-coated CdS nanocrystallites (168-170). Therefore, it seems that the PCs have the potential to be used as the chelating agent in nanoparticle synthesis. Gold and silver nanoparticles were obtained by exposing precursors at ambient temperature to a novel sundried biomass of *Cinnamomum camphora* leaf (171). Huang *et. al.* (172) in another study fabricated silver nanoparticles by lixivium of sundried *Cinnamomum camphora* in continuous-flow tubular microreactors and introduced polyols as possible reducing agents. Shankar *et. al.* (158) has reported the synthesis of stable gold, silver and bimetallic core-shell nanoparticles by reduction with neem leaves (*Azadirachta indica*). Gold nanoparticles formed were thin, planar structures rather than spherical. Planar particles were predominantly triangular and hexagon shaped in small percentages. Silver nanoparticles were found to be spherical and polydispersed with 5-35 nm dimension. Interestingly, rod shaped nanoparticles synthesized in pH dependent manner using *Avena sativa* (oat), suggest that biomass might contain more positive functional groups such as positive amino groups, sulfhydryl groups, and carboxylic groups (173) which allowed the Au(III) ions to get more close to the binding sites (174) and carry out the reduction of Au(III) to Au(0). Rapid synthesis of stable gold nanotriangles was achieved using *Tamarindus indica* (tamarind) leaf extract as reducing agent (161). These gold nanotriangles are used in photonics, optoelectronics, and optical sensing. Furthermore, *Emblica officinalis* fruit extract produced highly stable Au and Ag nanoparticles extracellularly (162). In other study, gold and silver nanoparticles produced by *Aloe vera* leaf extract were found to be of different shapes (spherical and triangular) and sizes (163). Recently, Harris and Bali (175) have investigated the uptake of metallic silver by two metallophytes, *Brassica juncea* and *M. sativa* and

suggested that both the plant could be utilized for phytosynthesis of silver nanoparticles.

Song and Kim (176) studied different plants (*Pinus desiflora*, *Diopyros kaki*, *Ginko biloba*, *Magnolia kobus* and *Platanus orientalis* leaves broth) to synthesize stable silver nanoparticles extracellularly. *M.kobus* and *D.kaki* leaf broths were able to convert silver nanoparticles faster after increase in reaction temperature (25-95^{0}C) but it is believed that, it might be a chemical conversion instead of an enzymatic one, because enzymes can not be active at higher temperatures. Bimetallic Au/Ag nanoparticles were formed by the interaction of bioinorganic capping molecules along with gold and silver nanoparticles. Spherical silver nanoparticles with size range 15-90 nm were obtained by the reduction of Ag ions with *D. kaki* (persimmom) leaf extract (177). Leguminous shrub, *Sesbania drummondii* seedlings could uptake high amounts of gold (III) ions, resulting in the formation of intracellular monodispersed spherical gold nanoparticles (178). Apiin (extracted from henna leaves) was employed to synthesize anisotropic gold and quasi-spherical silver nanoparticles. Secondary hydroxyl and carbonyl groups of apiin compounds were responsible for the reduction of nanoparticles and providing stability to them for upto 3 months. Different amounts of apiin were used to control the size and shape of nanoparticles (179). *Coriandrum sativum* (family: Apiaceae) leaf extract when exposed to the aqueous solution of gold ions, resulted in the extracellular production of gold nanoparticles with spherical, triangle, truncated triangles and decahedral morphologies (180).

Rapid precipitation of α-Se/protein was achieved at room temperature using proteins extracted from *Capsicum annuum* L. The protein and vitamin C present in *C. annuum* L. extract were responsible for the synthesis of α-Se nanoparticles. The proteins also stabilized nanoparticles on their surfaces (181). Interestingly, Green tea (*Camellia sinensis*) extract was capable to produce gold nanoparticles and silver nanostructures in aqueous solution in ambient conditions. Control of size, morphology and optical properties of the nanoparticles were investigated and suggests that the initial concentration of metal ions and the tea extract act as controlling factors (182). Silver-protein (core-shell) nanoparticles could be synthesized by spent mushroom substrate in the size range (30.5 ± 4.0 nm) (183). Synthesis of spherical silver nanoparticles (60–80 nm) using callus extract of *Carica papaya* was also achieved. Proteins and other ligands were found responsible for the synthesis and stabilization of

nanoparticles (184). Silver nanoparticles (10–20 nm) were fabricated by the latex of *Jatropha curcas* which acts as reducing and capping agent (185).

Algae:

Till date, few reports exist for algae mediated synthesis of nanoparticles. *Chlorella vulgaris*, dried cell suspension when incubated with $HAuCl_4$ solution accumulated elemental gold into the cells (186). *Phaeodactylum tricornutum* (marine phytoplanktonic algae), in response to Cd, formed PC-coated CdS nanocrystallites (186,187). PC-coated CdS nanocrystallites formation has been reported for the *Chlamydomonas reinhardtii* (freshwater microalgae) (188) and *P. tricornutum* (marine microalgae) (189). PC-coated CdS crystallites from *P. tricornutum* were similar to CdS nanocrystallites isolated from several plants and yeasts. *Sargassum wightii* was capable to form extremely stable extracellular gold nanoparticles in size range 8-12 nm (190). When *Spirulina platensis* biomass was exposed to aqueous solution of gold, silver ions, spherical gold (6-10 nm), silver (7-16 nm) and bimetallic Au-Ag nanoparticles (17-25 nm) were formed extracellularly (191). Cyanobacteria and eukaryotic alga genera such as *Lyngbya majuscule*, *Spirulina subsalsa* and *Rhizoclonium heiroglyphicum* could be used as cost-effective means for the biorecovery of gold and formation of gold nanoparticles (192). In another study, bioaccumulation and bioreduction of gold by *Rhizoclonium riparium*, *Navicula minima* and *Nitzaschia obtuse* had been reported (193,194). Recently, cell extract of marine microalga *Tetraselmis suecica* was used as a reducing agent for the synthesis of gold nanoparticles (195).

Viruses:

In recent years, biological methods have been developed for eco-friendly synthesis of inorganic materials. Biological materials like DNA (196,197), protein cages (198), biolipid cylinders (199, 200), viroid capsules (201), bacterial rapidosomes (202), S-layers (203) and multicellular superstructures (204) have been used in template-mediated synthesis of inorganic nanoparticles and microstructures. Interestingly, tobacco mosaic virus (TMV) was used as template for the synthesis of iron oxide, CdS, PbS and SiO_2 with different strategies. It appears to have happened due to glutamate and aspartate external groups present on the surface of viruses (205). Genetically engineered viruses (self-assembled viral capsids) were exploited as

biological templates for the assembly of quantum dot nanowires. Peptides like A7 and J140 which are capable to nucleate ZnS and CdS nanocrystals were expressed as fusion proteins (PVIII) into the capsid of virus, M13 bacteriophage. These template peptides were selected by phage display and exposure to precursor solution resulted in assembly of ZnS (5nm hexagonal wurtzite) nanocrystals on viral capsid and CdS (3-5nm) assemblies in the form of nanowires. Hybrid nanowires (ZnS–CdS) were achieved with a dual peptide virus engineered to express A7 and J140 within the same viral capsid (206, 207).

Some insight into the mechanisms of nanoparticle biosynthesis:

Researchers have focused their investigations to understand the exact mechanism of biosynthesis, but have been unable to find the exact ones. *Fusarium oxysporum* secrete at least four proteins in the aqueous extract which is indicated from polyacrylamide gel electrophoresis (PAGE). Reaction of these protein extracts with $CdSO_4$ solution did not produce CdS nanoparticles. Addition of ATP and NADH restored the CdS formation capability of the protein extract (124). It might be possible that these proteins are responsible for the *in vitro* synthesis of gold, silver and CdS nanoparticles (148-150). In depth investigation for intracellular formation of gold and silver nanoparticles by the fungus *Verticillium* sp. is not established at the moment. Since the particles are formed on the surface of mycelia, possibility is that negative carboxylate groups interact with silver ions by electrostatic interactions. Thereafter, the ions were reduced by enzymes present in the cell wall leading to the formation of silver nuclei which subsequently grow through further reduction of metal ions and accumulation of these nuclei occurs (120). In case of *Fusarium oxysporum* mediated extracellular gold nanoparticle synthesis, the NADH specific reductase secreted by the fungus leads to the formation of nanoparticles in solution (121).

In another study, reduction mechanism of H_2PtCl_6 and $PtCl_2$ platinum nanoparticles by hydrogenase enzyme isolated from the fungus was carried out. Result revealed that at pH 9 and 65°C, H_2PtCl_6 was reduced to Pt(II) which was later reduced to Pt(0) (126, 208). Previous studies suggest that H_2PtCl_6 might act as electron acceptor during the redox mechanism of hydrogenase enzyme from sulfate reducing bacteria (209). Several studies report the role of cytoplasmic and periplasmic hydrogenases produced by microorganisms in metal reduction (87, 126, 210-215,). In the case of *D. desulfuricans* and *E. coli*, partial inhibition of periplasmic hydrogenases with Cu(II) showed that these metal reductase enzymes play a role in Au(III) reduction (84). Possibly, hydrogenases play an important role in reduction but more investigations are needed to know the exact mechanisms of these reductions. Matsunaga and Takeyama (216) have shown that MagA gene and its protein (isolated from *Magnetospirillum* sp. AMB-1) were required for biomagnetic nanoparticle formation. Magnetotactic bacteria contain a membrane protein that plays an important role in biomineralization, therefore focus has shifted toward gene and protein identification (217, 218). Recent studies reveal a number of genes and proteins which play critical roles in the

biomineralization of bacterial magnetic particles (219). Chemical composition and microstructural characters were studied for bacterial magnetosomes extracted from *M. gryphiswaldense*. Cuboctahedral magnetite particles in dimensions of 46 ± 6.8 nm were obtained. The particles (Fe_3O_4) exhibit high chemical purity and the majority of them falls within a single magnetic-domain range (220). Plant based studies, explain that *C. annuum* L. extract contains proteins with amine groups which play reducing and controlling role during the formation of silver nanoparticles in the solutions (221). In case of neem (*Azadirachta indica*) leaf broth, stabilizing the nanoparticles was possibly facilitated by reducing sugars and/or terpenoids present in the leaf broth (158). Au, Ag and Au-Ag bimetallic nanoparticles were stabilized by polypeptide/ proteins of *S. platensis* alga (191).

Most of the studies were focused on controlling the morphology and size of nanoparticles by using proteins. Recently, association of proteins with spheroidal aggregates of biogenic ZnS nanocrystals was achieved and suggests that these extracellular proteins from microbes could limit the biogenic nanoparticles (222). Controlled formation of magnetite crystals with uniform size was achieved in the presence of Mms6 (a small acidic protein isolated from *M. Magneticum* AMB-1) (223). Mms6 also promoted the formation of uniform, isomorphic, superparamagnetic nanocrystals (224). The recombinant Mms6 protein was exploited for the synthesis of uniform, well-defined $CoFe_2O_4$ nanocrystals *in vitro* (225).

The case of CdS nanocrystals produced by *E. coli* cells indicates that nanocrystals synthesize intracellularly. CdS nanocrystals could be synthesized following Cd^{2+} and S^{2-} ions transported into the cells (95). ZnS nanoparticles too were synthesized by biological method (98). The results reveal that soluble sulfate diffused into immobilized beads and was then carried to the interior membrane of *R. sphaeroides* cell facilitated by sulfate permease. After that, ATP sulfurylase and phosphoadenosine-phosphosulfate reductase reduced sulfate to sulfite, and sulfite reductase reduced sulfite to sulfide which in turn reacted with O-acetylserine to synthesize cysteine via O-acetylserine thiolyase. Cysteine then produced S^{2-} by a cysteine desulfhydrase in the presence of zinc. After this process, spherical ZnS nanoparticles were synthesized following the reaction of S^{2-} with soluble zinc salt. These nanoparticles were discharged from immobilized *R. sphaeroides* cells into the solution.

Important parameters for biosynthesis:

Bio-based methods are a new approach for the development of natural nanofactories. Most of the important factors are constantly being researched upon to get nanoparticles with desirable features. The following mentioned parameters are considered as the most promising in biosynthesis of nanoparticles:

a). Bio-based sources for production of nanomaterials:

To choose the best source for the production of nanomaterials, intrinsic properties such as growth rate, enzyme production and metabolic pathways must be taken into consideration. *Fusarium oxysporum, Verticillium* sp. and *Trichothecium* sp. are some of the successfully used fungi for nanoparticles synthesis.

b). Biomolecules responsible for biosynthesis:

Biomolecules, especially enzymes and proteins are the major reducing and stabilizing agent for nanobiosyntheis. These can be exploited as whole cells of microorganisms, crude enzyme and in purified form obtained from microorganism. Nanoparticles production reaction seems to involve bio-reduction and needs coenzymes such as NADH, NADPH, FAD, etc. Nanomaterials synthesis will be cheaper with help of whole cells of the fungus as compred to purified enzymes from the same fungus.

c). Favorable conditions for growth:

Growth of organism and enzyme production are the key factors which can be tuned by the growth of organism. Therefore, nutrient, inoculum, pH, temperature, etc. should be optimized. Harvesting time is important in the case of using whole cells and crude enzymes. Therefore, it might be necessary to monitor the enzyme activity during the time course of growth.

d). Favorable reaction conditions:

Harvesting of cells was carried out to avoid unwanted residual nutrients and metabolites to avoid complications. Production rate and yield is crucial at industrial scale and needs to be optimized (including exposure time, pH, temperature, etc). Optimizing these factors could control morphology and properties of synthesizing nanoparticles. Therefore, researchers have focused their attention on finding optimal reaction conditions and mechanisms involved in the bio-reduction and production of nanoparticles.

Properties of nanomaterials:

The reduction in material dimensions has pronounced effect on their properties that are significantly different from their corresponding bulk materials. These different properties exhibited by nanomaterials are due to (a) large surface atom, (b) large surface energy, (c) spatial confinement and (d) reduced imperfections. The few properties of nanomaterials are discussed as follows:

I). Optical Property:

Fig 4: Size dependent optical properties of gold nanoparticles. (Image courtesy: http://images.google.com).

Metal nanoparticles (Fig 4) show different optical properties corresponding to their bulk form (226). These properties are dependent on composition, size, shape and surrounding medium of the nanoparticles (227). Depending on the size and shape of the nanoparticles, the optical properties vary from visible region to NIR region (228). This effect happens to appear due to the interaction of electron cloud present on the surface of metal nanoparticle with electromagnetic radiation. Metal nanoparticles (such as gold, silver and copper) are known to exhibit unique optical properties in visible and in NIR region within certain size limit of particles (226).

II). Surface Plasmon Resonance (SPR):

Electron clouds are contributed by the large number of atoms present on the surface of nanoparticles. These free electrons lead to a dipole excitation across the particles under the influence of the electric field vector of the incoming light (Fig 5). This induces positive polarization charge on cationic lattice. This charge acts as a restoring force and brings back electron cloud to its original position, thus causing the oscillations of the electron cloud.
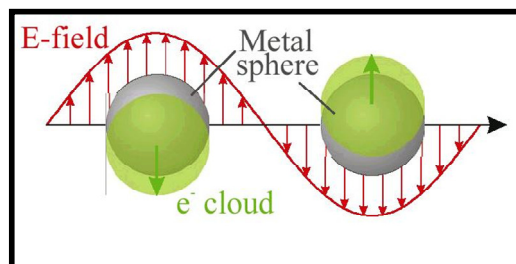

Fig 5: Collective excitation of the electrons: Surface Plasmon Resonance (SPR). (Image courtesy: http://images.google.com).

Thus, the electron density within the surface layer oscillates, whereas the density in the interior of the particle remains constant. This phenomenon is called as surface plasmon resonance and has been explained by Mie in 1908, based on the Maxwell's equation of scattering (21). Interestingly, any changes in the electron density near the surface of nanoparticles will lead to changes in the plasmon absorption. This surface sensitivity of colloidal nanoparticles has been used to study adsorption/ chemisorptions of biomolecules etc. (50a, 229-234). Several applications are emerging based on the surface plasmon resonance properties of nanoparticles.

III). Magnetic properties:

Magnetic properties of nanoscale materials are distinctly different from that of bulk materials. Ferromagnetic particles form single domains with large single magnetic moments at nanoscale. It changes magnetic properties drastically. Under thermodynamic equilibrium, magnetization behaviour of these nanoparticles is similar as that of atomic magnetization but with large magnetic moment. Below certain size, ferromagnetic particles become super-paramagnetic in nature (235). These particles do not show hysteresis in magnetization, since there is only one domain per particle.

IV). Mechanical Properties:

The mechanical properties of nanomaterials increase with the decrease in size. Most of the studies have been focused on the mechanical properties of one dimensional structure such as nanowire. The enhanced mechanical strength of nanowires or nanorods is ascribed to the high internal perfection of the nanowires. Generally, imperfections such as dislocations, micro-twins, impurities, etc. in crystals are highly energetic and should be eliminated from the perfect crystal structures. The smaller the cross-section of nanowires, the less is the probability of finding in it any imperfections as nanoscale dimension makes the elimination of such imperfections possible (236).

V). Thermal Properties:

Metal and semiconductor nanoparticles are found to have significantly lower melting point or phase transition temperature as compared to their bulk counterparts. The lowering of the melting points is observed when the particle size is below 100 nm and is attributed to increase in surface energy with a reduction of size. The decrease in the phase transition temperature can be ascribed to the changes in the ratio of surface energy to volume energy as a function of size (237).

Applications of nanomaterials:

Nanotechnology is of great vitality and offers immense opportunities. It offers an extremely broad range of potential applications including nanomedicine (detection, diagnostics and drug delivery), materials science, electronics, catalytic activities, photocatalytic activities, antimicrobial activities, etc. The variety of applications of nanomaterials is due to their unusual properties, large surface area, etc. Nanomaterials are explored and continuously being researched for various applications.

Nanoparticles for drug delivery in cancer:

There is a great potential of nanomaterials in the field of medicine (Nanomedicine). Few of the biomedical applications of nanomaterials includes detection of molecular interaction (238), cancer treatment by magnetic drug targeting (239), contrast agent in MRI (magnetic resonance imaging) (240), magnetic carriers for cell separation, enzyme immobilization (241), etc. Till date, there are many reports focusing on the application of nanomaterials in cancer therapy and diagnostics. The transport of a drug into tumor area is affected by the interstitial pressure as well as the composition, charge and characteristics of the drug (hydrophobicity, size) (242, 243). The dense packing of tumor cells restricts the movement of molecules into the interstitial compartments (244). The lack of tumor response to a drug (multi-drug resistance) can be due to poorly vascularized tumor regions and lack of drug accumulation in the tumor cells at a therapeutically effective concentration.

Nanomaterials of variable sizes can be synthesized with surface modifications that determine their properties in biological systems. Nanomaterials, whether bare or functionalized, below 100 nm and with at least one dimension can enter cells, even nuclear compartments and interact with the DNA and cellular proteins. Nanoparticles, undoubtedly, could be used in drug delivery systems due to their longer circulation time, larger effective surface area and lower sedimentation rate along with enhanced diffusion potential which makes them readily internalized in tumor cells through membrane.

Nanotechnology has the tremendous potential to improve cancer drug delivery in the following ways.

(1) Detect cancers at an early stage.

(2) Deliver the required concentration of the drug.

(3) Protect the drug from alterations and inactivation.

(4) Increase drug concentration at or near the target site.

(5) Prevent multi-drug resistance.

(6) Specifically destroy malignant cells without affecting the normal cells.

Nanoparticles injected into biological systems are rapidly coated with plasma proteins such as immunoglobulins and fibronectin. After injection, the macrophages internalize the opsonized nanoparticles through phagocytosis and deliver them to liver, spleen, kidney, lymph node and bone marrow (245). Cellular uptake mechanisms for nanoparticles and macromolecules are pinocytosis (246), endocytosis (247,248), and receptor-mediated endocytosis (249). Macromolecules and DNA, which are susceptible to lysosomal degradation, can be delivered by nanoparticles which escape lysosomal degradation.

The best way to increase the efficacy and reduce the toxicity of a cancer drug is to direct the drug to its target and to maintain its concentration at the site for a sufficient time for therapeutic action. Using nanoparticles to deliver drugs to tumors offers an attractive possibility to avoid obstacles that occur during conventional systemic drug administration. Nanoparticles can be directed to tumors by passive and active targeting. There are numerous examples of targeting nanoparticles and this area of research will offer important tools for cancer treatment (250, 254). Researchers have focused in investigating processes for the development for cancer treatment by using different types of nanomaterials (metal nanoparticles, magnetic nanoparticle, polymeric nanoparticles, fluorescent nanoparticles or quantum dots, silica nanoparticles), etc. and drugs such as taxol, doxorubicin, camptothecin, etc.

Nanotechnology in bio-imaging and detection:

Imaging and detection of live cells is important in cancer biology and tumor therapies. Successful development of the quantum dots as fluorescent probe, imaging for the live cell and detection of live cells become feasible (89). Quantum dots nanocrystals and the nanosized particles in the range of 1-10nm with unique properties would emit light in different color in size dependent manner. Quantum dots are excellent probes for *in vivo* imaging at molecular and cellular levels due to their stability and multicolor emissions. Remarkable advantage of quantum dots has been reported

because of their much stronger intensity and excellent photostability as compared to other fluorescent molecules. Modified quantum dots can be used as robust immunofluorescent probes for detection of cancer markers such as Her2 and other cellular targets on putative tumor cells. In addition, quantum dots can potentially be used for long-term labeling of live cells (255-257). The detection and diagnosis of cancers *in vivo* are promising applications of quantum dots. In early experiments in mice, multifunctional nanoparticle probes can bind to cancer targets in these animals allowing for visualization of the tumors *in vivo* (258). Since the utility of quantum dots as fluorescent labels, it is not surprising to develop a nanochip to carry out chemical analysis in future for separation and detection. Another important potential application is the use of nanomaterials as a drug carrier, where they can serve as nanobots to deliver drugs and also detectors which release the "drug" at or near the site of interest which will avoid the side effects associated with the drugs (259).

Nanoparticles as carrier for drug delivery:

Viral vectors, non-viral vectors and polymeric nanoparticles have been developed as carriers for delivery applications, but with little success. These carriers have some sort of immune response causing toxic changes to the cell and also affect certain proteins in the body. Polymeric nanoparticles also serve toxic effects due to degradation.

Nanotechnology offers synthesis and application of inorganic nanomaterials for drug delivery applications. There is great interest in inorganic nanoparticles as a carrier for delivery of DNA (260), proteins (261) etc. In the related investigation, inorganic nanoparticles such as gold (262), silica (263) and iron oxide nanoparticles (264-266) have been studied. These nanoparticles show low toxicity and controlled release property and offer surface functionality, biocompatibility and capability of targeted delivery of drugs (267). Conjugation of antibodies to nanomaterials is being used for targeted drug delivery. In another study, magnetite nanoparticles are used for hyperthermia of cancer (268). Thus, inorganic nanoparticles are gaining considerable importance for drug delivery and therapeutic applications.

Nanomaterials can be used for different applications such as catalysis (269), photocatalysis (270), optoelectronics (271), single-electron transistors, light emitters (272), nonlinear optical devices (273), hyperthermia treatment for malignant cells (274), magnetic memory storage devices, MRI enhancement (275), etc.

References:

1. Cao, G.Z. Imperial College Press, London, UK. **2004**.

2. Henglein, A. *Chem. Rev*. **1989**, *89*, 1861.

3. Khomutov, G. B.; Koksharov, Y. A. *Adv.Colloid Interface Sci*. **2006**, *1-3*, 119.

4. Bao, G. *In Mechanics in biology,* Casey, J.; Bao, G. Eds; ASME: New York, **2000**, *242*, 25.

5. Brown, C.L.; Bushell, G.; Whitehouse, M.W.; Agrawal, D.S.; Tupe, S.G.; Paknikar, K.M.; Tiekink, E.R.T. *Gold Bull*. **2007**, *40 (3)*, 245.

6. Antonii, F. *Panacea Aurea-Auro Potabile*, Bibliopolio Frobeniano, Hamburg. **1618**.

7. Kunckels, J. *Nuetliche Observationes oder Anmerkungen von Auro und Argento Potabili*, Schutzens, Hamburg. **1676**.

8. Faraday, M. *Philos. Trans*. **1857**, *147*, 145.

9. The Royal Institution of Great Britain, cited 18 Dec 2008. Available from: http://www.rigb.org/rimain/heritage/faraday page.jsp.

10. Thomson, D. *Gold Bulletin.* **2007**, *40*, 267.

11. Graham, T. *Philos. Trans. R. Soc*. **1861**, *151*, 183.

12. Taniguchi, N. On the Basic Concept of 'Nano-Technology'. In: *Proceedings of the international conference on production engineering. Tokyo, Part II,* Japan Society of Precision Engineering*,* **1974**: 18-23: Tokyo: JSPE.

13. Lansdown, A.B.G. In: Hipler, U.C.; Elsner, P. (Eds.), Biofunctional textiles and the Skin, *33*, Karger Publishers. **2006**.

14. Russell, A.D. In: Ellis, G.P.; Luscombe, D.K. (Eds.), Progress in Medicinal Chemistry, Elsevier Science Pub Co, Amsterdam, **1994**.

15. Rutkow, I.M. The History of Surgery in the United States, 1775-1900, Jeremy Norman Co. **1988**.

16. Lea, M.C. *Amer. J. Sci*. **1889**, *37*, 476.

17. Frens, G.; Overbeek, J.Th.G. *Colloid Poly. Sci*. **1969**, *233*, 922.

18. Savage, G. *Glass and Glassware*, Octopus Book, London. **1975**.

19. Wagner, F. E. *et. al. Nature*. **2000**, *407*, 691.

20. Turkevich, J. *Gold Bull.* **1985**, *18*, 86.

21. Mie, G. *Ann. Phys*. **1908**, *25*, 377.

22. Feynman, R. P. *Eng. Sci*. **1960**, *23*, 22.

23. Link, S.; El-Sayed, M. A. *J. Phys. Chem. B.* **1999**, *103*, 4212.

24. El-Sayed, M. A. *Acc. Chem. Res.* **2001**, *34*, 257.

25. Chen, S.; Ingram, R. S.; Hostetler, M. J.; Pietron, J. J.; Murray, R. W.; Schaaff, T. G.; Khoury, J. T.; Alvarez, M. M.; Whetten, R. L. *Science.* **1998**, *280*, 2098.

26. Templeton, A. C.; Pietron, J. J.; Murray, R. W.; Mulvaney, P. *J. Phys. Chem. B.* **2000**, *104*, 564.

27. Schmid G.; Simon U. *Chem. Commun.* **2005**, *6*, 697.

28. Raimondi, F.; Scherer, G. G.; Kötz, R.; Wokaun, A. *Angew. Chem. Int. Ed.* **2005**, *44*, 2190.

29. Kreibieg, U.; Vollmer, M. *Optical properties of metal clusters.* Springer: Berlin and New York. **1995**.

30. Hutter, E.; Fendler, J. H. *Adv. Mater.* **2004**, *16*, 1685.

31. Schaaf, T. G.; Shafigullen, M. N.; Khoury, J. T.; Vezmar, I.; Whetten, R. L.; Cullen, W. G.; First, P. N.; Guttierrez-Wing, C.; Ascencio, J.; Jose-Yacamun, M. J. *J. Phys. Chem. B.* **1997**, *101*, 7885.

32. Logunov, S. L.; Ahmadi, T. S.; El-Sayed, M. A.; Khoury, J. T.; Whetten, R. L. *J. Phys. Chem. B.* **1997**, *101*, 3713.

33. a). Alivisatos, A. P. *Science.* **1996**, *271*, 933. b). Brus, L. E. *J. Phys. Chem.* **1986**, *90*, 2555.

34. Brennan, J. G.; Seigrist, T.; Carroll, P. J.; Stuczynski, S. M.; Brus, L. E.; Steigerwalk, M. L. *J. Am. Chem. Soc.* **1989**, *111*, 4141.

35. Henglein, A.; Mulvaney, P.; Holtzworth, A.; Sosebee, T.E.; Fojitik, A. *Ber. Bunsenges. Phys. Chem.* **1992**, *96*, 754.

36. Henglein, A. *Langmuir.* **1999**, *15,* 6738.

37. El-Shall, M. S. *Appl. Surf. Sci.* **1996**, 106, 347.

38. Reetz, M. T.; Helbig, W. *J. Am. Chem. Soc.* **1994**, *116*, 7401.

39. Salkar, R. A.; Jeevanandam, P.; Kataby, G.; Aruna, S.T.; Koltypin,Y.; Palchik, O.; Gedanken, A. *J. Phys. Chem. B.* **2000**, *104*, 893.

40. a) Klabunde, K. J.; Timms, P. S.; Skell, P. S.; Ittel, S. *Inorg. Synth.* **1979**, *19*, 59. b). Davis, S. C.; Klabunde, K. J. *Chem. Rev.* **1982**, *82*, 153.

41. Frenot, A.; Chronakis, H. S. *Current opin. Colloid interf. Sci.* **2003**, *8*, 64.

42. Ginger, D. S.; Zhang, H.; Mirkin, C. A. *Angew. Chem. Int. Ed.* **2004**, *43*, 30.

43. Choy, K. L. *Prog. Mater. Sci.* **2003**, *48*, 57.

44. Wagener, M.; Gunther, B. *J. Magnet. Mag. Mater.* **1999**, *201*, 41.

45. Fojtik, A.; Henglein, A. *Ber. Bunsen-Ges. Phys. Chem.* **1993**, *97*, 252.

46. Cannas, C.; Musinu, A.; Peddis, D.; Piccaluga, G. *Chem. Mater.* **2006**, *18*, 3835.

47. Jayakumar, O. D.; Salunke, H. G.; Kadam, R. M.; Mohapatra, M.; Yaswant, G.; Kulshresshtha, S. K. *Nanotechnology.* **2006**, *17*, 1278.

48. Li, M.; Liu, X.L.; Cui, D.L.; Xu, H.Y.; Jiang, M.H. *Mater. Res. Bull.* **2006**, *41*, 1259.

49. Qu, L.; Shi, G.; Wu, X.; Fan, B. *Adv. Mater.* **2004**, *16*, 1200.

50. a) Brust, M.; Walker, M.; Bethell, D.; Schiffrin, D. J.; Whyman, R. J. *J. Chem. Soc.,Chem. Commun.* **1994**, 801. b) Brust, M.; Fink, J.; Bethell, D.; Schiffrin, D. J.; Kiely, C. J. *J. Chem. Soc., Chem. Commun.* **1995**, 1655. c) Cardenas-Trivino, G.; Klabunde, K. J.; Dale, E. B. *Langmuir.* **1987**, *3*, 986.

51. Kim, K.S.; Demberelnyamba, D.; Lee, H. *Langmuir.* **2004**, *20*, 556.

52. Chattopadhyay, P.; Gupta, R. B. *Ind. Eng. Chem. Res.* **2003**, *42*, 465.

53. Capek, I. *Advances in Colloid and Interface Science.* **2004**, *110*, 49.

54. Quinlan, F. T.; Kuter, J.; Tremel, W.; Knoll, W.; Risbud, S.; Stroeve, P. *Langmuir.* **2000**, *16*, 4049.

55. Braun, E.; Eichen, Y.; Sivan, U.; Ben-Yoseph, G. *Nature.* **1998**, *391*, 775.

56. a) Shenton, W.; Douglas, T.; Young, M.; Stubbs, G.; Mann, S. *Adv. Mater.* **1999**, *11*, 253. b) Fowler, C. E.; Shenton, W.; Stubbs, G.; Mann, S. *Adv. Mater.* **2001**, *13*, 126.

57. Zhang, M.; Drechsler, M.; Muller, A. H. E. *Chem. Mater.* **2004**, *16*, 537.

58. Wiesner, J.; Wokaun, A. *Chem. Phys. Lett.* **1989**, *57*, 569.

59. Qu, L.; Shi, G.; Wu, X.; Fan, B. *Adv. Mater.* **2004**, *16*, 1200.

60. Tan, Y.; Dai, X.; Li, Y.; Zhu, D. *J. Mater. Chem.* **2003**, *13*, 1069.

61. a). Beveridge, T.J.; Murray, R.G. *J Bacteriol.* **1980**, *141*, 876. b). Shivaji, S.; Madhu, S.; Singh, S. *Process Biochemistry* **2011**. DOI: 10.1016/ j.procbio.2011.06.008. c). Anil, K. Suresh.; Pelletier, D.A.; Wang, Wei.; Broich, M. L.; Moon, Ji-Won.; Baohua, Gu.; Allison, D. P.; Joy, D. C.; Phelps, T.J.; Doktycz, M.J. *Acta Biomaterialia.* **2011**, *7(5)*, 2148.

62. a). Aiking, H.; Kok, K.; Heerikhuizen, H.; Riet, J. *Appl Environ Microbiol.* **1982**, *44*, 938. b). Motamedi Juibari, M.; Abbasalizadeh, S.; Salehi Jouzani, Gh.; Noruzi, M. *Materials Letters.* **2011**, *65*, 1014. c). Fischer, A.; Schmitz,

M.; Aichmayer, B.; Fratzl, P.; Faivre, D. *J. R. Soc. Interface*. **2011**. DOI:10.1098/rsif.2010.0576.

63. a). Slawson, R.M.; Van, D.M.; Lee, H.; Trevor, J. *Plasmid.* **1992**, *27*, 73. b) Parikh, R.Y.; Ramanathan, R.; Coloe, P.J.; Bhargava, S.K.; Patole, M.S.; Shouche,Y.S.; Bansal,V. *Plos ONE*, **2011**, *6 (6),* e21401. c). Bai, H.J.; Yang, B.S.; Chai, C.J.; Yang, G.E.; Jia, W.L.; Yi, Z.B. *World J Microbiol Biotechnol.* **2011**, DOI 10.1007/s11274-011-0747-x.

64. Kumar, U.; Shete, A.; Harle, A.S.; Kasyutich, O.; Schwarzacher, W.; Pundle, A.; *et. al*. *Chem Mater.* **2008**, *20*, 1484.

65. Ahmad, A.; Senapati,S.; Khan, M.I.; Kumar, R.; Ramani, R.; Srinivas, V.; Sastry, M. *Nanotechnology.* **2003**, *14*, 824.

66. Niemeyer, C.M. *Nanobiotechnology.* Weinheim: Willey-VCH. **2005**.

67. Rouch, D. A.; Lee, B.T.O.; Morby, A. P. *J. Ind Micro.* **1995**, *14,* 132.

68. Beveridge, J.T.; Hughes, M.N.; Lee, H.; Leung, K.T.; Poole, R.K. *Adv Microb Physiol.* **1997**, *38*, 178.

69. Angell, P. *Curr Opin Biotechnol.* **1999**, *10*, 269.

70. Zierenberg, R.A.; Schiffman, P. *Nature.* **1990**, *348*, 155.

71. Pollmann, K.; Raff, J.; Merroun, M.; Fahmy, K.; Selenska-Pobell, S. *Biotechnol Adv.* **2006**, *24,* 58.

72. Southam, G.; Beveridge, T. J. *Geochim Cosmochim Acta*. **1994**, *58*, 4527.

73. Saifuddin, N.; Wong, C.W.; Yasumira Nur, A.A. *E-J Chem.* **2009**, *6(1),* 61.

74. Klaus, T.; Joerger, R.; Olsson, E.; Granqvist, C.G. *Proc Natl Acad Sci.* **1999**, *96*, 13611.

75. Klaus-Joerger, T.; Joerger, R.; Olsson, E.; Granqvist, C.G. *Trends Biotechnol.* **2001**, *19(1),* 15.

76. Brown, S.; Sarikaya, M.; Johnson, E. *J Mol Biol.* **2000**, *299*, 725.

77. Nair, B.; Pradeep, T.*Cryst Growth Des.* **2002**, *2*, 293.

78. Prasad, K.; Jha, A.K.; Kulkarni, A.R. *Nanoscale Res Lett*. **2007**, *2*, 248.

79. Konishi, Y.; Tsukiyama, T.; Tachimi, T.; Saitoh, N.; Nomura, T.; Nagamine, S. *Electrochimica Acta.* **2007**, *53(1),* 186.

80. Shahverdi, A.R.; Minaeian, S.; Shahverdi, H.R.; Jamalifar, H.; Nohi, A.A. *Biochemistry.* **2007**, *42*, 919.

81. He, S.; Guo, Z.; Zhang, Y.; Zhang, S.; Wang, J.; Gu, N. *Mater Lett.* **2007**, *61(18),* 3984.

82. He, S.; Zhang, Y.; Guo Z.; Gu, N. *Biotechnol Prog.* **2008**, *24*, 476.

83. Liangwei, D.; Jiang, H.; Liu, X.; Wang, E. *Electrochem Commun.* **2007**, *9*, 1165.

84. Deplanche, K.; Macaskie, L.E. *Biotechnol Bioeng.* **2008**, *99(5)*, 1055.

85. Lengke, M.; Fleet, M.E.; Southam, G. *Langmuir.* **2006**, *22*, 2780.

86. Lengke, M.; Ravel, B.; Fleet, M.E.; Wanger, G.; Gordon, R.A.; Southam, G.; *Environ Sci Technol.* **2006**, *40*, 6304.

87. Kashefi, K.; Tor, J.M.; Nevin, K.P.; Lovley, D.R. *Appl Envir Microbiol.* **2001**, *67*, 3275.

88. Wen, L.; Lin, Z.; Gu, P.; Zhou, J.; Yao, B.; Chen, G.; Fu, J. *J Nanopart Res.* **2008**, *11*, 279.

89. Chan, W.C.W.; Maxwell, D.J.; Gao, X.; Bailey, R.E.; Han, M.; Nie, S. *Curr Opin Biotechnol.* **2002**, *13*, 40.

90. Zhang, C.; Vali, H.; Romanek, C.S.; Phelps, T.J.; Liu, S.V. *Am Mineralogist Pages,* **1998**, *83*, 1409.

91. Watson, J.H.P.; Ellwood, D.C.; Soper, A.K.; Charnock, J. *J Magn Magn Mater.* **1999**, *203,* 69.

92. Lee, H.; Purdon, A.M.; Chu, V.; Westervelt, R.M. *Nano Lett.* **2004**, *4*, 995.

93. Cunningham, D.P.; Lundie, J.L.L. *Appl Environ Microbiol.* **1993**, *59*, 7.

94. Holmes, J.D.; Smith, P.R.; Evans-Gowing, R.; Richardson, D.J.; Russell, D.A.; Sodeau, J.R. *Arch Microbiol.* **1995**, *163*, 143.

95. Sweeney, R.Y.; Mao, C.; Gao, X.; Burt, J.L.; Belcher, A.M.; Georgiou, G.; Iverson, B.L. *Chem Biol*, **2004**, *11*, 1553.

96. Bai, H.J.; Zhang, Z.M.; Guo, Y.; Yang, G.E. *Colloids Surf B Biointerfaces.* **2009**, *70*, 142.

97. Matthias, L.; Gregory, K.D.; Thomsen-Ebert, T.; Gilbert, B.; Welch, S.A.; Kemner, K.M.; Logan, G.A.; Summons, R.E.; Stasio, D.G.; Bond, P.L.; Lai, B.; Kelly, S.D; Banfield, J.F. *Science.* **2000**, *290*, 1744.

98. Bai, H.J.; Zhang, Z.M. Gong, J. *Biotechnol Lett.* **2006**, *28*, 1135.

99. Bai, H.J.; Zhang, Z.M. *Mater Lett.* **2009**, *63(9-10),* 764.

100. Rogers, W.J.; Basu, P. *Atherosclerosis.* **2005**, *178(1),* 67.

101. Thorek, D.; Chen, A.; Czupryna, J.; Tsourkas, A. *Ann Biomed Eng.* **2006**, *34(1)*, 23.

102. Moroz, P.; Jones, S.K.; Gray, B.N. *Int J Hypertherm.* **2002**, *18*, 267.

103. Moroz, P.; Jones, S.K.; Gray, B.N. *J Surg Oncol.* **2002**, *80*, 149.

104. Roh, Y.; Lauf, R.J.; McMillan, A.D.; Zhang, C.; Rawn, C.J.; Bai, J.; Phelps, T.J. *Solid State Comm.* **2001**, *118*, 529.

105. Yeary, L.W.; Moon, J.W.; Love, L.J.; Thompson, J.R.; Rawn, C.J.; Phelps, T.J. *Robotics & Energetic Syst.* **2005**, *41*, 4384.

106. Philipse, A.P.; Maas, D. *Langmuir.* **2002**, *18*, 9977.

107. Lloyd, J.R.; Yong, P.; Macaskie, L.E. *Appl Environ Microbiol.* **1998**, *64*, 4607.

108. Yong, P.; Rowson, N.A.; Farr, J.P.G.; Harris, I.R.; Macaskie, L.E. *Biotechnol Bioeng.* **2002**, *80*, 369.

109. Windt, D.D.; Aelterman, P.; Verstraete, W. *Environ Microbiol.* **2005**, *7,* 314.

110. Konishi, Y.; Ohno, K.; Saitoh, N.; Nomura, T.; Nagamine, S.; Hishida, H.; Takahashi, Y.; Uruga, T. *J Biotechnol.* **2007**, *128*, 648.

111. Ahmad, A.; Senapati, S.; Khan, M.I; Kumar, R.; Sastry, M. *Langmuir.* **2003**, *19*, 3550.

112. Dameron, C.T.; Reese, R.N.; Mehra, R.K.; Kortan, A.R.; Carroll, P.J.; Steigerwald,M.L.; Brus, L.E.; Winge, D.R. *Nature.* **1989**, *338*, 596.

113. Yan, S.; Hea, W.; Sun, C.; Zhang, X.; Zhao, H.; Li, Z.; Zhou, W.; Tian, X.; Sun, X.; Han, X. *Dyes Pigm.* **2009**, *80(2),* 254.

114. Kowshik, M.; Vogel, W.; Urban, J.; Kulkarni, S.K.; Paknikar, K.M. *Adv Mater.* **2002**, *14(11),* 815.

115. Kowshik, M.; Deshmukh, N.; Vogel, W.; Urban, J.; Kulkarni, S.K.; Paknikar, K.M. *Biotechnol Bioeng.* **2002**, *78*, 583.

116. a). Kowshik, M.; Ashtaputre, S.; Kharrazi, S.; Vogel, W.; Urban, J.; Kulkarni, S.K.; Paknikar, K.M. *Nanotechnology.* **2003**, *14*, 95. b). Seshadri, S.; Saranya, K.; Kowshik, M. *Biotechnol Prog.* **2011**, DOI: 10.1002/btpr.651.

117. Jha, A.K.; Prasad, K.; Prasad, K. *Biochem Eng J.* **2009**, *43*, 303.

118. Agnihotri, M.; Joshi, S.; Kumar, A.R.; Zinjarde, S.; Kulkarni, S.K. *Mater Lett.* **2009**, *63(15),* 1231.

119. Mukherjee, P.; Ahmad, A.; Mandal, D.; Senapati, S.; Sainkar, S.R.; Khan, M.I.; Ramani, R.; Parischa, R.; Ajayakumar, P.V.; Alam, M.; Sastry, M.; Kumar, R. *Angew Chem Int Ed Engl.* **2001**, *40*, 3585.

120. Mukherjee, P.; Ahmad, A.; Mandal, D.; Senapati, S.; Sainkar, S.R.; Khan, M.; Parishcha, R.; Ajaykumar, P.V.; Alam, M.; Kumar, R.; Sastry, M. *Nano Lett* **2001**, *1(10)*, 515.

121. Mukherjee, P.; Senapati, S.; Mandal, D.; Ahmad, A.; Khan. M.I.; Kumar. R.; Sastry. M. *ChemBioChem*. **2002**, *3(5)*, 461.

122. Ahmad, A.; Mukherjee, P.; Senapati, S.; Mandal, D.; Khan, M.I.; Kumar, R.; Sastry, M. *Colloids Surf B Biointerfaces*. **2003**, *28*, 313.

123. Senapati, S.; Ahmad, A.; Khan, M.I.; Sastry, M.; Kumar, R. *Small,* **2005**, *1(5),* 517.

124. Ahmad, A.; Mukherjee, P.; Mandal, D.; Senapati, S.; Khan, M.I.; Kumar, R.; Sastry, M. *J. Am. Chem. Soc.* **2002**, *124*, 12108.

125. a). Gericke, M.; Pinches, A. *Hydrometallurgy*. **2006**, *83*, 132. b).Gericke, M.; Pinches, A. *Gold Bull.* **2006**, *39*, 22.

126. Riddin, T.L.; Gericke, M.; Whiteley, C.G. *Nanotechnology*. **2006**, *17*, 1.

127. Basavaraja, S.; Balaji, S.D.; Lagashetty, A.; Rajasab, A.H.; Venkataraman, A. *Mater Res Bull.* **2008**, *43(5),* 1164.

128. Vigneshwaran, N.; Ashtaputre, N.M.; Varadarajan, P.V.; Nachane, R.P.; Paralikar, K.M.; Balasubramanya, R.H. *Mater Lett.* **2007**, *61*, 1413.

129. Bhainsa, K.C.; D'Souza, S.F. *Colloids Surf B Biointerfaces.* **2006**, *47*, 160.

130. Vigneshwaran, N.; Kathe, A.A.; Varadarajan, P.V.; Nachane, R.P.; Balasubramanya, R.H. *Colloids Surf B Biointerfaces.* **2006**, *53*, 55.

131. Balaji, D.S.; Basavaraja, S.; Deshpande, R.; Bedre, M.D.; Prabhakar, B.K.; Venkataraman, A. *Colloids Surf B Biointerfaces.* **2009**, *68*, 88.

132. Kathiresan, K.; Manivannan, S.; Nabeel, M.A.; Dhivya, B. *Colloids Surf B Biointerfaces.* **2009**, *71*, 133.

133. Sadowski, Z.; Maliszewska, I.H.; Grochowalska, B.; Polowczyk, I.; Kozlecki, T. *Mater Sci Poland.* **2008**, *26(2),* 419.

134. Maliszewska, I.; Szewczyk, K.; Waszak, K. *J Phys Conf.* **2009**, *146*, 1.

135. Sanghi, R.; Verma, P. *Bioresour Technol.* **2009**, *100*, 501.

136. Ingle, A.; Gade, A.; Pierrat, S.; Sönnichsen, C.; Rai, M. *Current Nanosci.* **2008**, *4*, 141.

137. Philip, D. *Spectrochim Acta A Mol Biomol Spectrosc.* **2009**, *73(2),* 374.

138. a). Shankar, S.S.; Ahmad, A.; Pasricha, R.; Sastry, M. *J.Mater.Chem*. **2003**, *13*, 1822. b). Ahmad, A.; Senapati, S.; Khan, M. I.; Kumar, R.; Sastry, M. *J. Biomed Nanotechol.* **2005**, *1*, 47.

139. a). Castro-Longoria, E.; Vilchis-Nestor, A.R.; Avalos-Borjac, M. *Colloids and Surfaces B: Biointerfaces*. **2011**, *83 (1)*, 42. b). Vahabi, K.; Mansoori,

G.A.; Karimi, S. *Insciences J.* **2011**, *1(1)*, 65. c). Jain, N.; Bhargava,A.; Majumdar, S.; Tarafdar, J. C.; Panwar, J.*Nanoscale*, **2011**, *3*, 635. d). Ghodake V.P.; Kininge, P.T.; Magdum, S.P.; Dive, A. S.; Pillai, M.M. *Journal of Engineering Research and Studies (JERS).* **2011**, *II (I)*, 32. e). Mishra, A.; Tripathy, S.K.; Yun, Soon-Il. *Journal of Nanoscience and Nanotechnology.* **2011**, *11*, 243.

140. Kumar, S.A.; Ansary. A.A.; Ahmad, A.; Khan, M.I. *J Biomed Nanotechnol.* **2007**, *3*, 190.

141. Bansal, V.; Rautaray, D.; Ahmad, A.; Sastry, M. *J. Mater.Chem,* **2004**, *14*, 3303.

142. Bansal, V.; Rautaray, D.; Bharde, A.; Ahire, K.; Sanyal, A.; Ahmad, A.; Sastry, M. *J. Mater. Chem.* **2005**, *15*, 2583.

143. a).Rautaray, D.; Ahmad, A.; Sastry, M. *J.Am.Chem.Soc.* **2003**, *125*, 14656. b).Rautaray, D.; Sanyal, A.; Adyanthaya, S.D.; Ahmad, A.; Sastry, M. *Langmuir.* **2004**, *20*, 6827.

144. a). Bansal, V.; Sanyal, A.; Rautaray, D.; Ahmad, A.; Sastry, M. *Adv. Mater.* **2005**. *17*, 889. b).Bansal, V.; Syed, A.; Bhargava, S.K.; Ahmad, A.; Sastry, M. *Langmuir.* **2007**, *23*, 4993.   c). Bansal, V.; Ahmad, A.; Sastry, M. *J.Am.Chem.Soc.* **2006,** *128*, 14059.

145. a). Uddin, I.; Adyanthaya, S.; Syed, A.; Selvaraj, K.; Ahmad, A.; Poddar, P. *J. Nanosci. Nanotechnol.* **2008**, *8(8)*, 3909.   b).Bansal, V.; Poddar, P.; Ahmad, A.; Sastry, M. *J.Am.Chem.Soc.* **2006**, *128*, 11958.

146. Bharde, A.; Rautaray, D.; Bansal, V.; Ahmad, A.; Sarkar, I.; Yusuf, S.M.; Sanyal, M.; Sastry, M. *Small.* **2006**, *2*, 135.

147. Duran, N.; Marcato, P.D.; Alves, O.L.; DeSouza, G.I.H.; Esposito, E.J. *Nanobiotechnol.* **2005**, *3*, 8.

148. Ahmad, A.; Jagdale, T.; Dhas, V.; Khan, S.; Patil, S.; Pasricha, R.; Ravi,V.; Ogale, S. *Adv. Mater.* **2007**, *19*, 3295.

149. Mazumder, B.; Uddin, I.; Khan, S.; Ravi,V.; Selvraj,K.; Poddar, P.; Ahmad, A. *J.Mater.Chem*, **2007**, *17*, 3910.

150. a).Anil, S, Kumar.; Abyaneh, M. K.; Gosavi, S.W.; Kulkarni, S. K.; Ahmad, A.; Khan, M. I. *Biotechnol. Appl. Biochem.* **2007**, *47,* 191. b)Anil, S. Kumar., Abyaneh, M.K.; Gosavi, S. W.; Kulkarni, S.K.; Pasricha, R.; Ahmad, A.; Khan, M. I. *Biotechnol Lett.* **2007**, *29*, 439. c).Ansary, A.A.; Anil, S. Kumar.;

Krishnasastry, M. V.; Abyaneh,M.K.; Kulkarni, S.K.; Ahmad, A.; Khan, M. I. *J. Biomed. Nanotechnol.* **2007**, *3 (4)*, 406.

151. Gardea-Torresdey, J.L.; Parsons, J.G.; Gomez, E.; Videa, P.; Troiani, H.E.; Santiago, P.; Yacaman, M.J. *Nano Lett.* **2002**, *2*, 397.

152. Torresdey, J.L.G.; Gomez, E.; Videa, J.R.P.; Parsons, J.G.; Troiani, H.; Jos´e-Yacam´an, M. *Langmuir.* **2003**, *19*, 1357.

153. Gardea-Torresdey, J.L.; Tiemann, K.J.; Gamez, G.; Dokken, K.; Tehuacanero, S.; Jos´e-Yacam´an, M. *J Nanopart Res.* **1999**, *1*, 397.

154. Gardea-Torresdey, J.L.; Tiemann, K.J.; Armendariz, V.; Bess-Oberto, L.; Chianelli, R.R.; Rios, J.; Parsons, J.G.; Gamez, G. *J Hazard Mater.* **2000**, *80*, 175.

155. Herrera-Becerra, R.; Zorrilla, C.; Rius, J.L.; Ascencio, J.A. *Appl Phys.* A. **2008**, *91*, 241.

156. Shankar, S.S.; Ahmad, A.; Sastry, M. *Biotechnol Prog.* **2003**, *19*, 1627.

157. Shankar, S.S.; Ahmad, A.; Pasricha, R.; Sastry, M. *Mater Chem.* **2003**, *13*, 1822.

158. Shankar, S.S.; Rai, A.; Ahmad, A.; Sastry M. *J Colloid Interface Sci.* **2004**, *275*, 496.

159. Shankar, S.S.; Rai, A.; Ankamwar, B.; Singh, A.; Ahmad, A.; Sastry, M. *Nat Mater.* **2004**, *3*, 482.

160. Shankar, S.S.; Rai, A.; Ahmad, A.; Sastry, M. *Chem Mater.* **2005**, *17*, 566.

161. Ankamwar, B.; Chaudhary, M.; Sastry, M. *Synth React Inorg Metal-Org Nanometal Chem.* **2005**, *35*, 19.

162. Ankamwar, B.; Damle, C.; Ahmad, A.; Sastry, M. *J Nanosci Nanotechnol.* **2005**, *5(10),* 1665.

163. Chandran, S.P.; Chaudhary, M.; Pasricha, R.; Ahmad, A.; Sastry, M. *Biotechnol Prog.* **2006**, *22*, 577.

164. Rai, A.; Singh, A.; Ahmad, A.; Sastry, M. *Langmuir.* **2006**, *22*, 736.

165. a). Castro, L.; Blázquez, M. L.; Mu˜noz, J.A.; González,F.; García-Balboa, C.; Ballester, A. *Process Biochemistry.* **2011**, *46,* 1076. b). Elavazhagan, T.; Arunachalam, K.D. *International Journal of Nanomedicine.* **2011**, *6*, 1265. c). Andeani, J. K.; Kazemi, H.; Mohsenzadeh, S.; Safavi, A. Digest *Journal of Nanomaterials and Biostructures.* **2011**, *6 (3)*, 1011. d). Singh, C.; Sharma, V.; Naik, P.K.; Khandelwal, V.; Singh, H. *Digest Journal of Nanomaterials*

and Biostructures. **2011**, *6 (2)*, 535. e). Priya, M. M.; Selvia, B.K.; John Paul, J.A. *Digest Journal of Nanomaterials and Biostructures*. **2011**, *6(2)*, 869. f). Ahmad, N.; Sharma, S.; Singh, V. N.; Shamsi, S. F.; Fatma,A.; Mehta, B. R.; *Biotechnology Research International*. **2011**, Article ID 454090, DOI: 10.4061/2011/454090.

166. Grill, E.; Winnacker, E.L.; Zenk, M.H. *Science.* **1985**, *230*, 674.

167. a). Rauser, W.E. *Plant Physiol.* **1995**, *109*, 1141. b). Zenk, M.H. *Gene.* **1996**, *179*, 21.

168. Winge, D.R.; Dameron, C.T.; Mehra, R.K. In Stillman, M.J.; Shaw, C.F.; Suzuki, K.T. Eds. Metallothioneins (Pp. 257–270). New York: VCH Publishers. **1992**.

169. Kneer, R.; Zenk, M.H. *Phytochemistry.* **1997**, *44*, 69.

170. Rauser, W.E. *J Plant Physiol*. **2000**, *156*, 545.

171. Huang, J.; Li, Q.; Sun, D.; Lu, Y.; Su,Y.; Yang, X.; Wang, H.; Wang, Y.; Shao, W.; He, N.; Hong, J.; Chen, C. *Nanotechnology*. **2007**, *18*, 105104.

172. Huang, J.; Lin, L.; Li, Q.; Sun, D.; Wang, Y.; Lu, Y.; He, N.; Yang, K.; Yang, X.; Wang, H.; Wang, W.; Lin, W. *Ind Eng Chem Res.* **2008**, *47*, 6081.

173. Gardea-Torresdey, J.L.; Tiemann, K.J.; Parsons, J.G.; Gamez, G.; Jos´e-Yacam´an, M. *Adv Environ Res.* **2002**, *6*, 313.

174. Armendariz, V.; Herrera, I.; Peralta-Videa, J.R.; Jos´e-Yacam´an, M.; Troiani, H.; Santiago, P.; Gardea-Torresdey, J.L. *J Nanopart Res.* **2004**, *6*, 377.

175. Harris, A.T.; Bali, R. *J Nanopart Res.* **2008**, *10*, 691.

176. Song, J.Y.; Kim, B.S. *Bioprocess Biosyst Eng.* **2009**, *32*, 79.

177. Song, J.Y.; Kim, B.S. *Korean J Chem Eng.* **2008**, *25*, 808.

178. Sharma, N.C.; Sahi, S.V.; Nath, S.; Parsons, J.G.; Gardea-Torresdey, J.L.; Pal, T. *Environ Sci Technol.* **2007**, *41*, 5137.

179. Kasthuri, J.; Veerapandian, S.; Rajendiran, N. *Colloids Surf B Biointerfaces.* **2009**, *68*, 55.

180. Narayanan, B.K.; Sakthivel, N. *Mater Lett.* **2008**, *62*, 4588.

181. Li, S.; Shen, Y.; Xie, A.; Yu, X.; Zhang, X.; Yang, L.; Li, C. *Nanotechnology.* **2007**, *18*, 405101.

182. Vilchis-Nestora, A.R.; Sánchez-Mendieta, V.; Camacho-López, M.A.; Gómez- Espinosa, R.M.; Camacho-López, M.A.; Arenas-Alatorre, J.A. *Mater Lett*. **2008**, *62*, 3103.

183. Vigneshwaran, N.; Kathe, A.A.; Varadarajan, P.V.; Nachane, R.P.; Balasubramanya, R.H. *Langmuir.* **2007**, *23(13),* 7113.

184. Mude, N.; Ingle, A.; Gade, A.; Rai, M. *J. Plant Biochem Biotechnol.* **2009**, *18(1),* 83.

185. Bar, H.; Bhui, D.K.; Sahoo, G.P.; Sarkar, P.; De, S.P.; Misra, A. *Colloids Surf A. Physicochem Eng Asp.* **2009**, *339(1-3*), 134.

186. Hosea, M.; Greene, B.; McPherson, R.; Henzl, M.; Alexander, D.M.; Darnall, D.W. *Inorganica Chimica Acta.* **1986**, *123(3),* 161.

187. Scarano, G.; Morelli, E. *Plant Sci.* **2003**, *165(4*), 803.

188. Hu, S.; Law, K.W.K.; Wu, M. *Plant Sci.* **2001**, *161*, 987.

189. Morelli, E.; Cruz, B.H.; Somovigo, S.; Scarano, G. *Plant Sci.* **2002**, *163*, 807.

190. Singaravelu, G.; Arockiamary, J.S.; Kumar, G.V.; Govindaraju, K. *Colloids Surf B Biointerfaces.* **2007**, *57*, 97.

191. Govindaraju, K.; Basha, S.K.; Kumar, V.G.; Singaravelu, G. *J. Mater Sci.* **2008**, *43*, 5115.

192. Chakraborty, N.; Banerjee, A.; Lahiri, S.; Panda, A.; Ghosh, A.N.; Pal, R. *J. Appl Phycol.* **2009**, *21*, 145.

193. Chakraborty, N.; Pal, R.; Ramaswami, A.; Nayak, D.; Lahiri, S. *J. Radioanal Nucl Chem.* **2006**, *270*, 645.

194. Nayak, D.; Nag, M.; Banerjee, S.; Pal, R.; Laskar, S.; Lahiri, S. *J. Radioanal Nucl Chem*. **2006**, *268*, 337.

195. Shakibaie, M.; Forootanfar, H.; Mollazadeh-Moghaddam, K.; Bagherzadeh, Z.; Nafissi-Varcheh, N.; Shahverdi, A.R.; Faramarzi, M.A. *Biotechnol. Appl. Biochem.* **2010**, *57*, 71.

196. Alivisatos, A.P.; Johnsson, K.P.; Peng, X.; Wilson, T.E.; Loweth, C.J.; Bruchez, M.P. *et. al. Nature.* **1996**, *382*, 609.

197. a).Mirkin, C.A.; Letsinger, R.L.; Mucic, R.C.; Storhoff, J.J. *Nature.* **1996**, *382*, 607. b). Braun, E.; Eichen, Y.; Sivan, U.; Ben-Yoseph, G. *Nature.* **1998**, *391*, 775.

198. Wong, K.K.W.; Douglas, T.; Glider, S.; Awschalom, D.D.; Mann, S. *Chem Mater.* **1998**, *10*, 279.

199. Archibald, D.D.; Mann, S. *Nature.* **1993**, *364*, 430.

200. Baral, S.; Schoen, P. *Chem Mater.* **1993**, *5*, 145.

201. Douglas, T.; Young, M. *Nature.* **1998**, *393*, 152.

202. Pazirandeh, M.; Baral, S.; Campbell, J.R. *Biomimetics.* **1992**, *1*, 41.

203. Shenton, W.; Pum, D.; Sleytr, U.; Mann, S. *Nature.* **1997**, *389*, 585.

204. Davis, S.A.; Burkett, S.L.; Mendelson, N.H.; Mann, S. *Nature.***1997**, *385*, 420.

205. Shenton, W.; Douglas, T.; Young, M.; Stubbs, G.; Mann, S. *Adv Mater.* **1999**, *11*, 253.

206. Lee, S.W.; Mao, C.; Flynn, C.E.; Belcher, A.M. *Science.* **2002**, *296*, 892.

207. Mao, C.; Flynn, C.E.; Hayhurst, A.; Sweeney, R.; Qi, J.; Georgiou, G.; Iverson, B.; Belcher, A. M. *Proc Natl Aca Sci.* **2003**, *10*, 6946.

208. Govender, Y.; Riddin, T.; Gericke, M.; Whiteley, C.G. *Biotechnol Lett.* **2009**, 31, 95.

209. Rashamuse, K.; Whiteley, C.G. *Appl Microbiol Biotechnol.* **2007**, *75*, 1429.

210. Lovley, D.R.; Phillips, E.J.P. *Appl Environ Microbiol*. **1992**, *58*, 850.

211. Lovley, D.R.; Phillips, E.J.P. *Appl Environ Microbiol.* **1994**, *60*, 726.

212. Lloyd, J.R.; Nolting, H.F.; Sole, V.A.; Bosecker, K.; Macaskie, L.E. *Geomicrobiol J.* **1998**, *15*, 43.

213. Lloyd, J.R.; Ridley, J.; Khizniak, T.; Lyalikova, N.N.; Macaskie, L.E. *Appl Environ Microbiol.* **1999**, *65*, 2691.

214. Lloyd, J.R.; Thomas, G.H.; Finlay, J.A.; Cole, J.A.; Macaskie, L.E. *Biotechnol Bioeng.* **1999**, *166*, 122.

215. Lloyd, J.R.; Mabbett, A.M.; Williams, D.R.; Macaskie, L.E. *Hydrometallurgy*, **2001**, *59*, 327.

216. Matsunaga, T.; Takeyama, H. *Supramol Sci.* **1998**, *5(3-4),* 391.

217. Schüler, D. *J. Mol Microbiol Biotechnol.* **1999**, *1*, 79.

218. Grünberg, K.; Wawer, C.; Tebo, B.M.; Schüler, D. *Appl Environ Microbiol.* **2001**, *67*, 4573.

219. Arakaki, A.; Nakazawa, H.; Nemoto, M.; Mori, T.; Matsunaga, T. *J. R. Soc Interface.* **2008**, *5*, 977.

220. Moisescu, C.; Bonneville, S.; Tobler, D.; Ardelean, I.; Benning, L.G. *Mineral Mag*. **2008**, *72*, 333.

221. Li, S.; Shen, Y.; Xie, A.; Yu, X.; Qiu, L.; Zhang, L.; Zhang, Q. *Green Chem.* **2007**, *9,* 852.

222. Moreau, J.W.; Weber, P.K.; Martin, M.C.; Gilbert, B.; Hutcheon, I.D.; Banfield, J.F. *Science.* **2007**, *316(5831),* 1600.

223. Amemiya, Y.; Arakaki, A.; Staniland, S.S.; Tanaka, T.; Matsunaga, T. *Biomaterials.* **2007**, *28(35),* 5381.

224. Prozorov, T.; Mallapragada, S.K.; Narasimhan, B.; Wang, L.J.; Palo, P.; Nilsen- Hamilton, M.; Williams, T.J.; Bazylinski, D.A.; Prozorov, R.; Canfield, P.C. *Adv Funct Mater.* **2007**, *17(6),* 951.

225. Prozorov, T.; Palo, P.; Wang, L.; Nilsen-Hamilton, M.; Orr, D.; Jones, D.; Mallapragada, S.K.; Narasimhan, B.; Canfield, P.C.; Prozorov, R. *ACS Nano.* **2007**, *1(3),* 228.

226. Henglein, A. *J. Phys. Chem.* **1993**, *97*, 5457.

227. Burda, C.; Chen, X.; Narayanan, R.; El-Sayed, M. A. *Chem. Rev.* **2005,** *105*, 1025.

228. Kelly, K.L.; Coronado, E.; Zhao, L.L.; Schatz, G.C. *J.Phys. Chem. B.* **2003**, *107,* 668.

229. Malinsky, M.D.; Kelly, K.L.; Schatz, G.C.; VanDuyne, R.P. *J. Am. Chem. Soc.* **2001**, *123*, 1471.

230. Templeton, A.C.; Wvelfing, W.P.; Murray, R.W. *Acc. Chem. Res.* **2000**, *33*, 27.

231. Keating, C. D.; Kovaleski, K. M.; Natan, M. J**.** *J. Phys. Chem. B.* **1998**, *102*, 9404.

232. Xu, H.; Bjerneld, E. J.; Kall, M.; Borjesson, L. *Phy. Rev. Lett.* **1999**, *83*, 4357.

233. Crumbliss, A. L.; Perine, S. C.; Stonehuerner, J.; Tubergen, K. R.; Zhao, J.; O'Daly, J. P. *Biotech. Bioeng.* **1992**, *40*, 483.

234. Gole, A.; Dash, C.; Ramakrishnan, V.; Sainkar, S. R.; Mandale, A. B.; Rao, M.; Sastry, M. *Langmuir.* **2001**, *17*, 1674.

235. Volokitin, Y.; Sinzig, J.; Jongh, L. J.; Schmid, G.; Moiseev, I. I. *Nature.* **1996**, *384*, 621.

236. Weertman, J. R.; Averback, R. S.; Eds. Edelstein, A.S.; Cammarata, R.C. London Institute of Phys. Publ., Chapter 13, 323. **1996.**

237. Castro, T.; Reifenberger, R.; Choi, E.; Andres, R. P., *Phys. Rrev, B, Condens. Matter.* **1990**, *13*, 8548.

238. Nam, J. M.; Park, S.J.; Mirkin, C. A. *J. Am. Chem. Soc.* **2002**, *124*, 3820.

239. Lübbe, A. S.; Alexiou, C.; Bergermann, C. *J. Surg. Res.* **2001**, *95*, 200.

240. Illum, L.; Church, A. E.; Butterworth, M. D.; Arien, A.; Whetstone, J.; Davis, S. S. *Pharm. Res.* **2001**, *18*, 640.

241. Komissarova, L. Kh.; Kuznetsov, A. A.; Gluchoedov, N. P.; Kutushov, M. V.; Pluzan, M. A. *J. Magn. Mater.* **2001**, *225*, 197.

242. Jain, R. K. *Cancer Res.* **1987**, *47*, 3039.

243. Jain, R. K. *Sci. Am.* **1994**, *271*, 58.

244. Thorpe, P. E.; Burrows, F. J. *Breast Cancer Res. Treat.* **1995**, *36*, 237.

245. Lenaerts, V.; Nagelkerke, J. F.; Van Berkel, T. J.; Couvreur, P.; Grislain, L.; Roland, M.; Speiser, P. *J. Pharm. Sci.* **1984**, *73*, 980.

246. Weissleder, R.; Cheng, H.-C.; Bogdanova, A.; Bogdanov, A. Jr. *J. Magn. Reson. Imaging.* **1997**, *7*, 258.

247. Yeh, T.C.; Zhang, W.; Ildstad, S. T.; Ho, C. *Magn. Reson. Med.* **1993**, *30*, 617.

248. Schoepf, U.; Marecos, E. M.; Melder, R. J.; Jain, R. K.; Weissleder, R. *Biotechniqus.* **1998**, *24*, 642.

249. Moore, A.; Basilion, J. P.; Chiocca, E. A.; Weissleder, R. *Biochim. Biophys. Acta.* **1998**, *1402*, 239.

250. Vasir, J. K.; Reddy, M. K.; Labhasetwar, V. *Curr. Nanosci.* **2005**, *1*, 47.

251. Brannon-Peppas, L.; Blanchette, J. O. *Adv. Drug Deliv. Rev.* **2004**, *56*, 1649.

252. Cortez-Retamozo, V.; Backmann, N.; Senter, P. D.; Wernery, U.; Baetselier, P. D.; Muyldermans, S.; Revets, H. *Cancer Res.* **2004**, *64*, 2853.

253. Gillies, E. R.; Fréchet, J. M. J. *Drug Discov. Today.* **2005**, *10*, 35.

254. Schiffelers, R. M.; Ansari, A.; Xu, J.; Zhou, Q.; Tang, Q.; Storm, G.; Molema, G.; Lu, M. P.; Scaria, P. V.; Woodle, M. C. *Nucleic. Acids Res.* **2004**, *32*, e149.

255. Jaiswal, J. K.; Goldman, E. R.; Mattoussi, H.; Simon, S. M. *Nat. Methods.* **2004**, *1*, 73.

256. Jaiswal, J. K.; Mattoussi, H.; Mauro, J. M.; Simon, S. M. *Nat. Biotechnol.* **2003**, *21*, 47.

257. Michalet, X.; Pinaud, F. F.; Bentolila, L. A.; Tsay, J. M.; Doose, S.; Li, J. J.; Sundaresan, G.; Wu, A. M.; Gambhir, S. S.; Weiss, S. *Science.* **2005**, *307*, 538.

258. Gao, X.; Cui, Y.; Levenson, R. M.; Chung, L. W. K.; Nie, S. *Nat. Biotechnol.* **2004**, *22*, 969.

259. Haberzettl, C. A. *Nanotechnology.* **2002**, *13*, R9.

260. Sandhu, K. K., McIntosh, C. M., Simard, J. M., Rotello, V.M, *Bioconjugate Chem.* **2002**, *13*, 3.

261. Paciotti, G. F.; Myer, L.; Weinreich, D.; Goia, D.; Pavel, N.; McLaughlin, R. E.; Tamarkin, L, *Drug Deliv*. **2004**, *11*, 169.

262. Daniel, M. C.; Astruc, D. *Chem. Rev.* **2004**, *104,* 293.

263. Kneuer, C.; Haltner, E.G.; Schiestel, T.; Schirra, H.; Schmidt, H.; Lehr, C. S., *Inter. J. Pharm.* **2000**, *196*, 257.

264. Plank, C.; Schere, F.; Schillinger, U.; Bergemann, C.; Anton, M. *J. Liposome Res.* **2003**, *13*, 29.

265. Tartaj, P.; Morales, M. P.; Veintemillas-Verdaguer, S.; Gonzáles-Carreño, T.; Serna, C. J. *J.Phy. D: Appl. Phys.* **2003**, *36,* R182.

266. Gupta, A. K.; Gupta, M. *Biomaterials.* **2005**, *26*, 1565.

267. Xua, Z. P.; Zengb, Q. H.; Lua,G. Q.; BingYub, A. *Chem. Eng. Sci.* **2006**, *61* 1027.

268. Ito, A.; Shinkai, M.; Honda, H.; Kobayashi, T. *J. Biosci. Bioeng.* **2005**, *100*, 1.

269. Schmid, G. *Chem. Rev.* **1992**, *92*, 1709.

270. Brugger, P. A.; Cuendet, P.; Graetzel, M. *J. Am. Chem. Soc.* **1981**, *103*, 2923.

271. Wang, Y.; Herron, N. *J. Phys. Chem.* **1991**, *95*, 525.

272. (a) Klein, D. L.; Roth, R.; Lim, A. K. L.; Alivisatos, A. P.; McEven, P. L. *Nature.* **1997**, *389*, 699. (b) Weller, H. *Angew. Chem. Int. Ed. Engl.* **1998**, *37*, 1658.

273. Wang, Y. *Acc. Chem. Res.* **1991**, *24*, 133.

274. (a) Shi, J.; Gider, S.; Babcock, K.; Awschalom, D. D. *Science.* **1996**, *271*, 937. (b) Q. A. Pankhurst, J. Connolly, S. K. Jones, J. Dobson, *J. Phys. D: Appl. Phys.* **2003**, *36*, R167.

275. Mornet, S.; Vasseur, S.; Grasset, F.; Duguet, E. *J. Mater. Chem.* **2004**, *14*, 2161.

Chapter 2

Biological synthesis of metal nanoparticles using fungus

Part 1: Isolation and identification of the fungus *Humicola lanuginosa*

Summary:

We have isolated alkalophilic, alkalotolerant and thermophilic microorganisms from self-heating compost obtained from Pune district in Maharashtra, India, in order to synthesize highly monodispersed extracellular nanomaterials. The microorganisms obtained from above source represent different genera of bacteria, actinomycetes and fungi. All the cultures have been brought into pure culture and then screened for nanoparticles synthesis. Out of the 10 cultures screened, one fungus (AAH-SHC-1) was found to produce extracellular nanoparticles. It was maintained on alkaline MGYP (malt extract, glucose, yeast extract and peptone) agar slants. The fungal strain was aerobic and spore forming in nature showing optimum growth at temperature 50^0C and pH 9. The fungus (AAH-SHC-1) was identified as *Thermomyces lanuginosus* (*Humicola lanuginosa*) based on cultural and morphological characters and also by Internal Transcribed Spacer (ITS) sequence analysis.

Introduction:

Fungal taxonomy is traditionally based on comparative morphological features (1-3). However, special caution should be taken when closely related or morphologically similar fungi are identified, because the morphological characteristics of some fungi are medium dependent and cultural conditions can substantially affect vegetative and sexual compatibility (4-5). The earliest system for fungal classification and identification up to species level relied on morphological characters, mainly those of reproductive structures, spore morphology and the manner in which the spores are produced along with host range and secondary metabolites profile. However, this method of classification presents critical limitations such as sterility of fungal cultures that have not developed reproductive structures or morphological similarities among the members of different species (6). Now, it is clear from above that the conventional methods cannot be applied for identifying the fungal isolates that fail to sporulate in culture, which are categorized as mycelia sterilia (7). Various optimization of growth conditions have been used to promote sporulation of these fungi, such as potato dextrose agar (PDA), potato carrot agar (PCA), corn meal agar (CMA), oat meal agar (OMA), water agar as well as inclusion of host tissues in plate culture (8), UV treatment and grass leaf technique. Nevertheless, a large number of fungi still do not sporulate in culture, and these mycelia sterilia are considerably frequent in fungal studies (7).

The correct identification of fungi is of great practical importance not only in the industry but also in clinical pathology, biotechnology and environmental studies. Different names for the same fungus (anamorph and teleomorph stages) also results in a little confusion in their identification (9). In recent years, molecular biology techniques have provided newer tools for the correct identification of fungi up to species level.

Ribosomal RNA (rRNA) and ribosomal genes (rDNA) have been studied for their usefulness in fungal systematics. It is accepted that ribosomal genes are well characterized, ubiquitous and easily accessible via PCR technology. In ribosomal DNA sequencing, intergeneric transcribed spacers (ITS) and intergeneric regions (IGR) are more variable than the coding regions and these variable rDNA regions could offer valuable guidelines for characterizing and differentiating between two closely related species. It is possible that the ITS/IGR ratio could be suitable for designing species specific oligonucleotide probes for fungal identification. Based on

DNA sequence analysis or internal transcribed spacers of ribosomal DNA, phylogenetic studies have been carried out with important plant pathogenic fungi such as *Phytophthora* (10) and *Puccinia* (11). Lee *et. al.* have designed synthetic oligonucleotide probes from ITS sequence data to differentiate between different *Phytophthora* sp. (12). Phylogenetic relationship among *Fusarium solani* and its *formae speciales* is identified on the basis of their morphological and molecular characterization (13).

Different species of *Aspergillus* such as *Apergillus oryzae* [produces alpha amylase used as a digestive aid in pharmacology ("Taka Diastase")] and *Aspergillus flavus* (produces highly toxic aflatoxin) which are morphologically very close, have been identified and resolved with the help of molecular techniques. Similarly different species of *Trichoderma, Gliocladium* and *Verticillium* have been resolved using similar techniques.

From the foregoing brief outline of the recent studies on the use of molecular techniques for better characterization of strains taxonomically, it is obvious that newer avenues are being explored vigorously to make fungal taxonomy more meaningful. Several biochemists and molecular biologists believe in and recommended molecular taxonomy as the only realistic and reliable basis for classification and identification of fungi. Will it be possible to dispense with morphology-based taxonomy and fully switch over to molecular taxonomy and achieve reliable classification and identification is a question yet to be answered.

A careful analysis will show that the molecular data could contribute useful attributes for a better understanding of the phylogeny and evolutionary relationships of fungi, taxonomy and classification based on morphology would still be the most readily applicable and practical means for classification and differentiation of fungal strains. Hawksworth (1977) points out that it may not be realistic to expect molecular approaches to be the key for fungal classification (14). "As about 1800 fungi new to science are described every year and less than 100 species are sequenced each year, the gap widens rather than contracts. Technological developments including automated molecular and other biochemical procedures are unlikely to be of practical value for many years, except in certain fungi of medical and agriculture significance".

It can be safely assumed that in the immediate future atleast, industrial biotechnology and fermentation studies for fungal-based biomolecules will have to primarily rely upon morphology based taxonomy for discovering novel strains, while exploring

natural biodiversity. Further advances in molecular techniques may see the advent of an era in which molecular biology would play increasingly significant role, not only in aiding fungal taxonomy, but also in the augmented expression of heterologous genes and eukaryotic proteins in fungal systems through recombinant DNA technology.

Extremophiles are microorganisms which thrive under conditions which are lethal to human beings, such as extremes of temperature [from -14^0C (psychrophiles) to 45^0C (thermophiles) to 110^0C (hyperthermophiles)]; extremes of pH [from 1 (acidophiles) to 9 (alkalophiles)]; very high barostatic pressure (barophiles); nonaqueous environment containing 100% organic solvents; excess heavy metal concentrations; etc. These microorganisms have developed numerous special adaptations to survive in such extreme habitats, which include new mechanisms of energy transduction, regulating intracellular environment and metabolism, maintaining the structure and functioning of the membrane and enzymes, etc (15-17).

We have isolated 10 alkalophilic, alkalotolerant and thermophilic microorganisms (bacteria, actinomycetes and fungi) from self- heating compost obtained from Pune district in Maharashtra, India, in order to synthesize highly monodispersed extracellular nanomaterials. Out of 10 cultures screened, one fungus (AAH-SHC-1) was found to produce extracellular monodispersed nanoparticles. This fungus was identified on the cultural, morphological and molecular basis.

Materials and Methods:

Materials:

Malt extract, Glucose, Yeast extract and Peptone were purchased from HiMedia (India.), Agar agar (Qualigens), 2X CTAB buffer [CTAB: 2%, NaCl: 1. 5 M, EDTA: 20mM, Tris-HCL (pH-8): 100mM], Working CTAB solution [2X CTAB stock: 25ml, β-mercaptoethanol: 50µl, Polyvinylpyrrolidone (PVP): 0.25g], RNase A, Chloroform, Isoamyl alcohol, ethanol, TE buffer [10mM Tris-HCL, 1mM EDTA (pH-8)], agarose. ITS-1 and ITS-4 primers, deoxyribonucleotide triphosphate (dNTPs) and *Taq* DNA polymerase were purchased from Bangalore Genei, India. Thermal Cycler (Applied Biosystems, Veriti) and Nikon Microscope (Eclipse E200).

Collection of self heating compost:

The samples for the isolation of alkalotolerant, alkalophilic and thermophilic microorganisms were collected from Pune district of Maharashtra, India.

Isolation of alkalotolerant, alkalophilic and thermophilic microorganisms from self-heating compost:

For the isolation of extremophilic microorganisms (alkalotolerant, alkalophilic and thermophilic) in order to synthesize highly monodispersed inorganic nanomaterials, one gram of self heating compost was taken and suspended in 10mL of sterile distilled water and agitated for 10 min in a shaker at 200 rpm. One mL of suspension solution was diluted serially to 10^{-2} and 10^{-3} and 10^{-4} dilutions. Subsequently, 1mL of each dilution was placed on alkaline MGYP plates [(malt extract (0.3%), glucose (1%), yeast extract (0.3%), and peptone (0.5%), sterile 10% sodium carbonate was used to adjust the pH of the medium to 9.0]. The inoculated Petriplates were placed in B.O.D incubator at 50^0C in polythene bags with moist cotton to avoid desiccation. The polythene bags were opened daily to provide adequate aeration to cultures. Observations on appearance of various microorganisms (bacteria, actinomycetes and fungi) were taken from 2nd upto 5th day. After 2-5 days, microorganisms such as bacteria, actinomycetes and fungi were observed growing from the compost in the plates. Individual colonies and hyphal tips of the fungi were removed from alkaline MGYP plates and placed again on alkaline MGYP plates and incubated at 50^oC for at least 2-5 days. Each microbial culture was checked for purity and transferred to alkaline MGYP slants for highly monodispersed nanomaterials synthesis.

Cultural and morphological characters of the isolated fungus which produced highly monodispersed nanoparticles:

For studying the cultural and morphological characters the isolated fungus (AAH-SHC-1) was grown on alkaline MGYP agar plates. Cultural characters such as color and nature of the colony were determined by visual observations. Morphological features of the fungus such as mycelia, conidiophores and conidia were studied microscopically (Nikon Eclipse E200 Microscope).

Molecular characterization of the isolated fungus:

Isolation of fungal genomic DNA:

The genomic DNA of the alkalotolerant and thermophilic fungal strains was extracted according to the Cetyl Trimethyl Ammonium Bromide (CTAB) method (18). For the isolation of DNA, the fungus was grown in 250 ml Erlenmeyer flask containing 100 ml alkaline MGYP medium. The growth was initiated by inoculating agar plug containing mycelia from 7 days old alkaline MGYP slant. The flasks were incubated on a rotary shaker (200 rpm) for 4 days at 50°C and pH 9. The contents were centrifuged at 6000 rpm for 15 min, washed repeatedly to remove the media constituents. Fungal mycelia were lyophilized to dryness and crushed in liquid nitrogen. Crushed mycelia (0.5g) were taken in a 2 mL micro centrifuge tube. 1mL of pre warmed (65^{0}C) working CTAB solution was added in the same micro centrifuge tube. This mixture was incubated at 65^{0}C for 1 hr with interrupted gentle mixing after every 10 min. The mixture was cooled to room temperature and 500µL of chloroform: isoamyl alcohol (24:1) was added. The tubes were inverted for gentle mixing and then centrifuged at 10,000 rpm at RT for 10min. Supernatant was transferred into another tube and equal volumes of phenol (pH-8): chloroform (1:1) were added. The tubes were again inverted for gentle mixing and then centrifuged at 10,000 rpm at RT for 5min. To the supernatant, 10µL of 10mg/ml RNase A was added. The tubes were inverted for the mixing and incubated at 37^{0}C for 30 min. 500µL of pre chilled (-20^{0}C) isopropanol was added to precipitate the DNA. The tubes were inverted several times and kept at -20^{0}C for 30 min. The tubes were then centrifuged at 12,000 rpm for 15min at 4^{0}C. The supernatant was poured off and the tubes were inverted on a tissue paper. 1mL pre chilled (-20^{0}C) 70% ethanol was added to the tubes and centrifuged at 12,000 rpm for 15min at 4^{0}C. The supernatant was poured off and the tubes were kept for drying at RT for 3-4 hr. After complete drying, the DNA pellet

was re-suspended in 100 µL of TE buffer (4^0C). The quality of the isolated DNA was checked on 0.8 % agarose gel stained with Gel red.

PCR amplification of ITS regions:

Internal transcribed spacer (ITS) regions from the fungal strain were amplified using Applied Biosystems, Veriti 96-well thermal cycler with a final reaction mixture volume of 15 µL containing 0.5 µL fungal DNA solution (40ng), and 10 µL of PCR master mix which contains 2 µL 10X buffer (Bangalore Genei, India), 4 µL (0.2 mM) dNTPs, 1 µL (1 µM) each of the Universal Eukaryotic Primer **ITS1-TCCGTAGGTGAACCTGCGG** (forward primer), **ITS4-TCCTCCGCTTATTGATATGC** (reverse primer) and 0.5 U/µL Taq DNA polymerase (Bangalore Genei, India). Thermocycling parameters: Initial denaturation at 95^0C for 3 min, 35 cycles: 95^0C for 30 sec, 54^0C for 30 sec, 72^0C for 1 min; final extension was at 72^0C for 3 min. The resulting PCR products were analyzed on 1 % agarose gel containing Gel red.

DNA sequencing and sequence analysis:

PCR amplicon obtained using ITS1 and ITS4 primers was sequenced by Sangers dideoxy chain termination method (19) and was carried out at Chromous Biotech Pvt. Ltd, Bangalore, India. The sequence of PCR amplicon was then analyzed by performing nucleotide BLAST at NCBI. The hit matching with the sequence of PCR amplicon was then again used for the sequence alignment. The alignment of PCR amplicon and hit was done by using Clustal-W sequence alignment tool (20). Phylogenetic analysis was carried out using MEGA 4 software (21).

Results and Discussion:

Alkalotolerant, alkalophilic and thermophilic microorganisms from self heating compost:

A total of 10 (AAH-SHC-1 to AAH-SHC-10) microorganisms were isolated from above self heating compost collected from above location. These microorganisms were maintained on alkaline MGYP agar slants. After growing all the microorganisms at pH 9 and 50^0C, the slants were preserved at 15^0C. From an actively growing stock culture, subcultures were made on fresh slants and after 4 days of incubation at pH 9 and 50^0C were used as the starting material for the fermentation experiments.

For the synthesis of the gold and silver nanoparticles, all the microorganisms isolated from above source were grown in 250mL Erlenmeyer flasks containing 50mL of alkaline MGYP medium. The culture was grown with continuous shaking on a rotary shaker (200 rpm) at 50^0C for 96 h. After 96 h of fermentation, cells and mycelia were separated from the culture broth by centrifugation (5000 rpm) at 20^0C for 20 min and the cells and mycelia were then washed thrice with sterile distilled water under sterile conditions. The harvested cells and mycelial mass (10 g of wet mycelia) each was then resuspended in 50 mL of 10^{-3} M aqueous $HAuCl_4$ and $AgNO_3$ solution in 250 mL Erlenmeyer flasks at pH 9. The whole mixture was put into a shaker at 50^0C (200 rpm) and maintained in the dark. The bioreduction of the $AuCl4^-$ and Ag^+ ions in solution was monitored by periodic sampling of aliquots (2 mL) of the aqueous component and measuring the UV-vis spectra (200 nm to 800 nm) of the solution. Out of 10 microorganisms five were negative (AAH-SHC-3, AAH-SHC-4, AAH-SHC-6, AAH-SHC-7 and AAH-SHC-10) and four (AAH-SHC-2, AAH-SHC-5, AAH-SHC-8 and AAH-SHC-9) showed intracellular synthesis of gold and silver nanoparticles. Only AAH-SHC-1 produced extracellular highly monodispersed gold and silver nanoparticles. Further studies were carried out only on strain AAH-SHC-1 for extracellular synthesis of gold and silver nanoparticles.

Cultural and morphological characters of the fungus:

The fungus AAH-SHC-1 grown on alkaline MGYP medium produces fast growing colonies. Colonies which initially appear off-white and felt-like, turn grey with time on the upper side of Petriplate. Subsequently the reverse side of colony turns brown and the agar substratum stains a deep brown or wine color. The vegetative mycelium is hyaline, septate, thin walled, highly branched and is differentiated into conidia on

short lateral branches functioning as undistinguished conidiophores. Conidia are attached at bulging conidiogenous cells. Conidia produced were single, apically positioned, globose or subglobose, brown, single celled. Conidia are attached terminally on the conidiogenous cells. Based on the above cultural and morphological features the isolated strain has been identified as *Thermymyces lanuginosus* (*Humicola lanuginosa)* (22-25).
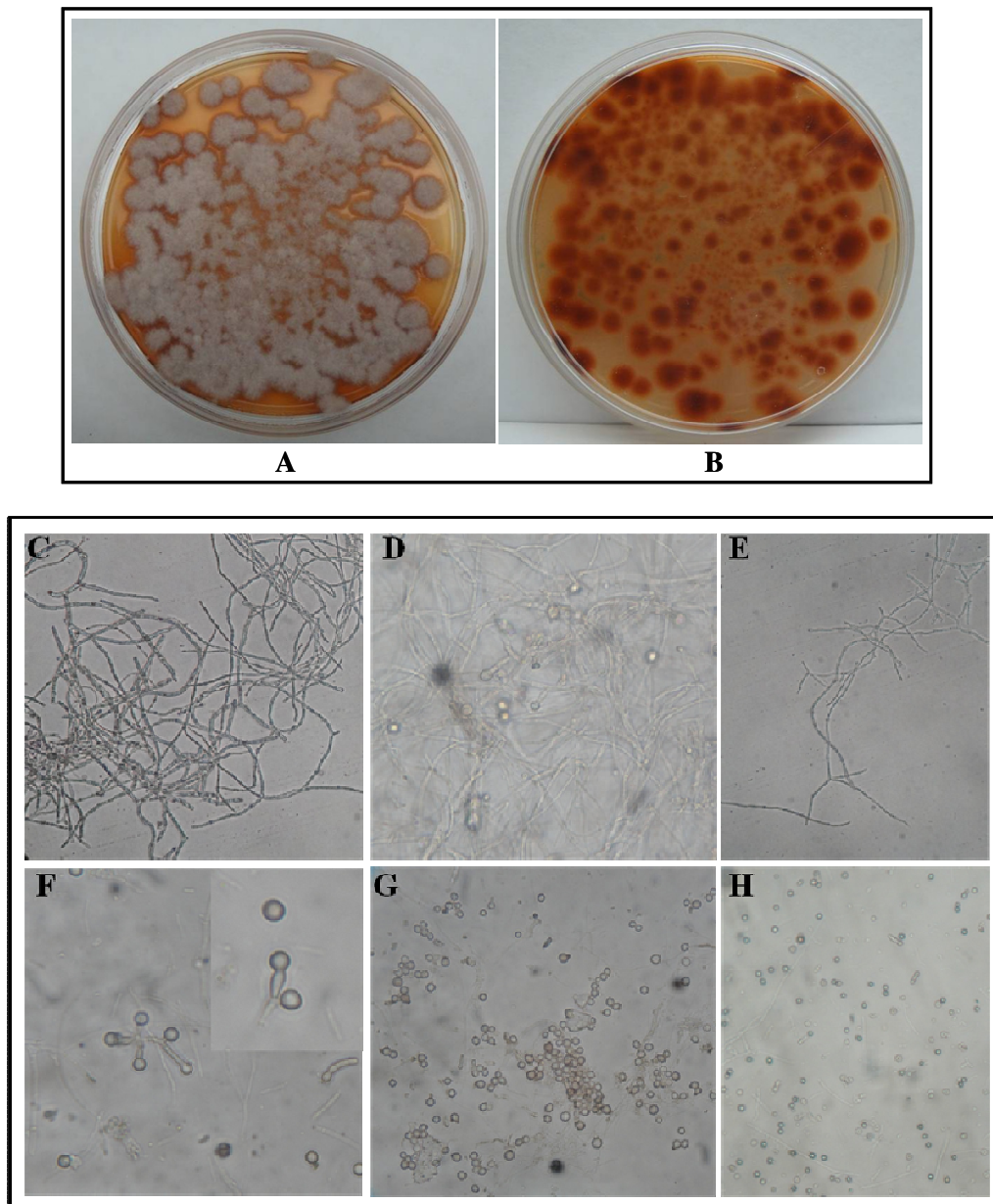

Fig 1: Morphological features of the fungus AAH-SCH-1. The fungal strain was grown on alkaline MGYP agar plate for microscopic observations. Fungal growth: front (A) and back (B) side of alkaline MGYP agar plate, (C-E) Mycelia, (F) Attachment of the conidia on conidiophore, (G-H) Conidia.

Genomic DNA, PCR amplification and sequence analysis:

Genomic DNA isolation by CTAB method resulted in obtaining high quality DNA (Fig. 2). Universal eukaryotic primers (ITS1 and ITS4) used for the amplification of ITS regions successfully amplified fungal genomic DNA producing fragments of 0.57 kb (Fig. 3). Sequence analysis was done using ChromasV 2.0 program and the sequence profile was obtained in FASTA format. BLAST analysis of the sequence determined the identical sequence from the data base. Majority of the hits from BLAST search were from *Thermomyces lanuginosus* (*Humicola lanuginosa*). The sequence analysis of the isolated fungus determined that the 570 bps fragment consist of a partial ITS1 region at 5' end (1 to 182 bps), 5.8 S ribosomal RNA (183 to 338 bps), ITS2 (339 to 512 bps) and partial 28S ribosomal RNA (513 to 570 bps) at 3' end. All the sequences were aligned using Clustal-W programme and the homology between the sequences was determined. The sequence has been submitted to Genebank nucleotide database and is accessible under accession number JN600618.

Phylogenetic analysis of the sequence:

The phylogenetic tree was constructed using MEGA 4 software employing neighbour joining method. This analysis was carried out by using ITS sequence of the isolated fungus (Fig. 4). The phylogenetic analysis also confirmed that the isolated fungal strain AAH-SHC-1 is closely related to *Thermomyces lanuginosus* (*Humicola lanuginosa*).

Genomic DNA of fungus AAH-SHC-1
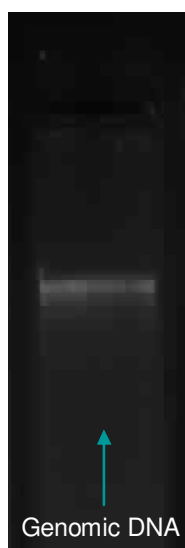
Fig 2: Genomic DNA of fungus AAH-SHC-1 on 0.8 % agarose gel.

PCR Amplification and Sequencing of ITS 1 gene
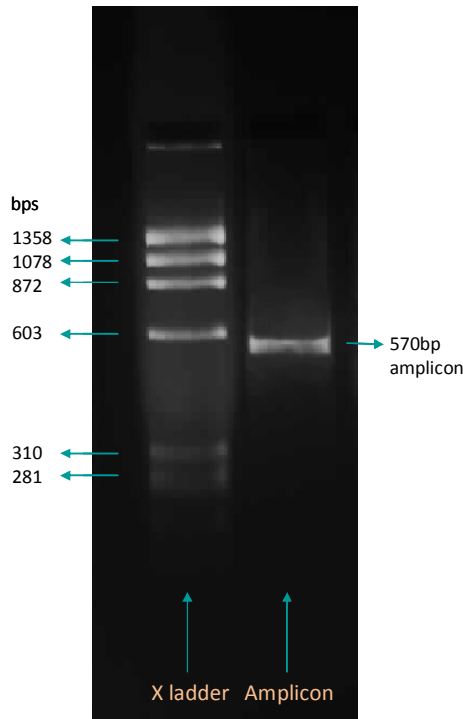
Fig 3: Lane 1: Low range standard molecular weight marker (Φx174) and Lane 2: 0.57 kb PCR amplicon obtained from fungus AAH-SHC-1.

ITS1 regions of fungus AAH-SHC-1:

```
5'
1    AATCTCCCAC CCGTGTCTAC CACACCTAGT GTTGCTTTGG CGGGCCCACT
51   CCTCCGGTGT TCCGCCGGGG GGGTCGTCCC GGGGCGCGGT GTGCCCCCGG
101  GGCCCGTGCC CGCCAGAGGC ACTCACTGTG AACGCTTTTG TGAATGCGAG
151  GATTGTCTGA GTGACGAAAT GCAATCGTTC AAAACTTTCA ACAATGGATC
201  TCTTGGTTCC GGCATCGATG AAGAACGCAG CGAAATGCGA TAAGTAATGT
251  GAATTGCAGA ATTCCGTGAA TCATCGAATC TTTGAACGCA CATTGCGCCC
301  TCTGGTATTC CGGGGGGCAT GCCTGTCCGA GCGTCATTGC GAACCCTCAA
351  GCACGGCTTG TGTGTTGGGC CGCCGTCCCC TCGTTTGGAG GGGACGGGCC
401  TGAAAGGCAG CGGCGGCGTC GCGTCCGGTC CTCGAGCGTA TGGGGCTCTG
451  TCACGCGCTC AAGGAGGGGT CCGGCCGGGG CCATAGCCTC TGAAGGTCAA
501  TTCTTCCAAG GTTGACCTCG GATCAGGTAG GAGTACCCGC TGAACTTAAG
551  CATATCAATA AGCGAAGGAA
3'
```

Internal Transcribed Spacer 1: 1….182bps
5.8 S ribosomal RNA: 183….338bps
Internal Transcribed Spacer 2: 339-512bps
28S ribosomal RNA: 513….570bps

Seq: Corresponding regions in ITS1 amplified PCR amplicon of fungus AAH-SHC-1.

Phylogenetic relationship of selected member with fungus AA-SHC-1:
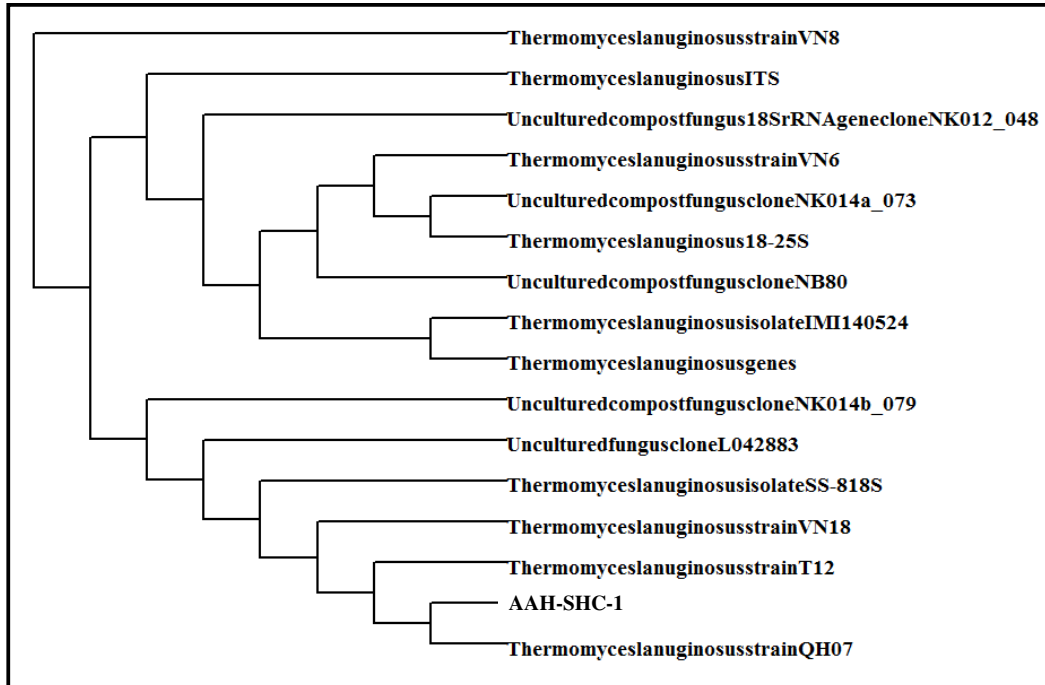
Fig 4: Phylogenetic relationships of selected members with fungus AAH-SHC-1.

Hits:

Sequences producing significant alignments:						
Accession	Description	Max score	Total score	Query coverage	E value	Max ident
GU441538.1	Thermomyces lanuginosus strain QH07 18S ribosomal RNA gene, part	1046	1046	99%	0.0	99%
AB085929.1	Thermomyces lanuginosus genes for 18S rRNA, ITS1, 5.8S rRNA, ITS	1046	1046	99%	0.0	99%
FJ548827.1	Thermomyces lanuginosus strain T12 18S ribosomal RNA gene, partia	1038	1038	99%	0.0	99%
EF550970.1	Thermomyces lanuginosus internal transcribed spacer 1, partial sequ	1037	1037	99%	0.0	99%

Clustal 2.1 multiple sequence alignment:

```
ITS1         ------------------------------------------------------------AAT  3
Thermomyces  TCCGTAGGTGAACCTGCGGAAGGATCATTACCGAGTGCGGGAACCCAGTCGGGTCCCAAT  60
                                                                        ***

ITS1         CTCCCACCCGTGTCTACCACACCTAGTGTTGCTTTGGCGGGCCCACTCCTCCGGTGTTCC  63
Thermomyces  CTCCCACCCGTGTCTACCACACCTAGTGTTGCTTTGGCGGGCCCACTCCTCCGGTGTTCC  120
             ************************************************************

ITS1         GCCGGGGGGGTCGTCCCGGGGCGCGGTGTGCCCCCGGGGCCCGTGCCCGCCAGAGGCACT  123
Thermomyces  GCCGGGGGGGTCGTCCCGGGGCGCGGTGTGCCCCCGGGGCCCGTGCCCGCCAGAGGCACT  180
             ************************************************************

ITS1         CACTGTGAACGCTTTTGTGAATGCGAGGATTGTCTGAGTGACGAAATGCAATCGTTCAAA  183
Thermomyces  CACTGTGAACGCTTTTGTGAATGCGAGGATTGTCTGAGTGACGAAATGCAATCGTTCAAA  240
             ************************************************************

ITS1         ACTTTCAACAATGGATCTCTTGGTTCCGGCATCGATGAAGAACGCAGCGAAATGCGATAA  243
Thermomyces  ACTTTCAACAATGGATCTCTTGGTTCCGGCATCGATGAAGAACGCAGCGAAATGCGATAA  300
             ************************************************************

ITS1         GTAATGTGAATTGCAGAATTCCGTGAATCATCGAATCTTTGAACGCACATTGCGCCCTCT  303
Thermomyces  GTAATGTGAATTGCAGAATTCCGTGAATCATCGAATCTTTGAACGCACATTGCGCCCTCT  360
             ************************************************************

ITS1         GGTATTCCGGGGGGCATGCCTGTCCGAGCGTCATTGCGAACCCTCAAGCACGGCTTGTGT  363
Thermomyces  GGTATTCCGGGGGGCATGCCTGTCCGAGCGTCATTGCGAACCCTCAAGCACGGCTTGTGT  420
             ************************************************************

ITS1         GTTGGGCCGCCGTCCCCTCGTTTGGAGGGGACGGGCCTGAAAGGCAGCGGCGGCGTCGCG  423
Thermomyces  GTTGGGCCGCCGTCCCCTCGTTTGGAGGGGACGGGCCTGAAAGGCAGCGGCGGCGTCGCG  480
             ************************************************************

ITS1         TCCGGTCCTCGAGCGTATGGGGCTCTGTCACGCGCTCAAGGAGGGGTCCGGCCGGGGCCA  483
Thermomyces  TCCGGTCCTCGAGCGTATGGGGCTCTGTCACGCGCTCAAGGAGGGGTCCGGCCGGGGCCA  540
             ************************************************************

ITS1         TAGCCTCTGAAGGTCAATTCTTCCAAGGTTGACCTCGGATCAGGTAGGAGTACCCGCTGA  543
Thermomyces  TAGCCTCTGAAGGTCAATTCTTCCAAGGTTGACCTCGGATCAGGTAGGAGTACCCGCTGA  600
             ************************************************************
```

Conclusion:

Morphology of the fungus AAH-SHC-1 obtained from self-heating compost which produced extracellular monodispersed nanoparticles mostly agrees with the description of Barron (22), Barnet and Hunter (23), Abbas *et.al* (24) and Eriksen *et.al* (25). The fungus AAH-SHC-1 is grown on alkaline MGYP medium and produces fast growing colonies. Colonies which initially appear off-white and felt-like, turned grey with time on the upper side of Petriplate. Subsequently the reverse side of colony turns brown and the agar substratum stains a deep brown or wine color. The vegetative mycelium is hyaline, septate, thin walled, highly branched and is differentiated into conidia on short lateral branches functioning as undistinguished conidiophores. Conidia are attached at bulging conidiogenous cells. Conidia produced were single, apically positioned, globose or subglobose, brown and 1-celled. Conidia are attached terminally on the conidiogenous cells (Fig 1). All the above mentioned characters are identical to those describe for the fungus *Thermomyces lanuginosus* (*Humicola lanuginosa*). Hence the fungus AAH-SHC-1 is referred to as *Thermomyces lanuginosus* (*Humicola lanuginosa*). The ITS sequence analysis and homology alignment of isolate AAH-SHC-1 using BLAST and Clustal-W programme respectively revealed similarity with genus *Thermomyces lanuginosus* (*Humicola lanuginosa*). The phylogenetic studies also indicate that the closest relative of the fungus AAH-SHC-1 is *Thermomyces lanuginosus.* Therefore, considering the cultural and morphological characters, we identified the fungus as *Thermomyces lanuginosus*. The sequence analysis and phylogenetic studies also support the identification. Although *Thermomyces lanuginosus* has wide spread occurrence in soils across India and different strain of *Thermomyces lanuginosus* have been isolated from self-heating compost and other substrates, no attempts have been made to synthesize inorganic nanomaterials from *Thermomyces lanuginosus*. The fungus *Thermomyces lanuginosus* (*Humicola lanuginosa),* which we have isolated, produces highly monodispersed gold and silver nanoparticles.

References:

1. Crous, P.W.; Braun, U.; Schubert, K.; Groenewald, J.Z. *Studies in Mycology*. **2007**, *58*, 33.

2. Sette, L.D.; Passarini, M.R.Z.; Delarmelina, C.; Salati, F.; Duarte, M.C.T. *World Journal of Microbiology and Biotechnology*. **2006**, *22*, 1185.

3. Zhang, Y., Fournier, J., Pointing, S.B and Hyde, K.D. *Fungal Diversity*. **2008**, *33*, 47.

4. Zhang, H.W.; Song, Y.C.; Tan, R.X. *Natural Product Reports*. **2006**, 23, 753.

5. Hyde, K.D.; Soytong, K. *Cryptogamie Mycologie*. **2007**, *28*, 281.

6. Santos, Z.C; Machado, P.; Branco, P.; Cadete, F. T.; Martins, A. R; José B.; Leal, P.; Dias, M.B. *Journal of Cell Science*. **2010**, *123*, 1414.

7. Lacap, D.C.; Hyde, K.D.; Liew, E.C.Y. *Fungal Diversity*. **2003**, *12*, 53.

8. Guo, L.D., Hyde, K.D. and Liew, E.C.Y. *New Phytologist*. **2000**, *147*, 617.

9. Maheshwari, R.; Bharadwaj, G.; Bhat, M.K. *Microbiol. Mol. Biol. Rev.* **2000**, *64 (3)*, 461.

10. Lee, S.B.; Taylor, J.W. Molec. *Biol. Evol*. **1992**, *9*, 636.

11. Zambino, P. J.; Szabo, L. J. *Mycologia*. **1993**, *85*,401.

12. Lee, S.B.; White, T.J.; Taylor, J.W. *Phytopathology*. **1993**, *83*, 177.

13. Lee, Y.M.; Choi, Y.K.; Min, B.R. *Mycobiology*. **2000**, *28*. 82.

14. Hawksworth, D.L. *Mycologist*. **1997**, *11,* 18.

15. Emerson, R. *Thermophiles. In: The Fungi - An Advanced Treatise* (Answorth, G.C. and Sussman, A.S (Eds.), Academic Press, London. **1968**, 105.

16. Cooney, D.G.; Emerson, R. *Thermophilic Fungi: An Account of their Biology, Activities and Classification*, Freeman, San Francisco, CA. **1964,** 80.

17. Ahmad, A.; Senapati, S.; Khan, M.I.; Kumar, R.; Sastry, M. *Langmuir*. **2003**, *19*, 3550.

18. Möller, E. M.; Bahnweg, G.; Sandermann, H.; Geiger, H. H. *Nucl. Acids Res.* **1992**, *20(22),* 6115.

19. Sanger, F.; Nicklen, S.; Coulson, A. R. *Proc Natl Acad Sci.* **1977**, *74(12)*, 5463.

20. Chenna, R.; Sugawara, H.; Koike, T.; Lopez, R.; Gibson, T.J.; Higgins, D.G.; Thompson, J.D. *Nucleic Acids Res.* **2003**, *31 (13),* 3497.

21. Tamura, K.; Dudley, J.; Nei, M.; Kumar, S. *Molecular Biology and Evolution.* **2007**, *24*, 1596.

22. Barron, G.L. *The genera of hyphomycetes from soil*. The Williams and Wilkins company, Baltimore. **1968**, Pp: 1-362.

23. Barnett, H.L. and Hunter, B.B. *Illustrated genera of Imperfecti fungi*. The American Phytopathological Society, U.S.A. **1998**, Pp: 1-218.

24. Abbas, S.Q.; Niaz, M.; Maan, A.; Iqbal, J.; Waqas, M.; Ahmed, H.; Liaqat, A.; Sidra **.** *Pak. J. Bot*. **2009**, *41(3),* 1429.

25. Eriksen, S.H.; Haasum, I.; Jensen, B.; Olsen, J. *FEMS Microbiology Letters*, **1992**, *93*, 279.

Part 2: Biological synthesis of gold and silver nanoparticles using fungus

Summary:

Nanomaterial synthesis using biological routes occurs at ambient conditions; therefore, focus has shifted toward biological routes as compared to chemical and physical methods which are currently available and extensively used for nanosynthesis. Biosynthesis of metal nanoparticles viz. gold and silver by *Humicola lanuginosa* was demonstrated when exposed to $HAuCl_4$ and $AgNO_3$ solutions respectively. The biogenic nanoparticles synthesized were characterized by UV, TEM, XRD, XPS, EDAX and FTIR. The fungus reduces the respective solution and leads to the formation of extracellular nanoparticles of spherical morphology with good dispersity. Cell viability assay was carried out on NIH3T3 mouse embryonic fibroblast cell line and MDA-MB-231 human breast carcinoma cell line. Biodistribution studies were also carried out by radiolabelling gold nanoparticles with Technetium-99m (Tc-99m). Conjugation of gold nanoparticles with anticancer drug doxorubicin was carried out for drug delivery applications.

Introduction:

Materials at nanoscale exhibit novel properties different from their bulk counterparts. The properties include chemical, physical, optical, electronic and magnetic. These unique properties are significantly dependent on the particle size and shape. Biosynthesis occurs at ambient reaction conditions and therefore attracts increasing attention as a novel synthesizing platform. Bacteria (1), actinomycetes (2), fungus (3) and even higher plants (4) have been employed for the production of nanomaterials. The creative use of magnetotactic bacteria (which synthesize magnetite nanoparticles) (5), diatoms (siliceous materials) (6) and S-layer bacteria (gypsum and calcium carbonate layers) (7) are some of the well known examples used for the nanoscale biosynthesis.

The bacteria, *Pseudomonas stutzeri* AG256 isolated from silver mines has been reported for the production of silver nanoparticles (8). Nair and Pradeep reported the formation of gold, silver and gold-silver alloy nanoparticles with well defined morphology by *Lactobacillus* strain found in buttermilk (9). Besides bacteria-mediated biosynthesis, eukaryotic organisms such as fungi are also a good choice for the production of nanomaterials as they secrete more enzymes when compared to bacteria and are easier to handle and grow on simple media. However, a novel bio-inspired process has been reported for the intra and extra-cellular synthesis of nanoparticles using the fungi, *Verticillium* sp. and *Fusarium oxysporum* respectively. These entrapped nanoparticles are produced in solution and may have the exciting possibility for industrial applications.

The fungus *Verticillium* sp. is found to produce gold nanoparticles with fairly well defined morphology and good dispersity (10). These results suggest that the trapping of $AuCl_4^-$ ions on the surface of fungal cells is due to the enzymes with positive charge groups. Although the fungal production of nanoparticles is higher as compared to bacterial synthesis, it might be so due to large amount of enzyme secretion from fungi. When incubated with Ag^+ ions, the fungus *Verticillium* sp. has shown the capability to produce silver nanoparticles (3).

Fusarium oxysporum, specific for NADH-dependent reductase, was successfully used for the reduction of $AuCl_4^-$ ions to gold nanoparticles. It has opened up exciting possibilities for novel fungal-enzyme based approach for nanoparticle synthesis (11). It was also used for the synthesis of stable silver hydrosol (12) and technologically important CdS nanoparticles (13). By controlling the amount of cofactor NADH,

synthesis of stable Au-Ag alloy nanoparticles has been achieved. This approach can be further employed for producing nanoparticles with different chemical compositions (14).

However, it is remarkable research toward elucidating the mechanism or the feasible conditions for the production of nanoparticles with desirable features. *Thermomonospora* sp. an extremophilic actinomycetes, when reacted with gold ions, resulted in efficient synthesis of monodispersed gold nanoparticles, extracellularly (2). It is believed that the reduction of metal ions and stabilization of nanoparticles occurs by an enzymatic process. This monodispersed synthesis of gold nanoparticles could be due to extremes of the conditions such as alkaline pH and slightly elevated temperature as compared to polydispersed gold nanoparticle synthesis by *Fusarium oxysporum*. Alkalotolerant *Rhodococcus* sp. has been reported for intracellular synthesis of good quality monodispersed gold nanoparticles (15). These extracellular nanoparticles were stabilized by the enzymes and reducing agents secreted by the fungi in the reaction mixture. Previous reports suggest that the fungal strain produces four high molecular weight proteins which are found associated with the nanoparticles. Out of these, one strain is found to be NADH-dependent reductase. An endophytic fungus, *Colletotrichum* sp. growing in the leaves of geranium was found to produce stable gold nanoparticles with variable morphology (16). Zirconia nanoparticles are also produced by the use of fungus *Fusarium oxysporum*, and the fungus is also having the capability of hydrolyzing aqueous ZrF_6^{2-} ions extracellularly (17). It is believed that the fungus secretes the protein similar in nature to silicatein, thus resulting in the formation of zirconia nanoparticles. In the biosynthesis of nanoparticles, the fungal growth plays an important parameter. *Trichothecium* sp. when grown under stationary conditions and reacted with gold ions produces extracellular gold nanoparticles, while under shaking conditions results in intracellular gold nanoparticle formation. There is a possibility that some sorts of enzymes or proteins are responsible for the synthesis. The fungus secretes the enzyme or protein under stationary conditions into the reaction mixture but not in shaking conditions (18). For the elucidation of the mechanism for nanobiosynthesis, α-NADPH-dependent sulfite reductase, nitrate reductase and phytochelatin isolated from *Fusarium oxysporum* has been used for *in vitro* gold and silver nanoparticle production respectively (19, 20).

Apart from microbes, biosynthesis of nanoparticles can also be possible using plants such as *Alfalfa* (21), Geranium (*Pelargonium graveolens*) (22), lemongrass plant (*Cymbopogon flexuosus*) (23) extracts, *Azadirachta indica* (24), *Emblica officinalis* (25), *Aloe vera* (26), *Cinnamomum camphora* plant extracts, sugar beet pulp, memecylon edule leaf extract and leaf extract of ginger (*Zingiber officinale*) (27).

Moreover, bio-based approaches have also been successfully achieved for the synthesis of nanomaterials of different chemical compositions. To control the shape and size of the synthesized nanoparticle is of great importance. There is growing need for the development of protocol for the synthesis of nanomaterials with desired features (in terms of size, shape and dispersity). Recently, lemongrass (*Cymbopogon flexuosus*) plant extracts have been exploited for the size and shape controlled biosynthesis of gold nanotriangles. Nanotriangle morphology could be controlled by halide ions.

Improvement in dispersity of gold nanoparticles has been achieved by *Thermomonospora* sp. as compared to *Fusarium oxysporum*, due to the alkaline pH and elevated temperature of the reaction medium. On the other hand, the size, shape and yield of biosynthesized nanoparticles significantly depend on the physiological parameters and are remarkably affected by the growth conditions which include temperature and environment of inorganic ions of the live organism. For example, biosynthesis yields of cadmium sulfide (CdS) nanocrystals increased about 20-fold in *Escherichia coli* cells grown to stationary phase as compared to late logarithmic phase. The use of live fungi for the size and shape control biosynthesis of nanoparticles is so far an unexplored and underexploited area of current research and would be of great prominence for a variety of applications.

The availability of nanoparticles with controlled optical and electrical properties has sparked widespread interest in their biologically relevant applications such as luminescent tagging and imaging, medical diagnostics, drug delivery and implantable nanoelectronics (28, 29). A number of templates have been used for enzyme immobilizations such as silica nanotubes (30), phospholipid bilayers (31, 32), self assembled monolayers (33, 34), etc. There are several reports on metal nanoparticle-enzyme conjugates which include the formation and enzyme activity of nanoparticles complexed with horse radish peroxidase (35), xanthine oxidase (36), glucose oxidase and carbonic anhydrase (37). Functionalized γ-Fe_2O_3 magnetic nanoparticles (38)

have been used for the support of the enzyme lipase. Conjugation of pepsin (39) and fungal protease (40) with nanoparticles has also been reported.

At the National Chemical Laboratory, Pune, our group has reported the conjugation of *in vitro* synthesized CdS nanoparticles to jacalin and chickpea lectin with 1-Ethyl-3-(3-methyl amino propyl)-carbodiimide (EDC) (41). Hrushikesh *et. al.* (42) reported the binding of the hormone insulin to gold nanoparticles and its application in transmucosal delivery for the therapeutic treatment of Diabetes mellitus. Conjugates of gold nanoparticles to doxorubicin have been reported (43).

Gold and magnetite nanoparticles are the most commonly used nanoparticles for hyperthermia and drug delivery. The unique chemical properties of colloidal gold make it a promising agent in targeted delivery approach for drugs or genes to specific cells. The physical and chemical properties of colloidal gold permit more than one protein molecule to bind to a single particle of colloidal gold. Tumor necrosis factor (TNF) can be bound to gold nanocrystals and delivered safely and effectively to tumor-burdened mice and dogs (44). This will form the basis of a new formulation of the potent anticancer drug TNF-α, which destroys tumors but is also very toxic to healthy tissues. By coupling TNF-α to colloidal gold, this will become a safe as well as an effective anticancer therapy.

Gold and silica composite nanoparticles have been investigated as nanobullets for cancer. Gold atoms bind to silicone atoms and serve as a seed for the growth of aluminium islands. The large electron affinity toward gold causes a significant change in the electronic structure of silica resulting in a substantial reduction in the highest occupied and lowest unoccupied molecular orbital and the optical gap, thus allowing it to absorb near IR radiations. This suggests that a small cluster can have a similar effect in the treatment of cancer as the large sized nanoshell but with a different mechanism (45). Carbon magnetic nanoparticles (CMNP) are composed of spherical particles 40-50 nm in diameter, with iron/ iron oxide particles dispersed in carbon-based host-structure (46). Free doxorubicin (DOX) molecules are immobilized onto the surfaces of activated CMNP particles to form CMNP-DOX conjugates. The *in vitro* antiproliferative activity of immobilized doxorubicin in the conjugates has been demonstrated in tumor cell toxicity assay. It is suggested that this CMNP-DOX system can be used for targeted drug delivery system in cancer. The use of magnetic nanoparticles for the delivery of chemotherapeutics has evolved since the 1970's. Zimmerman and Pilwat in 1976 used magnetic erythrocytes for the delivery of

cytotoxic drugs (47). In 1980's, several authors developed this strategy to deliver different drugs using magnetic microcapsules and spheres (48-51).

Hepatic cancer is the most prevalent primary cancer of the liver. Doxorubicin (DOX) is an anthracycline antibiotic which is one of the most widely used anticancer agents for the treatment of hepatic cancer (52). However, problems related to the development of multidrug resistance and acute cardiotoxicity have led the scientists to investigate alternative forms of administering DOX for the treatment of cancer. High hepatocellular uptake of DOX coupled with low systemic exposure remains the key issue in successful therapy. Free DOX (positively charged) enters the tumor cells by diffusion but is effluxed by P-glycoprotein receptors present on the tumor cell surface resulting in minimal intracellular concentrations of DOX (52,53). DOX loaded nanoparticles showed improvement of DOX concentrations in tumor cells as compared to free DOX and also revealed improvement in multiple drug resistance (54). Another severe problem with DOX therapy is its fatal normal tissue toxicity. DOX shows severe cardio-toxicity along with renal-toxicity with myelosuppression (55). Asialoglycoprotein receptors are present in abundance in liver and more importantly, known to be over expressed in hepatic cancer. Pullulan is known to have specific affinity for the asialoglycoprotein receptors. Pullulan has been used in liver targeted drug delivery system by covalent coupling with polymer/drug (52, 56).

Monoclonal antibody based therapeutics have been investigated in various experiments for targeting hepatic cells and growth factors on tumor vasculatures (57). The results of these experiments have been promising and have showed that antibody based therapeutics are efficient in delivering the cancer drugs to the desired site of action thus reducing systemic toxicity. Liposomes, nanoparticles, HEMA(N-2-hydroxypropyl) methylacryl amide)-DOX conjugate (58) and dendrimers were found to be clinically useful in the case of passive targeting of hepatic cancer. Use of ligand targeted therapeutics for treatment of hepatic cancer is also reported. This strategy utilizes targeting to specific tumor factors, receptors or protein over express on the cancerous cells thereby increasing the exposure of malignant cells.

In the present work, the fungus *Humicola lanuginosa* was used for the first time in the synthesis of gold and silver nanoparticles. Biodistribution studies of the gold nanoparticles were conducted and these gold nanoparticles were then conjugated with anticancer drug doxorubicin.

Materials and Methods:

Materials:

Chloroauric acid ($HAuCl_4$) and silver nitrate ($AgNO_3$) were obtained from Sigma Aldrich, malt extract, yeast extract, glucose and peptone were obtained from HiMedia and used as-received.

Fungal growth and maintenance:

The fungus *Humicola lanuginosa* was isolated from self-heating compost obtained from Pune district in Maharashtra, India. It was maintained on MGYP [malt extract (0.3%), glucose (1%), yeast extract (0.3%), and peptone (0.5%)] agar slants. Stock cultures were maintained by sub-culturing at monthly intervals. After growing the fungus at pH 9 and 50^0C for 4 days, the slants were preserved at 15^0C. From an actively growing stock culture, subcultures were made on fresh slants and after 4 days of incubation at pH 9 and 50^0C, the same were used as the starting material for biosynthesis of gold nanoparticles.

Extracellular biosynthesis of gold and silver nanoparticles by *Humicola lanuginosa*:

For the biosynthesis of gold and silver nanoparticles, the fungus was grown in 250 mL Erlenmeyer flasks containing 100 mL of MGYP medium. Sterile 10% sodium carbonate was used to adjust the pH of the medium to 9. After the pH of the medium was adjusted, the culture was grown with continuous shaking on a rotary shaker (200 rpm) at 50^0C for 96 hr. After 96 hr of fermentation, mycelia were separated from the culture broth by centrifugation (5000 rpm) at 20^0C for 20 min and then the mycelia were washed thrice with sterile distilled water under sterile conditions. The harvested mycelial mass (20 g of wet mycelia) was then resuspended in 100 mL of aqueous solution of 1mM $HAuCl_4$ (for gold nanoparticles) and 1 mM $AgNO_3$ (for silver nanoparticles) solutions in 250 mL Erlenmeyer flasks and the same was put onto a shaker at 50^0C (200 rpm). The reaction was carried out for a period of 96 hr and fungal biomass was separated by filter-paper to collect biomass and filtrate in sterile conditions. Periodically, aliquots of the reaction solution were removed and subjected to UV-Vis spectroscopy to check the formation of nanoparticles extracellularly.

Characterization of biosynthesized gold and silver nanoparticles:

The optical properties of metal nanoparticles were examined by using UV-Vis spectroscopy. The measurements were performed on a Shimadzu dual-beam spectrophotometer (model UV-1601 PC) operated at a resolution of 1 nm. The nanoparticles were also characterized by using Transmission Electron Microscopy (TEM) and X-ray Diffraction (XRD) measurements. The biosynthesized nanoparticles solution was drop cast on a carbon coated copper grid and analyzed using JEOL 1200EX instrument operated at a voltage of 80 kV. The Selected Area Electron Diffraction (SAED) analysis was carried out on the same grid. HRTEM images were scanned on FEI Technai G2 system operated at an accelerating voltage of 300 kV at room temperature. The XRD patterns were obtained on a Philips PW 1830 instrument operating at 40 kV and at a current of 30 mA with Cu K_α radiation (λ = 1.5404 Å). X-ray photoelectron spectra were recorded on VG MicroTech ESCA 3000 instrument. FTIR spectra of metal nanoparticle solution was recorded on Perkin Elmer spectrum one B in diffuse reflectance (DRS) mode at a resolution of 2 cm^{-1}. Energy Dispersive Analysis of X-ray (EDAX) analysis was carried out on a Leica Stereoscan-440 SEM equipped with a Phoenix EDAX attachment. EDAX spectra were recorded in the spot-profile mode by focusing the electron beam onto a region on the surface coated with nanoparticles.

Cell Viability Assay:

The effect of nanoparticles on the proliferation of NIH3T3 mouse embryonic fibroblast cell line and MDA-MB-231 human breast carcinoma cell line was assessed by MTT [3-(4,5-Dimethylthiazol-2-yl)-2,5-diphenyltetrazolium bromide] assay. Briefly, the cells ($2x10^4$ for NIH3T3 and $1x10^5$ for MDA-MB-231) grown in 96-well plates were treated with varying concentrations of nanoparticles (0-1000 µg/ml) for 24 hr at 37^0C. The cells were further incubated with MTT (0.5 mg/ml) at 37^0C for 3 hr followed by addition of 200 µl of isopropanol. The color intensity was measured at 570 nm using an enzyme linked immunosorbent assay (ELISA) reader. The experiments were performed in triplicates. The cell viability was plotted as percent of control (59).

Radiolabelling and biodistribution studies:

a) Radiolabelling of gold nanoparticles with Tc-99m:

Tc99m-gold nanoparticles were prepared by dissolving 10 mg of gold nanoparticles in 1 ml of distilled water followed by the addition of 100 µg of $SnCl_2.2H_2O$ and the pH was adjusted to 6.5. Approximately Tc-99m (2mCi) was added to the content, mixed and incubated for 10-15min. The percent radiolabel was determined by using instant thin layer chromatography (ITLC) method (60).

b) Radiochemical purity (RCP):

The radiochemical purity of Tc-99m with gold nanoparticle was estimated by instant thin layer chromatography (ITLC) using silica gel coated fibre sheets. ITLC was performed using 100% acetone and 0.9% saline as the mobile phase. A measured amount of 2-3 µl of the radiolabelled complex was applied at a point 1 cm from one end of an ITLC-SG strip and allowed to run for approximately 10 cm. Amount of reduced/hydrolyzed Tc-99m was determined using pyridine: acetic acid: water (3:5:1.5 v/v) as mobile phase and ITLC as the stationary phase and the radioactivity distribution over the strip was determined with a well counter (ECIL). Radiochemical purity (RCP) was calculated as the fraction of radioactivity that remained at the origin and was designated as percent (%) RCP.

c) Biodistribution of radiolabelled nanoparticles:

Male Sprauge Dawley rat weighing (180-220 gm) was selected for evaluating the localization of the labelled complex. Tc99m-gold nanoparticles of 14.8 MBq (400uCi) were administered through the penile vein of rat. The biodistribution studies of labelled gold nanoparticles were evaluated after 45 min post injection.

Conjugation of anticancer drug doxorubicin with gold nanoparticles:

Biosynthesized gold nanoparticles were conjugated with anticancer drug doxorubicin. As mentioned earlier, biosynthesized nanomaterials are capped by a protein layer secreted by the fungus in the reaction mixture during the process of biosynthesis. Free amino as well as carboxylic groups are present in the capped protein layer. The free carboxyl group present on these proteins was targeted to couple with the free amino

group present on the doxorubicin. Carboxyl group on the nanoparticles surface was estimated as described by Ansary *et. al.* 2007 (41).

The gold nanoparticles were conjugated to doxorubicin, with free carboxyl by using the activator 1-Ethyl-3- (3-dimethylaminopropyl)-carbodiimide (EDC). The coupling reaction was carried out in a 5 ml reaction volume, of 50 mM MES/HEPES buffer containing 250 µg of gold nanoparticles and 250 µg of doxorubicin was added to 5 mM of EDC. Conjugation was performed at 30^0C. After stirring for 12 h at room temperature, the reaction mixture was concentrated under high vacuum and further purification of the doxorubicin-gold conjugate was done by HPLC (Waters) using C_{18} symmetry reverse phase column and gradient elution was carried out using Acetonitrile : Water (5% : 95%). At a flow rate of 0.5 ml/min. A dual wavelength recorder set at 253nm and 530nm was used to detect the doxorubicin and gold nanoparticles respectively from the column. Fluorescence measurements were carried out using a Perkin Elmer LS-50B spectrofluorimeter.

Results and Discussion:

Biological synthesis of gold nanoparticles by *Humicola lanuginosa*

The fungus, *Humicola lanuginosa* when incubated with aqueous solution of 1mM HAuCl$_4$ at temperature 50^0C and pH 9 for 96 hr under shaking condition on a rotary shaker (200 rpm) resulted in the production of extracellular monodispersed, stable and water dispersible gold nanoparticles.
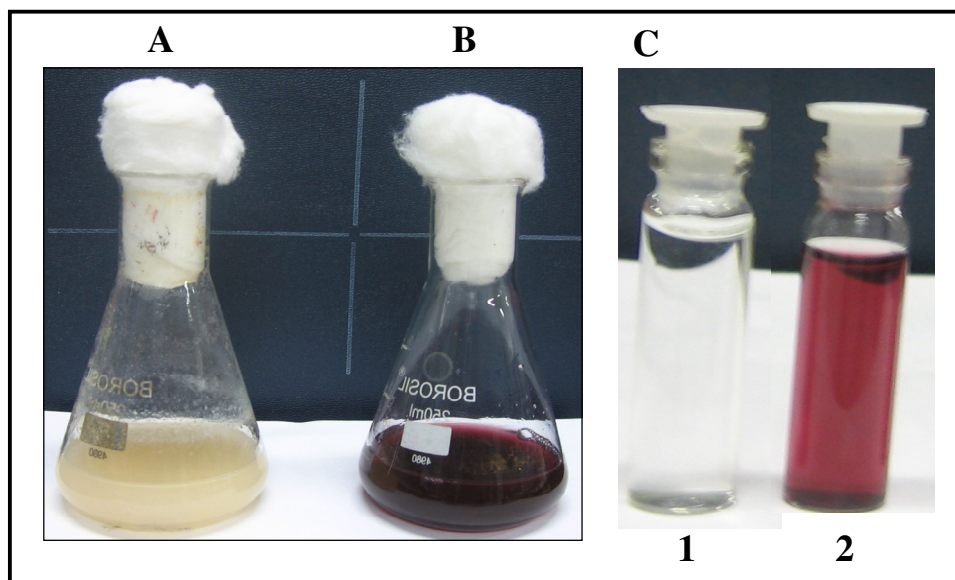
Fig 1: Conical flasks with fungus *Humicola lanuginosa* before (A) and after (B) exposure to HAuCl$_4$ ion for 96 hr. (C). Filtrate of the control flask (1) and filtrate of treated flask (2).

Figure 1 shows two conical flasks with the *Humicola lanuginosa* fungal biomass before (A, conical flask on the left side) and after (B, conical flask on the right side) exposure to 1 mM HAuCl$_4$ solution at 50^0C for 96 hr. The change in the color from pale yellow to vivid ruby red after incubation with fungus could clearly be seen in Figure 1(B), which demonstrates the formation of Au nanoparticles by the fungal biomass. The color ruby red appears due to excitation of the surface plasmon resonance, of Au nanoparticles (61). By simple filtration of the reaction mixture we have established the extracellular nature of the gold nanoparticles (Fig 1 C).

UV-Vis spectroscopy of gold nanoparticles:

Biosynthesis of gold nanoparticles was monitored by the UV-Vis spectroscopy. After the $HAuCl_4$ solution reacted with the fungus *Humicola lanuginosa*, it was observed that the surface plasmon band that occurs at ~530 nm, corresponds to the surface plasmon resonance of gold nanoparticles (11, 61). These gold nanoparticles were separated from the fungal biomass by filtration after completion of the reaction. The biomass upon filtration was found to be colorless, indicating that the reduction of the gold ions took place extracellularly. It was observed that these gold nanoparticles were stable toward aggregation. These nanoparticles are thus stabilized in solution by capping agent that is secreted by the fungus which is likely to be a protein or set of proteins. An absorption band centered at 270 nm which can be attributed to the presence of protein secreted by the fungus in the reaction mixture, can be clearly seen in the UV-Vis spectrum of the biosynthesized gold nanoparticles.
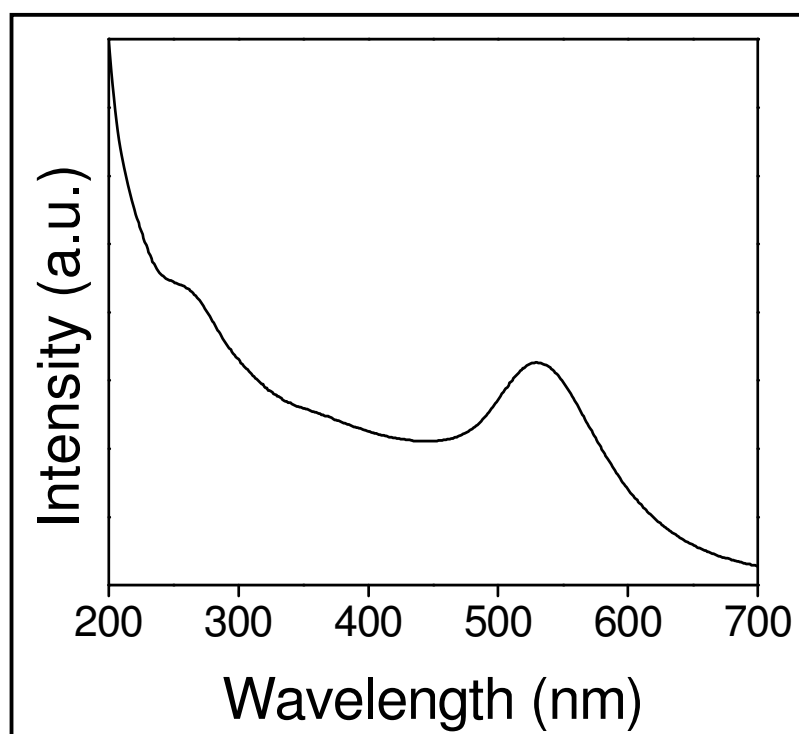
Fig 2: UV-Vis spectra recorded for the gold nanoparticles.

Transmission Electron Microscopy of gold nanoparticles:

Morphology and size distribution profile of the biosynthesized nanoparticles was obtained by TEM analysis. These gold nanoparticles are monodispersed, sized in between 18-24 nm with average size approximately 20 nm (Fig 3 D). These particles are very well dispersed in solution, which is due to the capping agent likely to be a protein secreted by the fungus which also prevents their aggregation. Fig. 3. B shows the Selected Area Electron Diffraction (SAED) pattern obtained from gold nanoparticles shown in Fig 3 A. The Scherrer ring pattern characteristic of face centered cubic (fcc), gold is clearly observed, showing that the structures seen in TEM images are nanocrystalline in nature. The HRTEM micrograph showed that interplaner distance is 2.35 A, which exactly matches with the (111) plane of the gold nanoparticles.
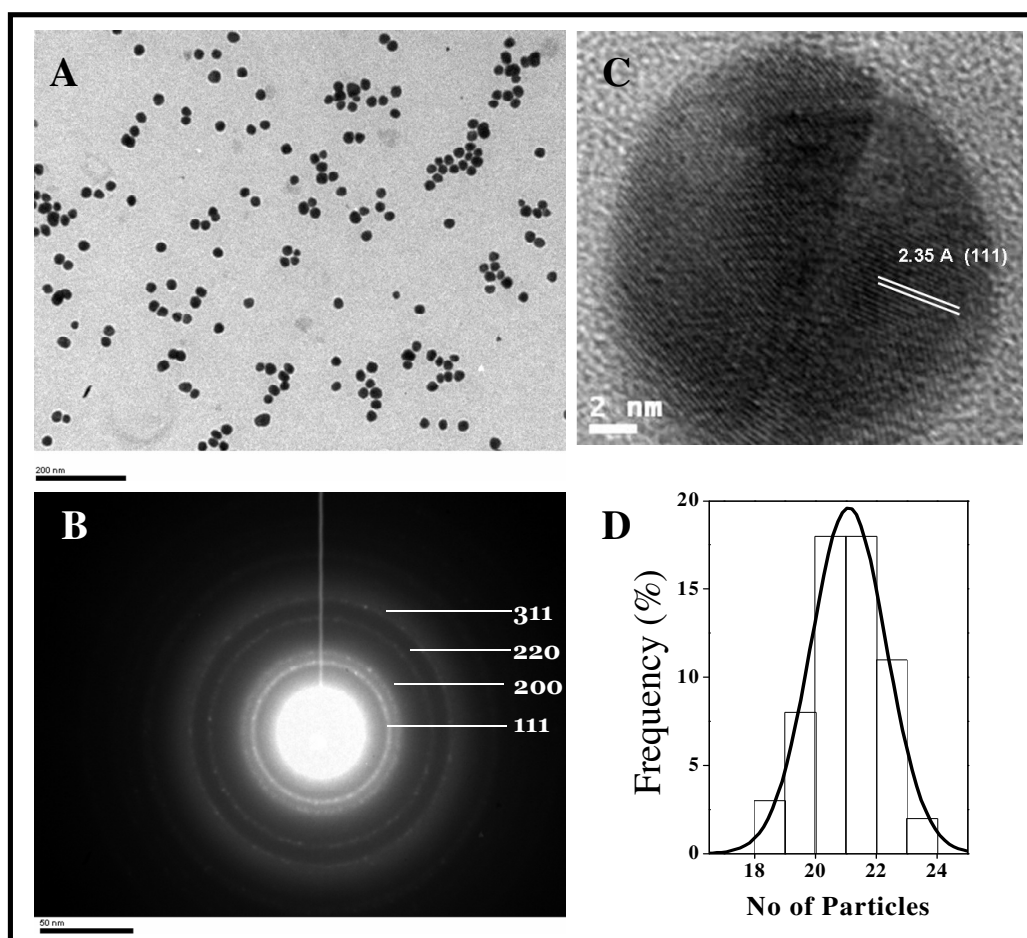
Fig 3. A). TEM micrograph recorded for gold nanoparticles. B). Selected area diffraction pattern recorded from extracellular gold nanoparticles shown in Fig 3.A. C). HRTEM micrograph. D). Particle size distribution histogram. The solid line is a Gaussian fit to the histogram.

X-ray Diffraction analysis of gold nanoparticles:

XRD analysis can provide information of the crystalline nature of the nanoparticles. The presence of four prominent Bragg's reflection corresponding to the (111), (200), (220) and (311) orientations agree with those reported for gold nanoparticles (15). These reflections are broad which indicates that the formed particles are in the nanoscale dimension.
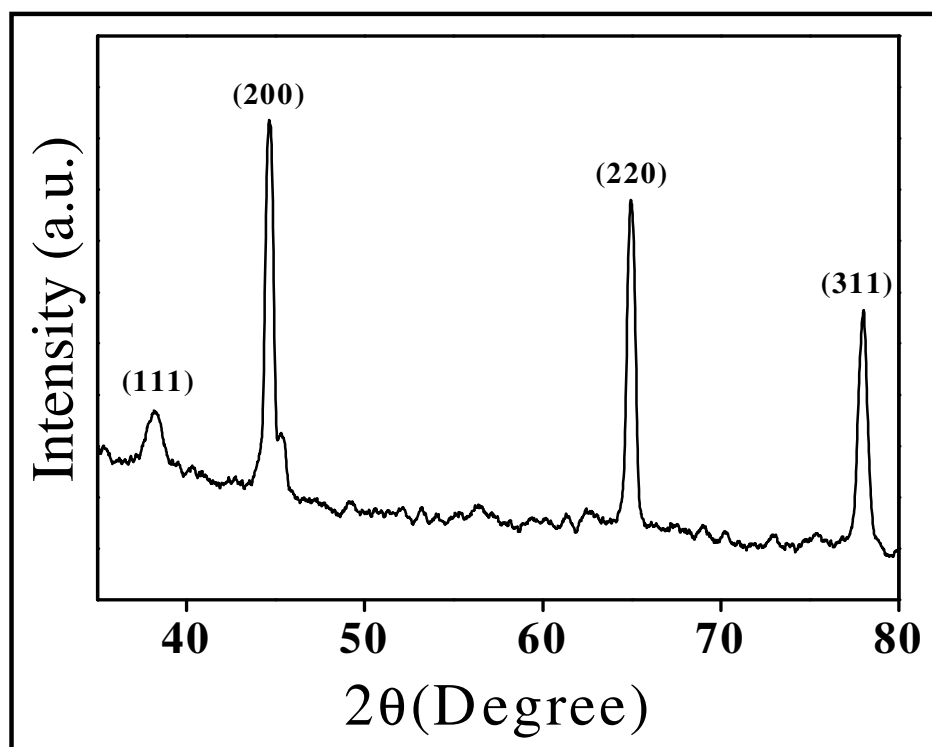
Fig 4: XRD pattern recorded for gold nanoparticles.

X-ray photoelectron spectroscopy of gold nanoparticles:

The presence of gold nanoparticles was also confirmed by analyzing the sample by XPS is shown in Fig 5. The results showed in Fig 5 confirm the presence of Au, C, O, N as the prominent elements. Peaks corresponding to C 1s core levels (Fig 5 A) appear from the proteins with binding energies (BE) 283, 285 and 286 eV. The peaks in (Fig 5 B and C) corresponds to chemically distinct N 1s and O 1s core levels with binding energies 400 eV and 531.5 eV respectively. The Au 4f spectrum could be resolved into two peaks (Au $4f_{7/2}$ and $4f_{5/2}$) due to the spin-orbit coupling with binding energy of 84.2 and 87.6 eV respectively. These binding energies are characteristic of metallic gold (Fig 5 D) and agree with those reported for gold nanoparticles (19).
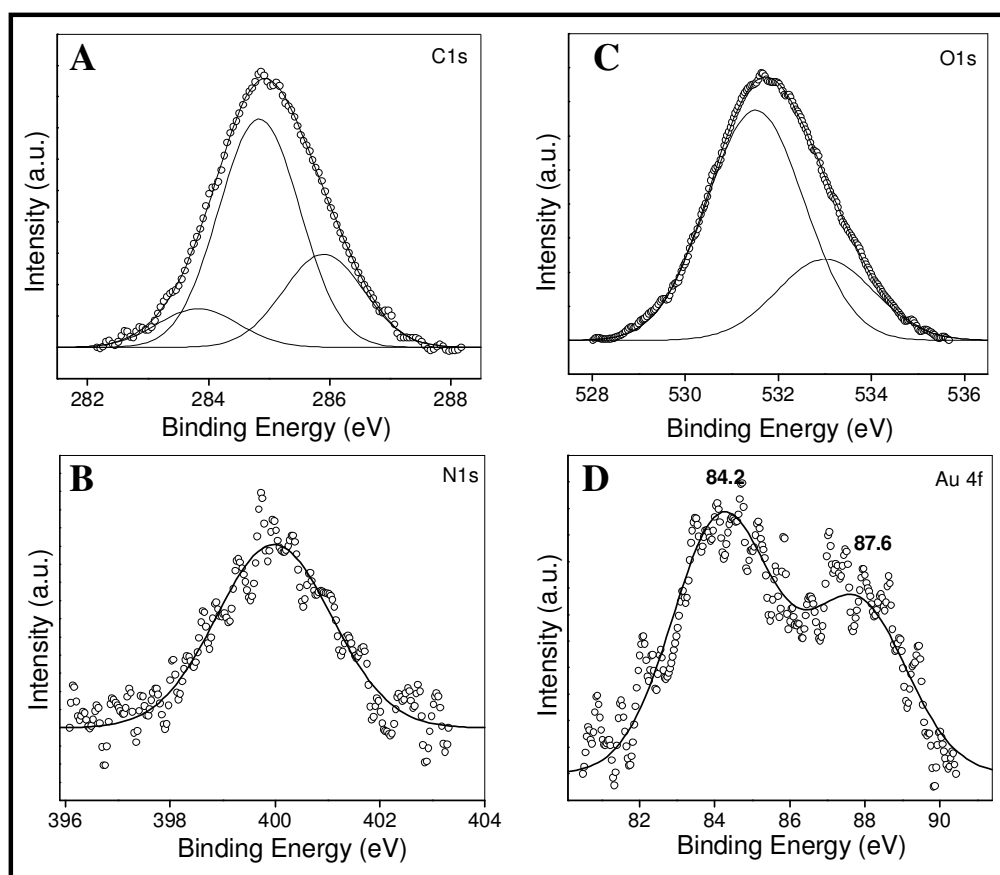
Fig. 5: X-ray photoelectron spectrum of gold nanoparticles.

Fourier transform infrared spectroscopy of gold nanoparticles:

FTIR spectrum recorded for the biosynthesized gold nanoparticles shows the presence of two bands at 1654 and 1541 cm^{-1} as seen in the Fig 6. The band at 1654 and 1541 cm^{-1} may be assigned to the amide I and II bands of proteins respectively (2). Moreover, there is a possibility of stabilization of the gold nanoparticles by surface binding protein either by free amino group or by cysteine residues present in the protein.
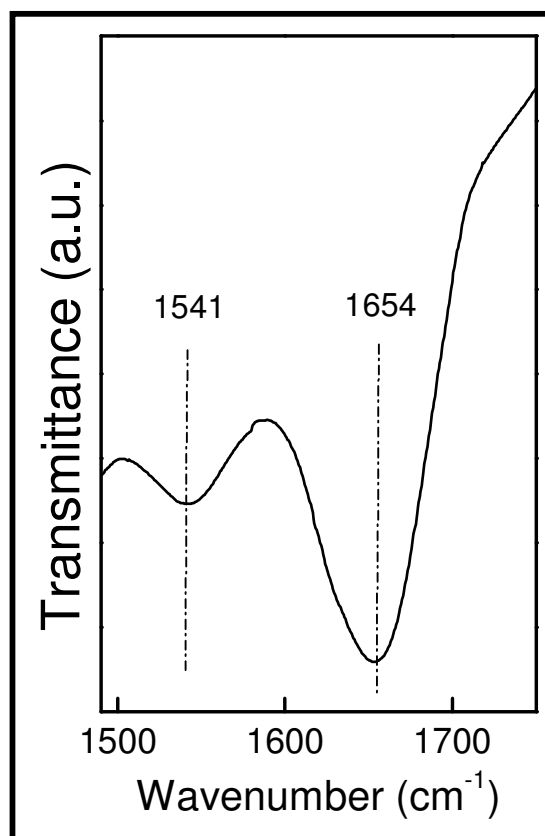
Fig 6: FTIR spectrum of gold nanoparticles.

Energy Dispersive Analysis of X-ray (EDAX) of gold nanoparticles:

EDAX spectrum is recorded in the spot profile mode from one of the densely populated gold nanoparticles. Signals are observed from Au, together with C, O and Si. Presence of gold was confirmed by two peaks which appear to be at 2.15 and 9.70 keV. The C and O signals are likely to be due to X-ray emission from proteins or enzymes present on the biosynthesized nanoparticle surfaces. The Si signal likely appears due to X-ray emission from the glass substrate used for EDAX analysis.
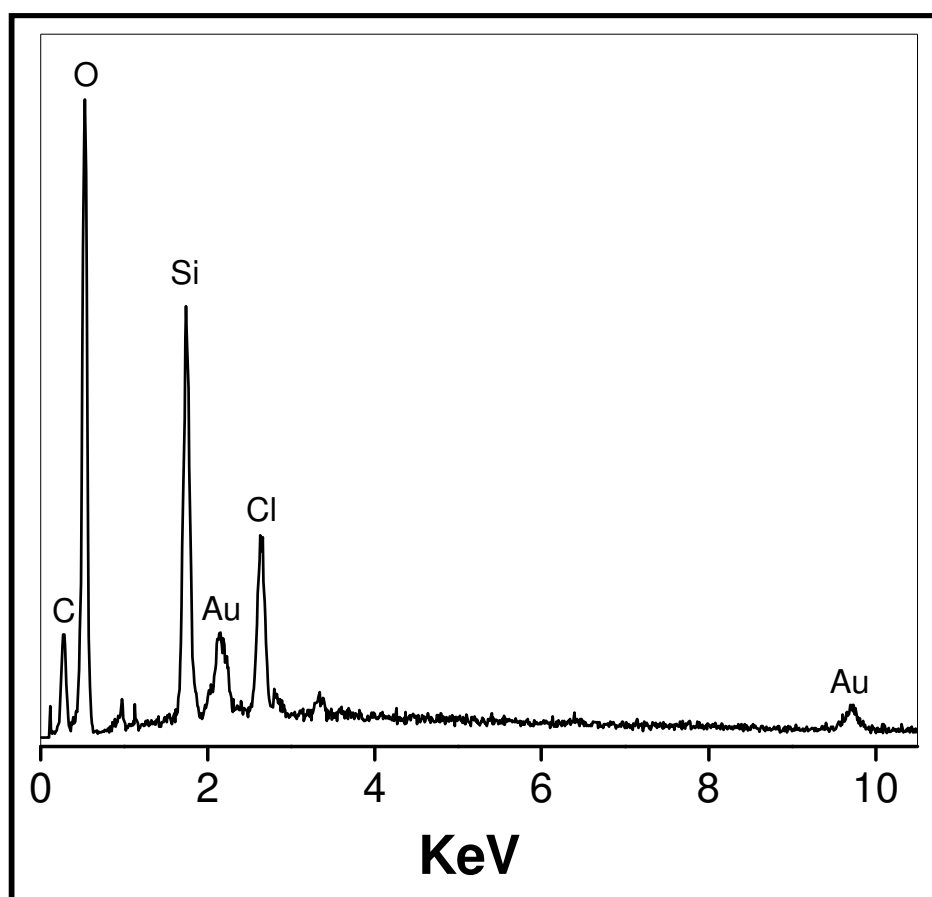
Fig 7: EDAX analysis of gold nanoparticles.

Cell viability assay of gold nanoparticles:

The effect of Au nanoparticles on the cell viability of NIH3T3 mouse embryonic fibroblast cell line and MDA-MB-231 human breast carcinoma cell line was checked by MTT assay. The cells were treated with varying concentrations of Au nanoparticles (50µg/ml, 250µg/ml, 5000µg/ml and 1000µg/ml) for 24 hr. There is no significant difference on cell viability at concentration of 50µg/ml. The cell viability was reduced in a dose-dependent manner in both the cell lines and the significant cytotoxicity of the nanoparticle was observed from concentrations of 250µg/ml for both the cell lines. The cell viability was reduced by 52% in case of NIH3T3 and 71.17% for MDA-MB-231 cell line at 1000µg/ml concentration.
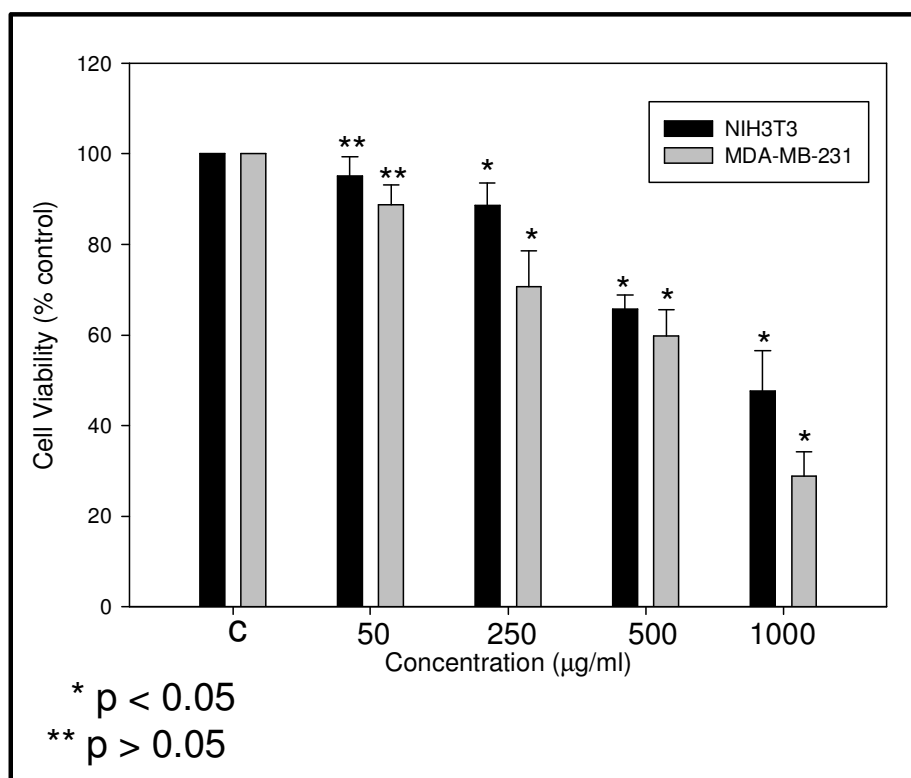
Fig 8: Cell viability assay of gold nanoparticles against NIH3T3 mouse embryonic fibroblast cell line and MDA-MB-231 human breast carcinoma cell line. The data represented in the form of a bar graph and plotted using means + S.E. of triplicate determinations. The values were analyzed by Student's *t*-test (p < 0.005). Statistical analysis, P values for significantly different means, *P< 0.005 and **P> 0.05 vs control.

Radiolabelling and biodistribution studies:

a) Complex formation study:

On the basis of chromatographic analysis, the radiolabelling efficiency was found to be more than 99% consistently. The optimal labelling efficiency was obtained with 100 µg of stannous chloride (the concentration of $SnCl_2.2H_2O$ was varied from 50-100 µg) and at pH 6.5.

b) Biodistribution and gamma scintigraphic imaging of Tc99m-gold nanoparticles:

Localization and biodistribution study of Tc99m-gold nanoparticle in normal healthy rat over time was determined by gamma camera imaging, as shown in Figure 9. The study clearly indicates the biodistribution of the complex (Tc99m-gold nanoparticle) in above mentioned rat. These gold nanoparticles reach out to the liver, heart, kidneys and pass out through the urine within 45 minutes.
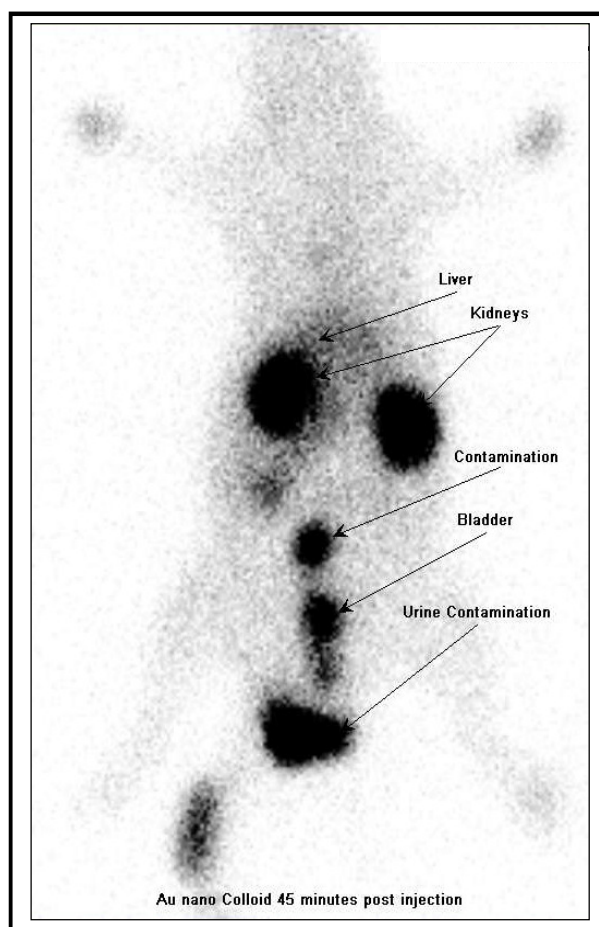
Fig 9: Gamma scintigraphic image showing biodistribution of biosynthesized gold nanoparticles in rat.

Conjugation of gold nanoparticles with anticancer drug doxorubicin:

The HPLC profile showed distinct peaks at 253 nm and at 530 nm (Fig 10). The peak having maximum absorbance at 253 nm and 530 nm was collected and further purified by HPLC (Fig 11).
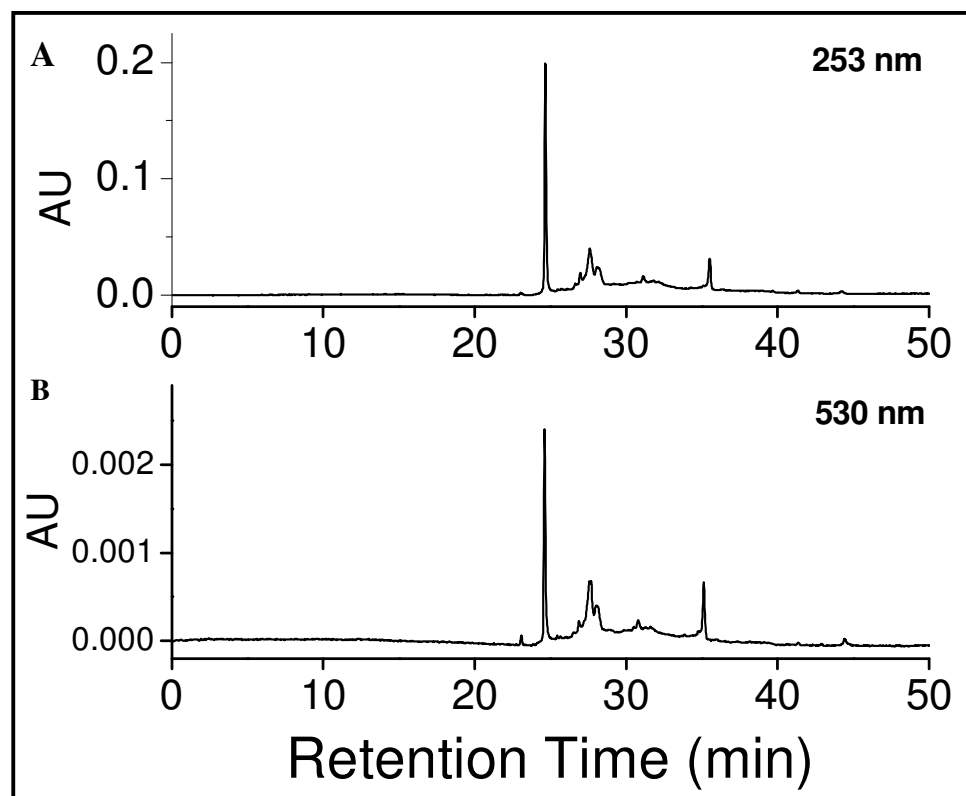
Fig 10: HPLC profile of the crude (gold nanoparticles-doxorubicin conjugate) at two different wavelengths A) 253 nm for doxorubicin detection and B) 530 nm to detect gold nanoparticles.
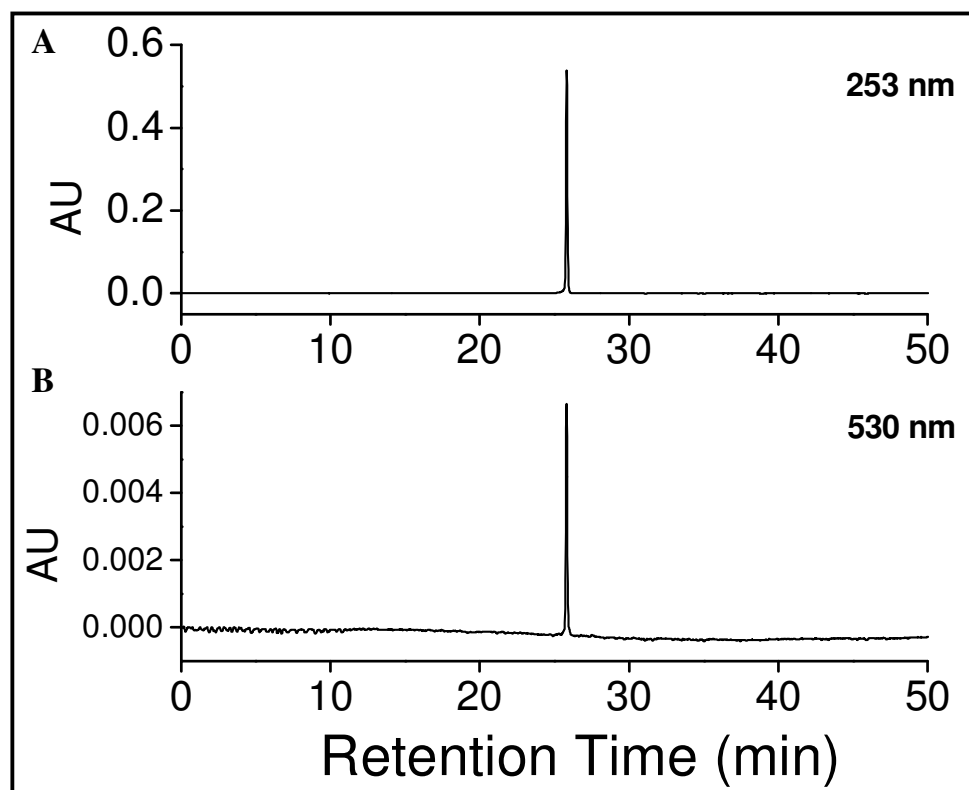
Fig 11: HPLC profile of the purified (gold nanoparticles-doxorubicin conjugate) at two different wavelengths A) 253 nm for doxorubicin detection and B) 530 nm to detect gold nanoparticles.

Fluorescence measurement:

Fluorescence measurement was carried out for the anticancer drug doxorubicin and gold nanoparticle-doxorubicin conjugate by exciting both the samples at 480 nm (Fig 12). There are no significant changes in the fluorescence spectrum. Decrease in the peak intensity of doxorubicin after conjugation with gold nanoparticles is due to slight quenching of doxorubicin by gold nanoparticles.
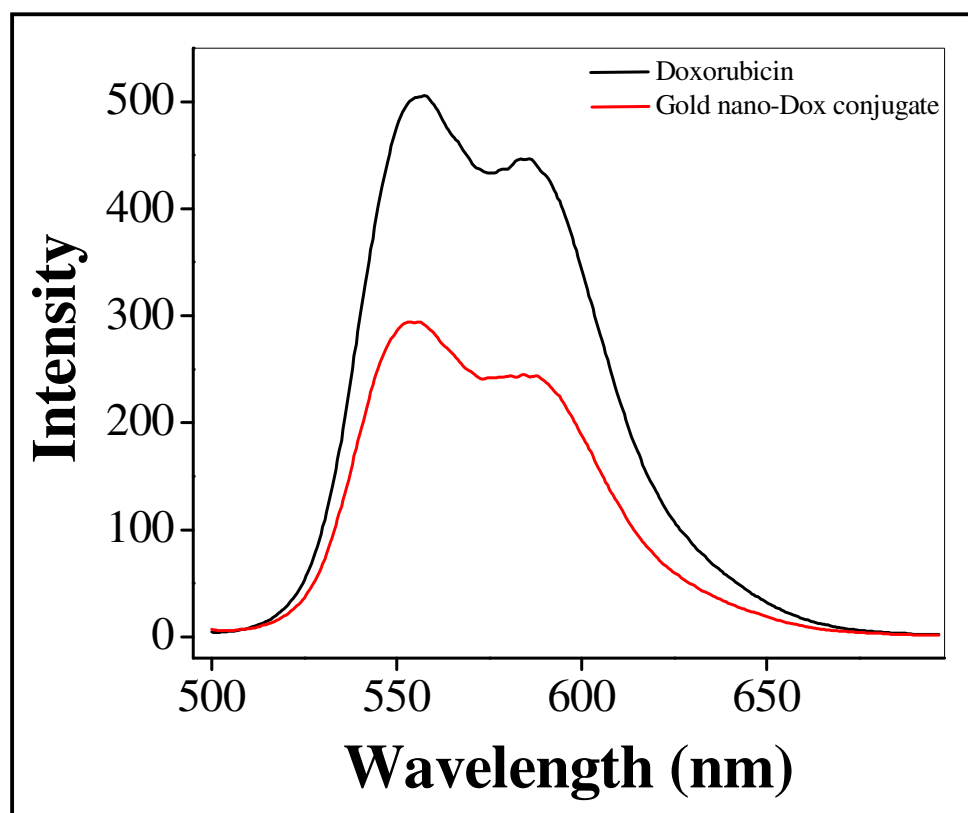
Fig 12: Fluorescence emission spectrum of doxorubicin and gold nanoparticle-doxorubicin conjugate excited at 480 nm.

Biological synthesis of silver nanoparticles by *Humicola lanuginosa*

Silver nanoparticles obtained by reacting the fungal biomass (20g) with 1mM aqueous solution of $AgNO_3$ in 250 ml Erlenmeyer flask at temperature 50^0C and pH 9. The reaction mixture was put onto a shaker under shaking conditions. The change in the color from yellowish to brown indicates the formation of silver nanoparticles.

Figure 13 shows two conical flasks with the fungal biomass before (A) and after (B) exposure to 1 mM $AgNO_3$ solution at temperature 50^0C and pH 9 for 96 hr. The change in the color from yellow to brown clearly demonstrates the formation of silver nanoparticles. The brown color arises because of the excitation of surface plasmon vibrations in the silver nanoparticles (61). After filtration, it was observed that the biomass was still pale yellow and that the aqueous solution contained the silver nanoparticles, characterized by an intense brown color. This demonstrates that the reduction of the Ag^+ ions takes place extracellularly (Fig 13 C).
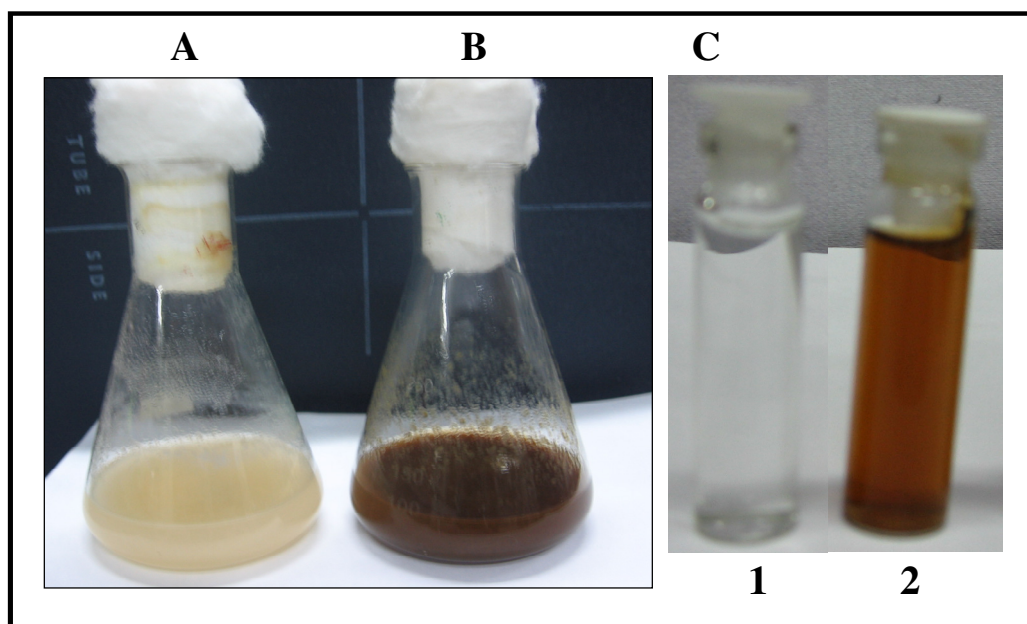
Fig 13: Conical flasks with fungus (*Humicola lanuginosa*) before (A) and after (B) exposure to $AgNO_3$ ions. (C) Filtrate of the control flask (1) and filtrate of treated flask (2).

UV-Vis spectroscopy of silver nanoparticles:

Bio-reduction of the aqueous Ag^+ ions after exposure to the fungal biomass was monitored by UV-Vis spectroscopy (Fig 14). It was observed that the biomass has a pale yellow color before reaction with the silver ions, which changes to a brownish color after completion of the reaction. This indicates the formation of silver nanoparticles in the reaction mixture and is due to the excitation of surface plasmon vibrations (61). It was observed that the surface plasmon band centered at ~415 nm that corresponds to the surface plasmon resonance of silver nanoparticles (12). These silver nanopartices are also stabilized by the secreted protein in the reaction. The protein band also appears around 270 nm in the UV spectrum.
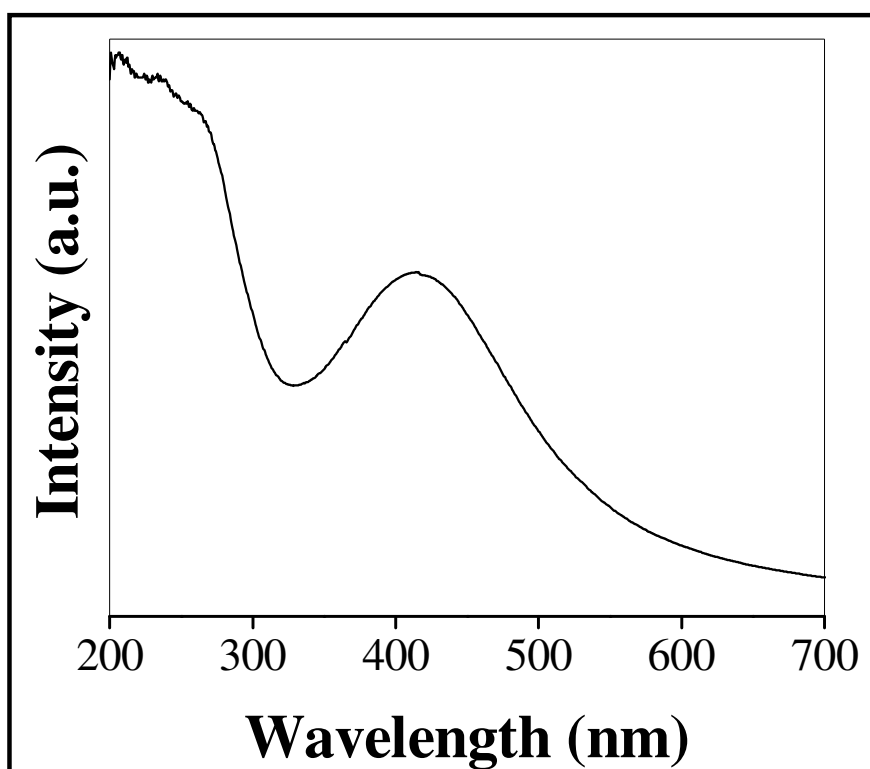
Fig 14: UV-Vis spectrum for the silver nanoparticles.

Transmission Electron Microscopy of silver nanoparticles:

A representative TEM micrograph Fig (15) recorded from the silver nanoparticle solution deposited on a carbon coated copper TEM grid. The silver nanoparticles are very well dispersed. The morphology is predominantly spherical but quite polydispersed in size ranging from 5-20 nm. These nanoparticles are stabilized by protein of the fungus present in the reaction mixture. As per earlier discussion, silver nanoparticles synthesized by incubating $AgNO_3$ by fungus are stable toward aggregation. Fig 15. B shows the Selected Area Electron Diffraction (SAED) pattern obtained from gold nanoparticles shown in Fig 15 A. The Scherrer ring pattern characteristic of face centered cubic (fcc), silver is clearly observed, showing that the structures seen in TEM images are nanocrystalline in nature. HRTEM results show the inteplaner distance which matches with (111) plane of the silver nanoparticles.
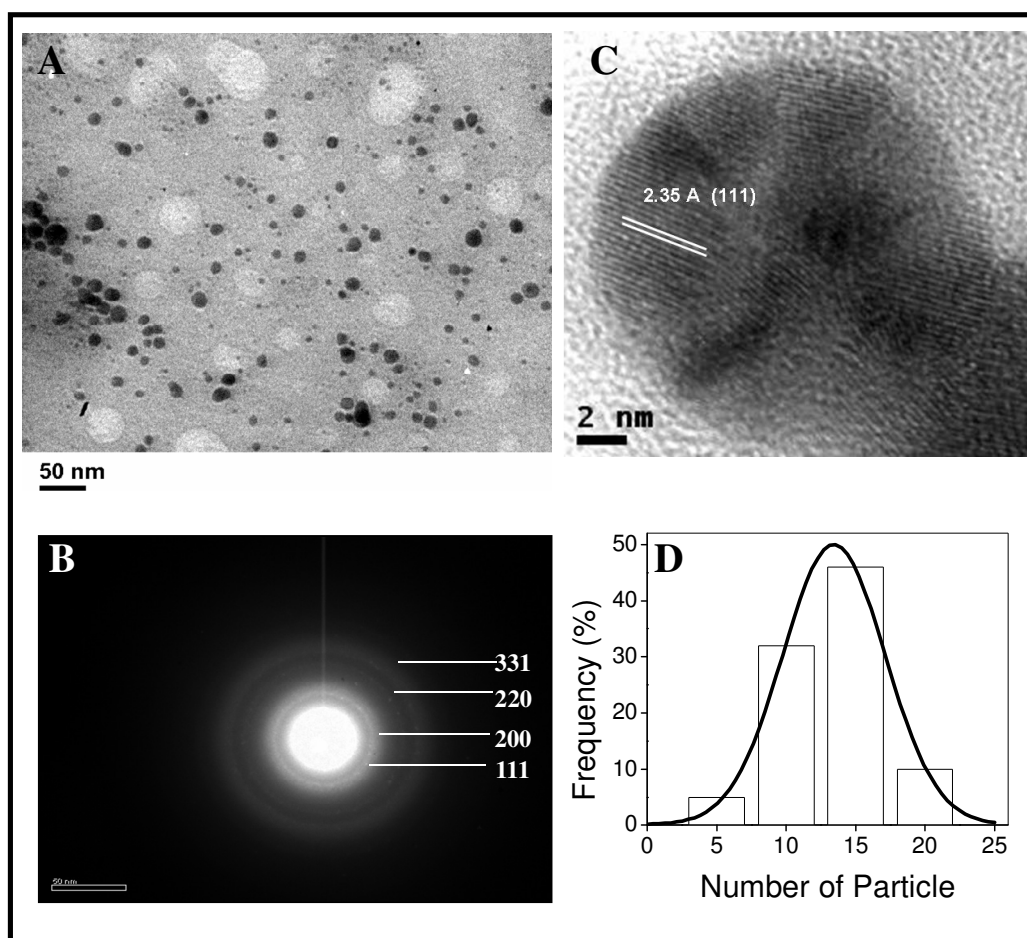
Fig 15: (A) Representative TEM micrograph recorded of silver nanoparticle. (B). Selected area diffraction pattern recorded from extracellular silver nanoparticles shown in Fig 15.A. (C). HRTEM micrograph. (D). Particle size distribution histogram of silver nanoparticles synthesized by the fungus.

X-ray Diffraction analysis of silver nanoparticles:

The XRD pattern for silver nanoparticles is provided in Figure 16. The presence of Braggs reflections arises due to (111), (200), (220) and (311) planes and agree well with those reported for fcc silver. The XRD pattern thus clearly shows that the silver nanoparticles formed are crystalline in nature (4).
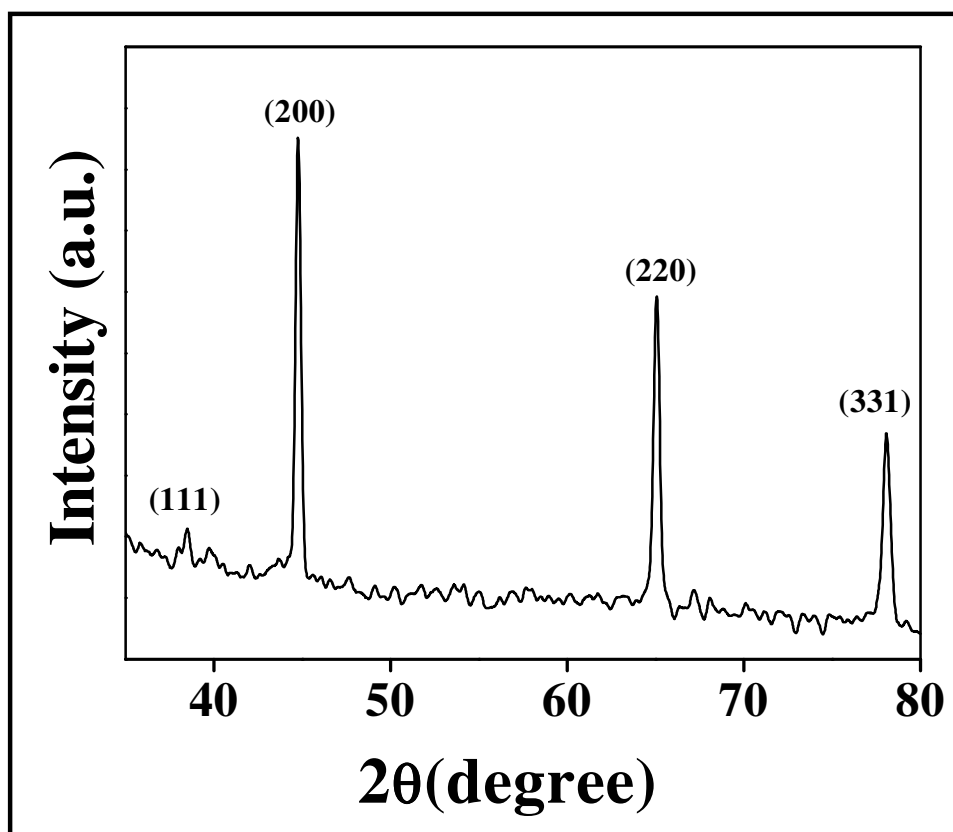
Fig 16: XRD pattern recorded for silver nanoparticles.

X-ray photoelectron spectroscopy of silver nanoparticles:

X-ray photoelectron spectroscopy (XPS) analysis supports the reduction of Ag^+ ions to elemental silver by the fungus (Fig 17). The peaks corresponding to chemically distinct C1s (282, 285 and 286), O1s (531.5 and 533) and N 1s (400) core level with binding energies are also represented in the figure. The Ag 3d spectrum could be decomposed into a single spin-orbit pair. The Ag $3d_{5/2}$ and $3d_{3/2}$ peaks occur at binding energies (BE) of 367.8 eV and 374.2 eV respectively and are assigned to the metallic Ag. It clearly indicates that all the silver ions are reduced by the fungus (20).
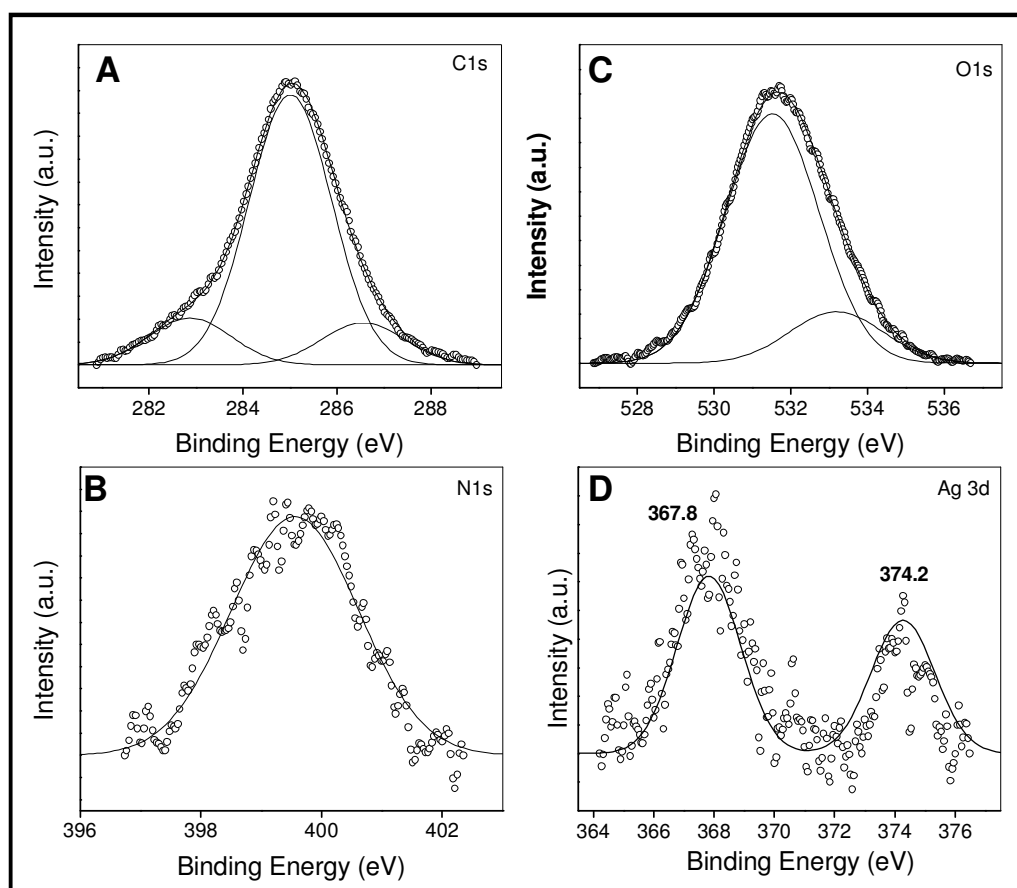
Fig 17: XPS spectrum for silver nanoparticles.

Fourier transform infrared spectroscopy of silver nanoparticles:

The amide bond between amino acid in protein thus gives rise to signature in the FTIR spectrum (Fig 18). The FTIR spectrum shows two bands at around 1644 and 1523, these bands are assigned to Amide I and Amide II of the proteins and are due to –C=O and –N-H stretch vibrations present in the amide linkages of the proteins, respectively. Role of the protein in stabilization of the silver nanoparticles by free amino group or others present in the protein may be a possibility.
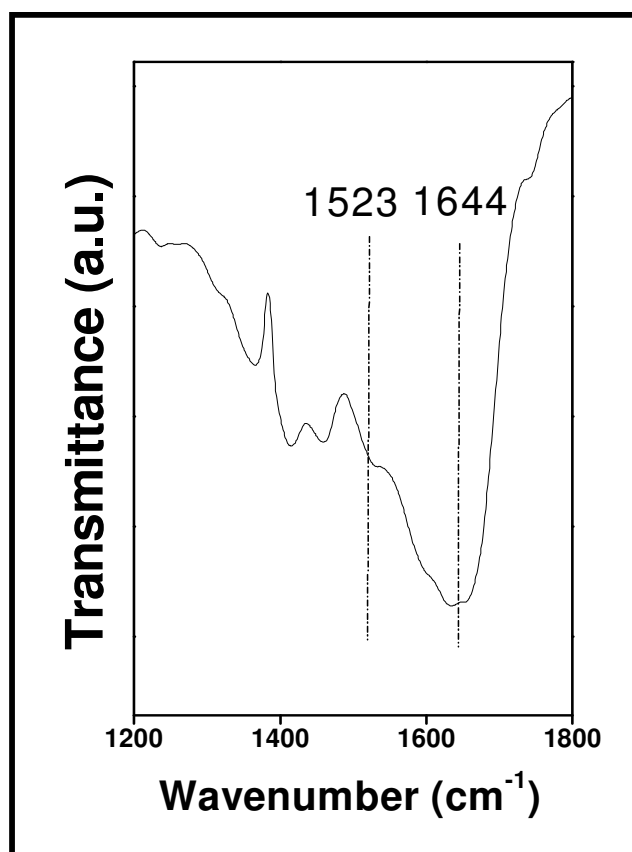
Fig 18: FTIR spectrum for silver nanoparticles.

Energy Dispersive Analysis of X-ray (EDAX) of silver nanoparticles:

EDAX spectrum (Fig 19) represents the signal from densely populated silver nanoparticles. Signals from Ag, together with C, O and Si are present. The presence of signals appear from C, O due to the X-ray emission from the biomolecules likely to be of proteins. The Si signal appears from the glass substrate used in EDAX analysis.
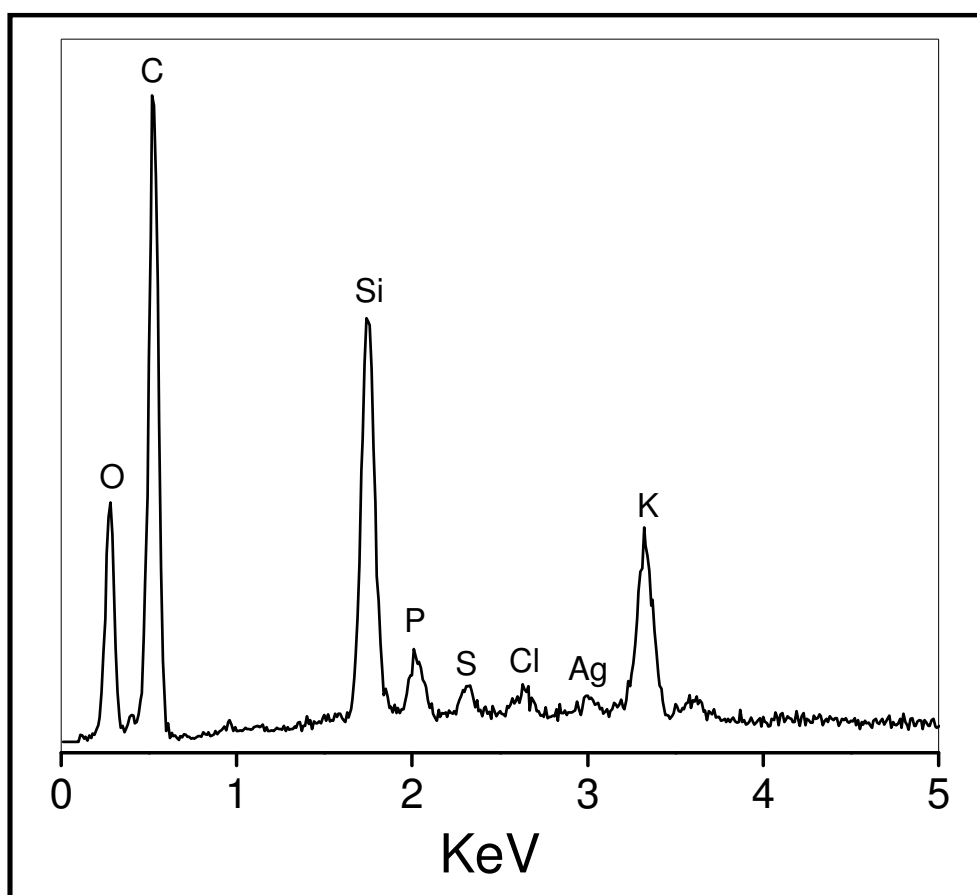
Fig 19: EDAX spectrum for silver nanoparticles

Cell viability assay of silver nanoparticles:

The effect of Ag nanoparticles on the cell viability of NIH3T3 mouse embryonic fibroblast cell line and MDA-MB-231 human breast carcinoma cell line was checked by MTT assay. The cells were treated with varying concentrations of Ag nanoparticles (50µg/ml, 250µg/ml, 5000 µg/ml and 1000 µg/ml) for 24 h. There is no significant difference on cell viability at concentration of 50µg/ml. The cell viability was reduced in a dose-dependent manner in both the cell lines and the cytotoxicity of the nanoparticle was observed from concentrations 250µg/ml in both the cell lines. The cell viability was reduced by 20.83% in case of NIH3T3 and 42.18% for MDA-MB-231 cell line at 1000µg/ml concentration.
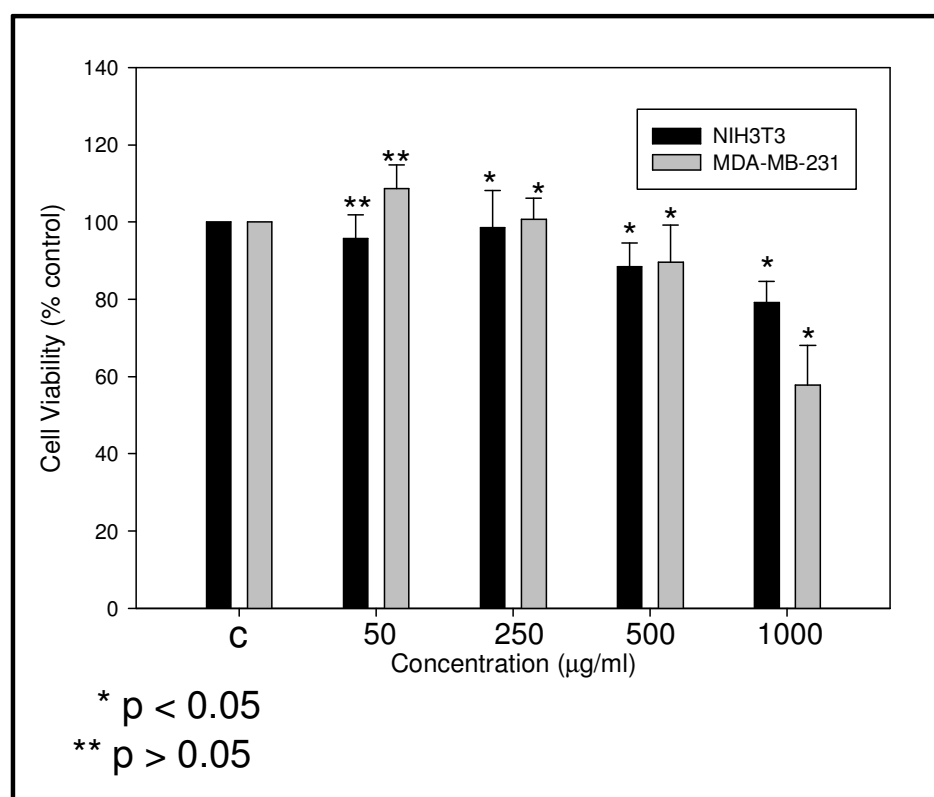
Fig 20: Cell viability assay of silver nanoparticles against NIH3T3 mouse embryonic fibroblast cell line and MDA-MB-231 human breast carcinoma cell line. The data is represented in the form of a bar graph and plotted using means + S.E. of triplicate determinations. The values were analyzed by Student's *t*-test (p < 0.005). Statistical analysis, P values for significantly different means, *P< 0.005 and **P> 0.05 vs control.

The exact mechanism by which the nanoparticle biosynthesis takes place is not so clear. Extracellular biosynthesis of gold nanoparticles using the fungus *Fusarium oxysporum* has been reported to occur by NADH-dependent reductase secreted by the fungus into the solution (11). Purified enzymes from the fungus *Fusarium oxysporum* were employed for the successful synthesis of metal and sulfide nanoparticles. The enzymes sulfite reductase and nitrate reductase were used for the *in vitro* synthesis of gold (19) and silver nanoparticles respectively (20). Even more interesting, *in vitro* synthesis of technologically important and highly stable semiconductor CdS nanoparticles capped by phytochelatin was also observed by the use of sulphite reductase enzyme purified from the fungus (41). Shahverdi et. al. suggests that, cell supernatant of *Enterobacter* contains the enzyme nitroreductase that may be involved in the biosynthesis of silver nanoparticles (62). Gold nanowire biosynthesis has been achieved by the protein present in the cell free extract of *Rhodopseudomonas capsulata*. The cell free extract reduced the gold ions resulting in gold nuclei which further formed nanoparticles. Due to the insufficient capping in the solution, these gold nanoparticles are unstable and form liner assembly (63). Gold nanoplates were synthesized by incubation of aqueous solution of chloroauric acid with extract of *Chlorella vulgaris* (unicellular green alga) at room temperature. The result suggests that proteins are involved in the synthesis of nanomaterials as well as control the shape and size of the nanomaterials. A protein with an approximate molecular weight 28 kDa was isolated, purified and tested for the reduction of chloroauric acid in aqueous solution (64). Silver nanoplates have been obtained by the extract of *Chlorella vulgaris* at room temperature. The protein content in the extract involved in the biosynthesis provides dual functions i.e. Ag ion reduction and shape controlled synthesis of nanosilver. Hydroxyl groups in Tyr residues and carboxyl groups in Asp and/or Glu residues were further identified as the most active functional groups for Ag ion reduction and for directing the anisotropic growth of Ag nanoplates, respectively (65). In case of plant, in particular, Neem leaf broth, rapid synthesis of stable gold, silver and bimetallic Au-Ag core shell has been achieved. It is assumed that flavanones and terpenoids act as the stabilizing agents for nanoparticles and that the reduction of metal ions is possibly also facilitated by these and/or sugars (24).

The present study suggests the size controlled synthesis of gold and silver nanoparticle synthesis using fungus *Humicola lanuginosa*. This is an enzyme-mediated process also supported by FTIR analysis. Remarkably, the reduction of ions

and stabilization of the synthesized nanomaterials is by the secreted biomolecules, likely to be a protein in the reaction mixture. These secreted proteins cap the nanoparticle's surface and prevent their aggregation thus making them water dispersible. In an attempt to synthesize metal nanoparticles with control over size and shape, a novel thermophilic fungus was isolated, and identified as *Humicola lanuginosa* by morphological and molecular techniques. The biosynthesized nanoparticles were characterized by UV-Vis spectroscopy, TEM, XRD, XPS, FTIR and EDAX. These gold nanoparticles were radiolabelled and injected in rat to see the biodistribution. Conjugation of gold nanoparticles with anticancer drug doxorubicin was achieved.

In the earlier reports, none of the above studies give mechanisms for nanobiosynthesis, instead they only give the possibility or role of a biomolecule in the biosynthesis process. The complete elucidation of the mechanisms for nanoparticle biosynthesis needs extensive efforts and thorough analysis which includes purification of the active biomolecules responsible for the synthesis, sequence analysis and structure analysis. Our efforts are still on for controlling the shape and size of nanoparticles and the mechanism for biosynthesis. Complete elucidation of mechanism for the biosynthesis of nanoparticles is beyond the scope of this thesis.

Conclusion:

In the present work, a novel alkalotolerant and thermophilic fungus was isolated and identified as *Humicola lanuginosa* in the laboratory. This fungus produces metal nanoparticles such as gold and silver when reacted with aqueous solutions of $HAuCl_4$ and $AgNO_3$ which leads to the production of extracellular nanoparticles with good dispersity and stability. The fungus *Humicola lanuginosa* has been employed for the first time for the biosynthesis of metal (viz. gold and silver) nanoparticles. Characterization of biosynthesized nanoparticles has been carried out by different techniques. FTIR results suggest that the biomolecules likely to be proteins are responsible for the stabilization and formation of nanoparticles. The biocompatibility and cytotoxicity of gold and silver nanoparticles was assessed by cell viability assay. Biodistribution profile also suggests further exploitation of these gold nanoparticles to the particular site. Conjugation of gold nanoparticles to doxorubicin also opens up the exciting possibility for drug delivery applications.

References:

1. a). Beveridge, T.J.; Murray, R.G. *J Bacteriol*. **1980**. *141,* 876. b). Shivaji, S.; Madhu, S.; Singh, S. *Process Biochemistry,* **2011**, DOI:10.1016/j.procbio. 2011.06.008. c).Anil, K. Suresh.; Pelletier, D.A.; Wang, Wei.; Broich, M. L.; Moon, Ji-Won.; Baohua, Gu.; Allison, D. P.; Joy, D. C.; Phelps, T.J.; Doktycz, M.J. *Acta Biomaterialia.* **2011**, *7(5)*, 2148. d). Motamedi Juibari, M.; Abbasalizadeh, S.; Salehi Jouzani, Gh.; Noruzi, M. *Materials Letters.* **2011**, *65*, 1014. e). Fischer, A.; Schmitz, M.; Aichmayer, B.; Fratzl, P.; Faivre, D. *J. R. Soc. Interface*. **2011**. DOI:10.1098/rsif.2010.0576. f). Parikh, R.Y.; Ramanathan, R.; Coloe, P.J. Bhargava, S.K.; Patole, M.S. Shouche, Y.S. Bansal, V. *Plos ONE*, **2011**, *6 (6),* e21401. g). Bai, H.J.; Yang, B. S.; Chai, C. J.; Yang, G.E.; Jia, W.L.; Yi, Z.B. *World J Microbiol Biotechnol.* **2011**, DOI: 10.1007/s11274-011-0747-x.

2. Ahmad, A.; Senapati, S.; Khan, M.I.; Kumar, R.; Sastry, M. *Langmuir.* **2003**, *19*, 3550.

3. a). Mukherjee, P.; Ahmad, A.; Mandal, D.; Senapati, S.; Sainkar, S.R.; Khan, M.I.; Parishcha, R.; Ajaykumar, P.V.; Alam, M.; Kumar, R.; Sastry, M. *Nano Lett*. **2001**, *1(10),* 515. b). Castro-Longoria, E.; Vilchis-Nestor, A. R.; Avalos-Borjac, M. *Colloids and Surfaces B: Biointerfaces*. **2011**, *83 (1),* 42. c). Vahabi, K.; Mansoori, G.A.; Karimi, S. *Insciences J.* **2011**, *1(1)*, 65. d). Jain, N.; Bhargava, A.; Majumdar, S.; Tarafdar, J.C. Panwar, J. *Nanoscale.* **2011**, *3*, 635. e). Ghodake, V.P.; Kininge, P.T.; Magdum, S.P.; Dive, A. S.; Pillai, M.M. *Journal of Engineering Research and Studies* (JERS). **2011**, *II (I)*, 32. f). Mishra, A.; Tripathy, S.K.; Yun, Soon-Il. *Journal of Nanoscience and Nanotechnology.* **2011**, 11, 243.

4. Shankar, S.S.; Ahmad, A.; Sastry, M. *Biotechnol Prog*. **2003**, *19,* 1627.

5. Loveley, D. R.; Stolz, J. F.; Nord, G. L.; Phillips, E.J.P. *Nature.* **1987**, *330*, 252.

6. Mann, S. *Nature,* **1993**, *365*, 499.

7. Pum, D.; Sleytr, U.B. *Trends Biotechnol.* **1999**, *17*, 8.

8. Klaus, T.; Joerger, R.; Olsson, E.; Granqvist, C. G. *Proc. Natl. Acad. Sci.* **1999**, *96*, 13611.

9. Nair, B.; Pradeep, T. *Cryst. Growth Des*. **2002**, *2*, 293.

10. Mukherjee, P.; Ahmad, A.; Mandal, D.; Senapati, S.; Sainkar, S.R.; Khan, M.I.; Ramani, R.; Pasricha, R.; Ajayakumar, P.V.; Alam, M.; Sastry, M.; Kumar, R. *Angew. Chem. Int. Ed.* **2001**, *40*, 3585.

11. Mukherjee, P.; Senapati, S.; Mandal, D.; Ahmad, A.; Khan, M.I.; Kumar, R.; Sastry, M. *ChemBiochem.* **2002**, *3*, 461.

12. Ahmad, A.; Mukherjee, P.; Senapati, S.; Mandal, D.; Khan, M I.; Kumar, R.; Sastry, M. *Colloids and Surfaces B: Biointerfaces.* **2003**, *28*, 313.

13. Ahmad, A.; Mukherjee, P.; Mandal, D.; Senapati, S.; Khan, M I.; Kumar, R.; Sastry, M. *J. Am. Chem. Soc.* **2002**, *124,* 12108.

14. Senapati, S.; Ahmad, A.; Khan. M. I.; Sastry, M.; Kumar, R. *Small.* **2005***, 1*, 517.

15. Ahmad, A.; Senapati, S.; Khan, M I.; Kumar, R.; Ramani, R.; Srinivas, V.; Sastry, M. *Nanotechnology.* **2003**, *14*, 824.

16. Shankar, S.S.; Ahmad, A.; Pasricha, R.; Sastry, M. *J.Mater.Chem.* **2003**, *13*, 1822.

17. Bansal,V.; Rautaray, D.; Ahmad, A.; Sastry, M. *J. Mater.Chem.* **2004**, *14*, 3303.

18. Ahmad, A.; Senapati,S.; Khan, M.I.; Kumar, R.; Sastry, M. *J. Biomed Nanotechol.* **2005**, *1*, 47.

19. Anil, S. Kumar.; Abyaneh,M. K.; Gosavi,S. W.; Kulkarni,S. K.; Ahmad, A.; Khan, M. I. *Biotechnol. Appl. Biochem.* **2007**, *47*, 191.

20. Anil, S. Kumar.; Abyaneh, M.K.; Gosavi, S. W.; Kulkarni, S.K.; Pasricha, R.; Ahmad, A.; Khan, M. I. *Biotechnol Lett.* **2007**, *29*, 439.

21. Gardea-Torresdey, J. L.; Parsons, J.G.; Gomez, E.; Peralta-Videa, J.; Troiani, H.E.; Santiago, P.; Yacaman, M.J. *Nano Lett.* **2002**, *2*, 397.

22. Shankar, S.S.; Ahmad, A.; Pasricha, R.; Sastry, M. *J. Mater. Chem.* **2003**, *13*, 1822.

23. Shankar, S.S.; Rai, A.; Ankamwar, B.; Singh, A.; Ahmad, A.; Sastry, M. *Nat. Mater.* **2004**, *3*, 482.

24. Shankar, S.S.; Rai, A.; Ahmad, A.; Sastry, M. *J. Colloid Interface Sci.* **2004**, 275, 496.

25. Ankamwar, B.; Chinmay, D.; Ahmad, A.; Sastry, M. *J. Nanosci. Nanotechnol.* **2005**, *5,* 1665.

26. Chandran, S.P.; Chaudhary, M.; Pasricha, R.; Ahmad, A.; Sastry, M. *Biotechnol. Prog.* **2006**, *22*, 577.

27. a). Huang, J.; Li, Q.B.; Sun, D.H.; Lu, Y.H.; Su, Y.B.; Yang, X.; Wang, H.X.; Wang, Y.P.; Shao, W.Y.; He, N. *Nanotechnology.* **2007**, *18*, 105104. b). Castro, L; Blázquez, L.M.; Mu˜noz, J.A.; González, F.; García-Balboa, C; Ballester, A. *Process Biochemistry.* **2011**, *46,* 1076. c). Elavazhagan, T.; Arunachalam, K.D. *International Journal of Nanomedicine.* **2011**, *6,* 1265. d). Singh, C.; Sharma,V.; Naik, P. K.; Khandelwal, V.; Singh, H. *Digest Journal of Nanomaterials and Biostructures.* **2011**, *6(2)*, 535.

28. Niemeyer, C.M. *Angew. Chem. Int. Ed.* **2001**, *40*, 4128.

29. Niemeyer. C.M. *Angew. Chem. Int. Ed.* **2003**, *42*, 5796.

30. David, T.M.; Sang, B.L.; Lacra, T.; Li, N.; Nevanen, T.K.; Soderlund, H.; Martin, C.R. *J. Am. Chem. Soc.* **2002**, *124*, 11864.

31. Hamachi, I.; Fujita, A.; Unitake. T.K. *J. Am. Chem. Soc.* **1994**, *116*, 8811.

32. Chen, X.; Hu, N.; Zeng, Y.; Rusling, J.F.; Yang, J. *Langmuir.* **1999**, *15*, 7022.

33. Mrksich, M.; Sigal, G. B.; Whitesides, G. M. *Langmuir.* **1995**, *11*, 4383.

34. Fang, J.; Knobler, C.M. *Langmuir.* **1996**, *12*, 1368.

35. Stonehuerner, J.G.; Zhao, J.; O'Daly, J.P.; Crumbliss, A.L.; Henkens, R.W. *Biosens. Bioelectron.* **1992**, *7*, 421.

36. Zhao, J.; O'Daly, J.P.; Henkens, R.W.; Stonehuerner, J.; Crumbliss, A.L. *Biosens. Bioelectron.* **1996**, *11*, 493.

37. Crumbliss, A.L.; Perine, S.C.; Stonehuerner, J.; Tubergen, K.R.; Zhao, J.; Henkens, R.W.; O'Daly. J.P. *Biotech. Bioeng.* **1992**, *40*, 483.

38. Dayal, A.; Loos, K.; Noto, M.; Chang, S.W.; Spagnoli, C.; Shafi, K.V.P.M.; Ulman, A.; Cowman, M.; Gross, R.S. *J. Am. Chem. Soc.* **2003**, *125*, 1684.

39. Gole, A.; Dash, C.; Ramakrishnan, V.; Sainkar, S.R.; Mandale, A.B.; Rao, M.; Sastry, M. *Langmuir* **2001**, *17*, 1674.

40. Gole, A.; Dash, C.; Mandale, A.B.; Rao, M.; Sastry, M. *Anal. Chem.* **2001**, *72,* 4301.

41. Ansary, A.A.; Anil, S. Kumar.; Krishnasastry, M. V.; Abyaneh, M. K.; Kulkarni, S.K.; Ahmad, A.; Khan, M. I. *Journal of Biomedical Nanotechnology.* **2007**, *3 (4)*, 406.

42. Joshi, H.M.; Bhumkar, D. R.; Joshi, K.; Pokharkar, V.; Sastry, M. *Langmuir.* **2006**, *22*, 300.

43. Anil, S. Kumar.; Peter, Y.A.; Nadeau, J.L. *Nanotechnology*. **2008**, *19,* 495101.

44. Paciotti, G. F.; Myer, L.; Weinreich, D.; Goia, D.; Pavel, N.; McLaughlin, R.E.; Tamarkin, L. *Drug Delivery.* **2004**, *11,*169.

45. Sun,Q.; Wang,Q.; Rao,B. K.; Jeena, P. *Phys Rev Lett.* **2004**, *93*, 186803.

46. Ma, Y.; Manolache, S.; Denes, F. S.; Vail, D.; Thamm, D.; Kurzman, I. *Journal of Biomaterials Science, Polymer Edition.* **2004**, *15(8),*1033.

47. Zimmerman, U.; Pilwat, G. *J. Biosci.* **1976**, *31,*372.

48. Kato, T.; Nemoto, R.; Mori, H.; Aabe, R.; Unno,K.; Goto, A.; Murota, H.; Hrada, M.; Homma, M.*Applied Biochem. Biotechnol.* **1984**, *10*, 199.

49. Widder, K. J.; Morrist, R. M.; Gerry, P.; Howard, D.P. JR.; Senyeit, A.E. *Proc. Natl. Acad. Sci*. **1981**, *78*, 579.

50. Gupta, P.K.; Hung, C.T.; Rao, N. S. *J. Pharm. Sci.* **1989**, *78*, 290.

51. Morimoto, Y.; Sugibayashi, K.; Okumura, M.; Kato, Y. *J. Pharmacobio-dynamics*. **1989**, *3(5),* 264.

52. Guhagarkar, S.A.; Majee, S.B.; Samad, A.; Devarajan,P.V. *Cancer Nanotechnology.* **2011**, DOI 10.1007/s12645-011-0012-x.

53. Némati, F.; Dubernet, C.; Verdière, A.C.; Poupon, M.F.; Treupel-Acar, L.; Puisieux, F.; Couvreur, P. *International Journal of Pharmaceutics.* **1994**, *102 (1-3)*, 55.

54. Verdière, A. C.; Dubernet, C.; Nemati, F.; Poupon, M. F.; Puisieux, F.; Couvreur, P. *Cancer Chemotherapy and Pharmacology.* **1994**, *33(6),* 504.

55. Hortobágyi, G.N. *Drugs.* **1997**, *54*, 1.

56. Managit, C.; Kawakami,S.; Yamashita,F.; Hashida, M. *Journal of Pharmaceutical Sciences.* **2005**, *94 (10)*, 2266.

57. Allgaier,H.P.; Deibert, P.; Olschewski, M.; Spamer,C.; Blum, U.; Gerok, W.; Blum, H. E. *International Journal of Cancer.* **1998**, *79*, 601.

58. Kopeček, J.; Kopečková, P.; Minko, T.; Lu, Z.R.; Peterson, C.M. *Journal of Controlled Release*. **2001**, *74 (1-3)*, 47.

59. Philip, S.; Kundu, G.C. *J. Biol Chem.* **2003**, *278 (16)*, 14487.

60. a). Reddy, L. Harivardhan.; Sharma, R.Kumar.; Chuttani, K.; Mishra, A.K.; Murthy, R. R. *The AAPS Journal.* **2004**, *6 (3)*, Article 23. b).Fu, C. M.; Wang, Y. F.; Chao, Y. C.; Hung, S. H.; Yang, M. D. *IEEE Transactions on Magnetics.* **2004**, *40 (4)*, 3003. c). Wang, Y.F.; Fu, C.M.; Chuang, M.H.; Cham, T.M. Chung, M.I. *Journal of Nanomaterials* **2011**, Article ID 851520,

doi:10.1155/2011/851520. d). Devarajan, P. V.; Jindal, A. B.; Patil, R.R.; Mulla, F.; Gaikwad, R.V.; Samad, A. *Journal of Pharmaceuticals Sciences.* **2010**, *99 (6)*, 2576.

61. Mulvany, P. *Langmuir.* **1996**, *12(3),* 788.

62. Shahverdi, A.; Minaeian, S.; Shahverdi, H.R.; Jamalifar, H.; Nohi, A.A. *Proc Biochem.* **2007**, *42*, 919.

63. Shiying, H, Zhang, Y.; Guo, Z.; Gu, N. *Biotechnol Prog.* **2008**, *24*, 476.

64. Xie, J.; Lee, J.Y.; Wang, D.I.; Ting, Y. P. *Small.* **2007**, *3 (4)*, 672.

65. Xie, J.; Lee, J.Y.; Wang, D.I.; Ting, Y.P. *ACS Nano.* **2007**, *1 (5)*, 429.

Part 3: Biological synthesis of platinum nanoparticles using fungus

Summary:

The present work emphasizes on nanoparticle synthesis protocol which occurs in ambient conditions**.** In our laboratory, fungi, actinomycetes and plant extracts are exploited for their potential to synthesize nanoparticles of different chemical compositions, sizes and shapes. *Fusarium oxysporum* when incubated with Hexachloroplatinic acid (H_2PtCl_6) in ambient conditions reduces the precursor and leads to the formation of stable extracellular platinum nanoparticles. The nanoparticles are in the size range of ~15 ± 5 nm and are stabilized by proteins present in the solution. The reduction process is believed to occur enzymatically, thus creating the possibility of a rational, fungal-based method for the synthesis of nanoparticles over a wide range of chemical compositions.

Introduction:

Materials with at least one dimension are in the nanometer range (1-100 nm) which exhibit significantly different properties from those of the corresponding bulk materials (1). Due to their extremely small size, they exhibit unusual properties such as electronic, optical, magnetic and chemical. Nanomaterials have great potential applications in catalysis (2), photocatalysis (3), optoelectronics (4), hyperthermia for malignant cells (5), cell labeling (6), cell tracking (7), in vivo imaging (8), DNA detection (9) etc. In particular, platinum nanoparticles are of great importance for their excellent catalytic activity (10-12). Synthesis of nanoparticles for catalytic application is an area of current interest due to the difficulty in synthesis and stability of nanoparticles. The available process for the preparation of platinum nanoparticles requires toxic chemicals (sodium borohydrate) (13), polymers (10), electrolytes (11), and thiol groups (14) to maintain the stability of nanoparticles. The synthesis of platinum nanoparticles of different shapes has been achieved (15) in aqueous solutions. Chemical and physical methods for nanomaterial synthesis are usually energy intensive, employ toxic chemicals and require higher temperatures. Therefore, a clean, nontoxic and environment friendly process for the synthesis of nanoparticles is in great demand. Researchers have turned toward biological systems (microbes and plants) for inspiration, which could provide a possible route for the development of nanoparticle synthesis. Biological systems are characterized by the processes that occur at ambient temperature and pressure. Therefore microbial and plant based processes for the synthesis of nanoparticles are an emerging technologies with great potential in industry.

Bacteria, among microbial system, was studied and considered a potential source for nanoparticle synthesis (16). In our laboratory, we have investigated eukaryotic organism such as fungi, instead of bacteria for the synthesis of nanoparticles. After the extensive screening programme, two fungi, viz. *Fusarium oxysporum* (17, 18) and *Verticillium* sp. (19, 20) were found to produce nanoparticles.

Moreover, earlier reports suggest intracellular nanoparticle synthesis using microbial routes. But it requires some additional steps for isolating the nanoparticles from microbial biomass. The difficulty in its downstream processing and time consumption hampers the process and evokes the purpose for development of a simple and cheap route for nanoparticle synthesis. Thus, there is a need for a more applicable and practical way if nanoparticles are to be formed extracellularly. The extracellular

synthesis of nanoparticles has been reported by bacteria (21), actinomycetes (22), fungi (23, 24) and plants (25).

Cis-platin (cis diaminedichloroplatinum), a well-known platinum compound is used as an antitumor agent (26). Yolkshell nanocrystals of FePt@CoS$_2$ have been found to be more potent in killing HeLa cells as compared to cis-platin (27). Considering the importance of the platinum nanoparticle, there is a growing need for the development of a protocol which will occur in ambient conditions. Biological synthesis of platinum nanoparticle using bacteria (28), fungi (29), plant (30), enzymes (31) and aqueous honey solution (32) has been suggested as possible eco-friendly alternatives to the available methods. These methods produce variable morphology of nanoparticles and there is no specific control on the shape and size of nanoparticles. A variable morphology (triangles, squares and spheres) has been observed for these processes. Leaf extracts of *Diopyros kaki* plant were used as a reducing agent for platinum nanoparticles. In the process, nearly complete conversion (~90%) was achieved at higher temperature of 95^{0}C. Enzymatic transformation of metal salts for the production of nanomaterials is superior over other methods, even though it has limitations. The major problem associated with the process is that the enzyme works at its optimum condition and at different pH and temperature metals can inhibit the enzyme activity. Despite earlier reports of bio-based methods for platinum nanoparticles, none of them provide control over size and shape for nanoparticle synthesis which occur in ambient conditions.

We have established the biosynthesis of metals, metal sulfides, oxides and suggested enzymatic reduction by the fungus and found *Fusarium oxysporum* as an efficient biocatalyst for the nanosynthesis. In the present work, we have employed the fungus *Fusarium oxysporum* for the extracellular synthesis of platinum nanoparticles.

Materials and Methods:

Materials:

Hexachloroplatinic acid (H_2PtCl_6) was obtained from Sigma Aldrich. Malt extract, yeast extract, glucose and peptone were obtained from HiMedia and used as-received.

Fungal growth and maintenance:

The fungus *Fusarium oxysporum* was maintained on Potato Dextrose Agar [PDA (potato 25% w/v, dextrose 2% w/v, and agar 2% w/v)] slants at 25^0C. Stock cultures were maintained by subculturing at monthly intervals. The fungus was grown at pH 7.0 and 25^0C for 5 days; the slants were preserved at 15^0C. From an actively growing stock culture, subcultures were made on fresh slants and after 5 days of incubation at pH 7.0 and 25^0C, were used as the starting material for synthesis of nanoparticles.

Biological synthesis of platinum nanoparticles:

For the extracellular synthesis of platinum nanoparticles, the fungus was grown in 500 mL Erlenmeyer flasks each containing MGYP media (100 mL), composed of malt extract (0.3 %), glucose (1.0 %), yeast extract (0.3 %) and peptone (0.5 %) at $25-27^0C$ under shaking at 200 rpm for 96 hr. After 96 hr of fermentation, mycelia were separated from the culture broth by centrifugation (5000 rpm) at 10^0C for 20 min and then the mycelia were washed thrice with sterile distilled water under sterile conditions. The harvested mycelial mass (20 g of wet mycelia) was then resuspended in 100 mL of aqueous solution of 1mM H_2PtCl_6 solutions in 500 mL Erlenmeyer flasks and the same was put into a shaker at $25-27^0C$ (200 rpm). The reaction was carried out for a period of 96 hr and fungal biomass was separated by filter-paper to collect biomass and filtrate in sterile conditions. Periodically, aliquots of the reaction solution were removed and subjected to UV-Vis spectroscopy to check the formation of nanoparticles extracellularly.

Characterization of platinum nanoparticles:

Optical measurement of the platinum nanoparticles was studied by UV-visible spectrophotometer over the spectral range of 200-800 nm. The measurements were carried out on a Shimadzu dual-beam spectrophotometer (model UV-1601 PC) operating at a resolution of 1 nm. TEM measurements were performed on a JEOL model 1200 EX TEM operating at an accelerated voltage of 80 KV. Samples for TEM

analysis were prepared by drop coating the nanoparticle solutions on carbon coated copper grids. SAED analysis was performed on the same grid. X-ray diffraction analysis was carried out for nanoparticle powder on Panalytical 'X' Pert PRO system with CuKα radiation (λ) 1.5418 Å). Nanoparticle powder samples were used for XPS measurements. The measurements were performed on a VG microtech ESCA 3000 instrument. The FTIR measurements were performed on a Perkin–Elmer Spectrum One instrument operated in the diffuse reflectance mode at a resolution of 2 cm^{-1}. The samples for the measurement were prepared by mixing platinum-nanoparticle powder with KBr.

Results and Discussion:

The fungus, *Fusarium oxysporum* when reacted with aqueous solution of Hexachloroplatinic acid (H_2PtCl_6) at room temperature for 96 hr under shaking conditions on a rotary shaker (200 rpm) resulted in the formation of extracellular and highly stable platinum nanoparticles of nearly ~15±5 nm in size and spherical in shape.

UV-Vis spectroscopy of platinum nanoparticles:

The Figure 1A shows glass vial of the Hexachloroplatinic acid (H_2PtCl_6) reaction solution at the beginning (time $t = 0$, glass vial on the left side) and after 96 hr of reaction (glass vial on the right side) with the *Fusarium oxysporum* biomass. The dark brown color of the solution after reaction indicates the presence of platinum nanoparticles in the solution.

The UV-Vis spectrum recorded for the reaction mixture before and after the reaction of Hexachloroplatinic acid (H_2PtCl_6) with fungus *Fusarium oxysporum* is shown in Figure 1B. When Hexachloroplatinic acid (H_2PtCl_6) is dissolved in water, it forms $2H^+$ and $PtCl_6^{2-}$. The absorption peak at 260nm appears due to the presence of $PtCl_6^{2-}$ in water. But after reduction with the fungus *Fusarium oxysporum*, the absorption peak disappeared which indicates the complete reduction of precursor salt to zero-valent platinum.

Absorption band at 270-280 nm which is contributed by proteins present in the extracellular broth, suggesting a possible reducing enzyme based process for the synthesis of platinum nanoparticles. The solution was extremely stable, with no evidence of flocculation of the particles even a month after reaction. The long-term stability of the platinum nanoparticle solution could be due to the presence of the capping protein/peptide in solution that binds to the surface of the nanoparticle and prevents its flocculation.
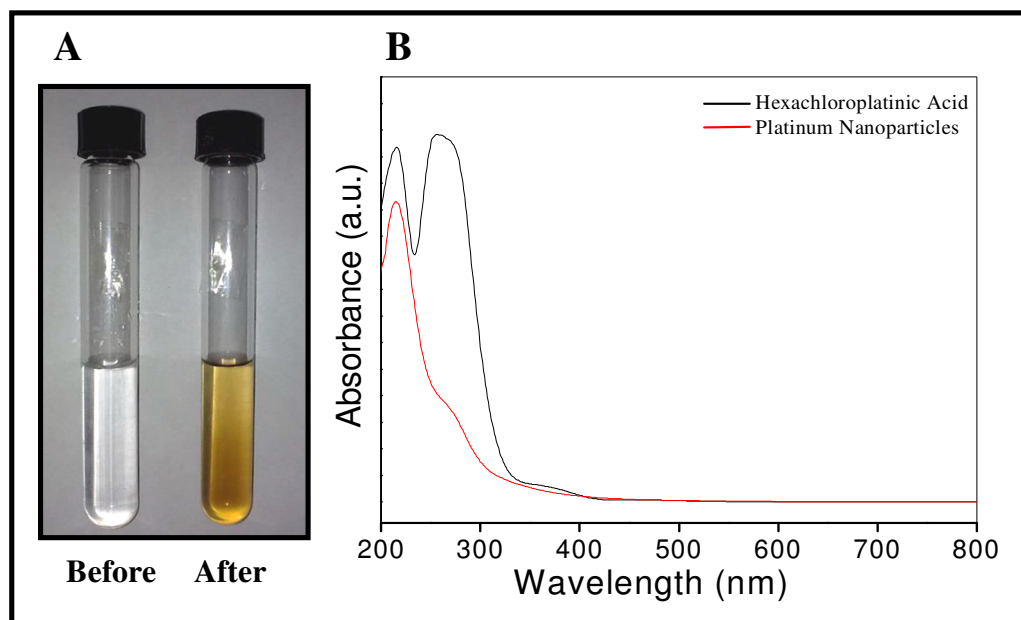
Fig 1. A). Shows glass vial containing H_2PtCl_6 solution before (glass vial on the left) and after reaction with the fungal biomass (glass vial on the right). B).UV-Vis spectra recorded from the aqueous 1mM H_2PtCl_6 solution after 96 hr of reaction with the fungal biomass.

Transmission Electron Microscopy of platinum nanoparticles:

Transmission electron micrograph analysis was performed in order to determine the size and shape of the biosynthesized nanoparticles. The transmission electron micrographs (Fig. 2A) bring out the formation of nanoparticles in size range of ~15 ± 5 nm. The morphology of the nanoparticles was found to be spherical. Fig 2. B shows the Selected Area Electron Diffraction (SAED) pattern obtained from platinum nanoparticles shown in Fig 2 A. The Scherrer ring pattern characteristic of face centered cubic (fcc), platinum is clearly observed, showing that the structures seen in TEM images are nanocrystalline in nature. The histogram shown in (Fig 2C) brings out the size distribution of nanoparticles, sized in between 5-30 nm with average size approximately 15 nm (Fig 2 C).

As stated earlier, fungus secretes the proteins which play a role of reducing and capping agents in the process. As the dissolved components (Hexachloroplatinic acid) get into the solution, they form reactive molecular complexes, which leads to the formation of inorganic nanoparticles and are also capped by the secreted proteins in the reaction media.
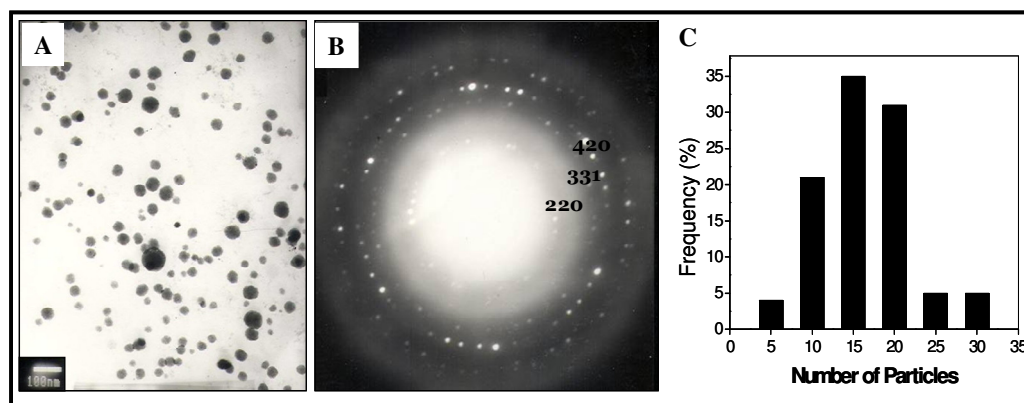
Fig 2. A. TEM micrograph of the platinum-nanoparticle formed by the reaction of H_2PtCl_6 with *Fusarium oxysporum* biomass for 96 hr. B).Selected area diffraction pattern recorded from extracellular platinum nanoparticles shown in Fig 2.A. C) Particle size distribution histogram determined from the TEM micrograph.

X-ray Diffraction analysis of platinum nanoparticles:

X-ray diffraction (XRD) analysis of platinum nanoparticles was carried out by depositing them as a biofilm on a glass substrate which showed intense Bragg's peaks corresponding to (111), (200) and (220) in the 2 θ range 35 θ-80 θ (Fig.3) and in agreement with those reported for the platinum nanocrystals (33). The broadening of the Bragg's peaks indicates that the platinum particles formed are of nanoscale dimensions.
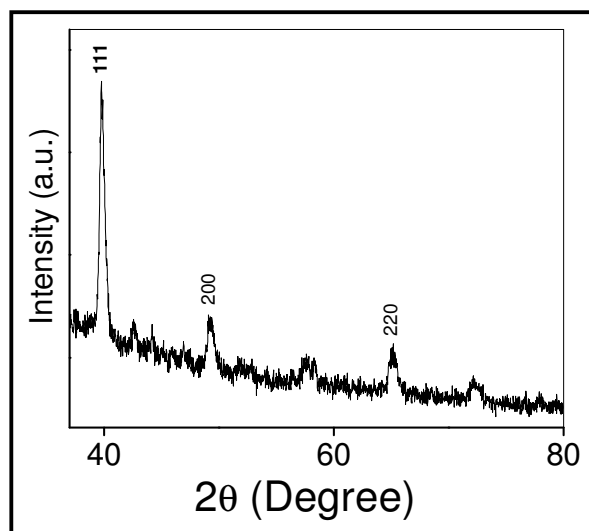
Fig 3: X-ray Diffraction pattern for the platinum nanoparticles synthesized by using *Fusarium oxysporum.*

X-ray photoelectron spectroscopy of platinum nanoparticles:

The presence of platinum nanoparticles was also confirmed by analyzing the sample by XPS is shown in Fig 4. The results showed the presence of Pt, C, O, N as the prominent elements. In Figure 4, we have presented the background corrected XPS results of the platinum nanoparticles. In Fig 4A, peaks correspond to chemically distinct C 1s core levels originating from the hydrocarbon chains, α-carbon and –COOH groups present in the proteins with binding energies 284.8, 286.4 and 288.4 eV respectively. The peaks in (Fig 4B and Fig 4C) corresponds to chemically distinct N 1s and O 1s core levels with binding energies 400 eV and 531.5 eV respectively. Fig 4D shows Pt 4f spectrum which could be resolved into two peaks ($4f_{5/2}$ and $4f_{7/2}$) due to the spin-orbit coupling with binding energies 71.3 and 74.8 eV respectively (13).
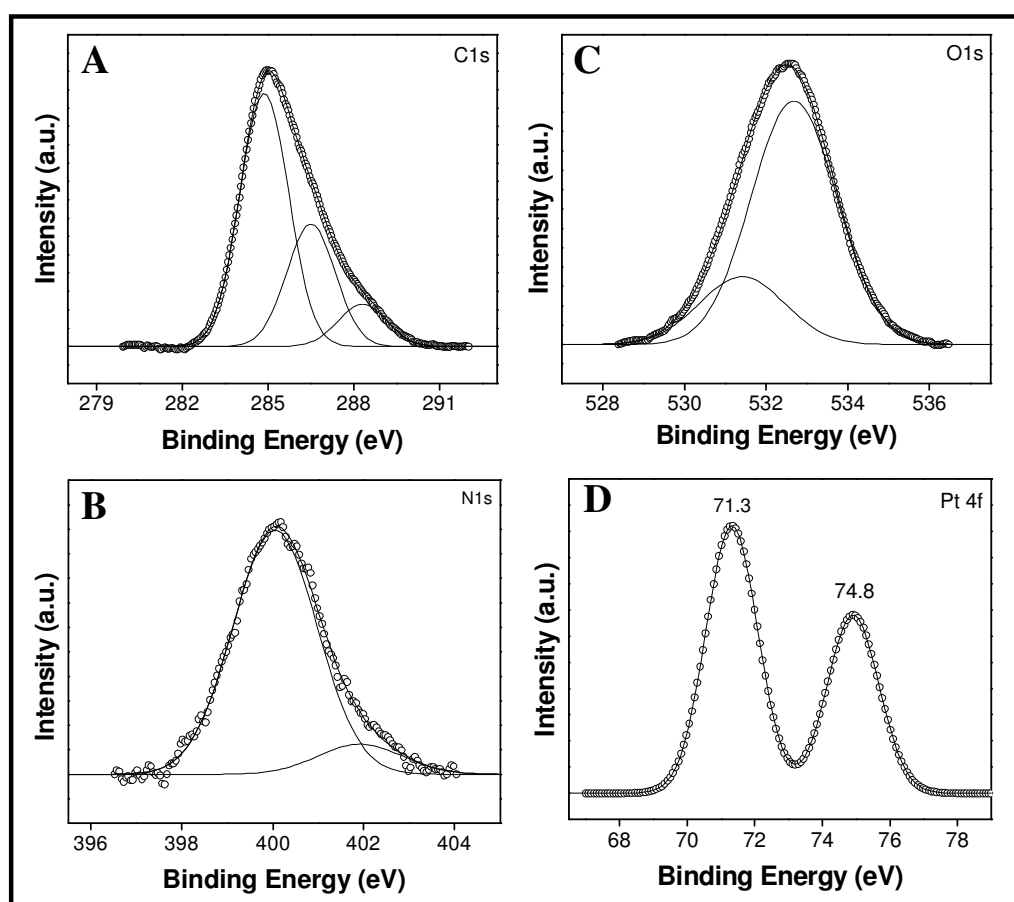
Fig. 4: X-ray photoelectron spectrum of platinum nanoparticles.

Fourier transform infrared spectroscopy of platinum nanoparticles:

Figure 5 shows the FTIR spectrum recorded from the Hexachloroplatinic acid solution after reaction with the fungus *Fusarium oxysporum* for 96 hr. In case of platinum nanoparticles, the presence of two bands at 1650 and 1536 cm^{-1} are seen in the figure. The 1650 and 1536 cm^{-1} bands may be assigned to the amide I and II bands of proteins, respectively (22). It is well-known that proteins can bind to platinum nanoparticles through either free amine groups or cysteine residues in the proteins and therefore, stabilization of the platinum nanoparticles by surface-bound proteins is a possibility.
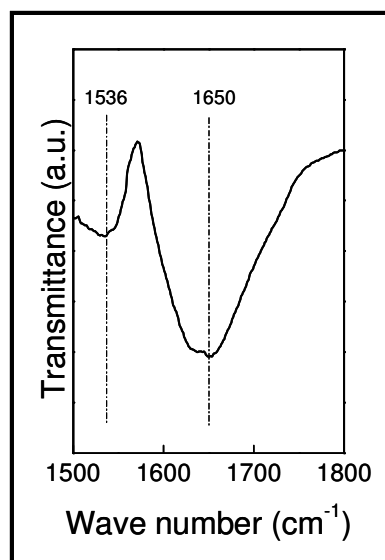
Fig 5: FTIR spectrum for the fungus synthesized platinum nanoparticles. The amide I and II bands are identified in the figure.

Conclusion:

In conclusion, the fungus *Fusarium oxysproum* was employed for the extracellular synthesis of platinum nanoparticles. The fungus reduces the Hexachloroplatinic acid (H_2PtCl_6) in solution, stabilizes them by secreting proteins at room temperature. The morphology of the nanoparticles was found to be spherical, nearly ~15 ± 5 nm in size.

References:

1. Henglein, A. *Chem. Rev.* **1989**, *89*, 1861.

2. Schmid, G. *Chem. Rev*. **1992**, *92*, 1709.

3. Brugger, P. A.; Cuendet, P.; Graetzel, M. *J. Am. Chem. Soc*. **1981**, *103*, 2923.

4. Wang,Y.; Herron, N. *J. Phys. Chem*. **1991**, *95*, 525.

5. Shi, J.; Gider, S.; Babcock, K.; Awschalom, D.D. *Science.* **1996**, *271*, 937.

6. Wu, X.; Liu, H.; Liu, J.; Haley, K. N.; Treadway, J. A.; Larson, J. P.; Ge, N.; Peale, F.; Bruchez, M. P. *Nature Biotechnol.* **2003**, *21*, 41.

7. Parak, W. J.; Boudreau, R.; Gros, M. L.; Gerion, D.; Zanchet, D.; Micheel, C. M.; Williams, S. C.; Alivisatos, A. Larabell, P.C. *Adv. Mater.* **2002**, *14*, 882.

8. Dubertret, B.; Skourides, P.; Norris, D. J.; Noireaux, V.; Brivanlou, A. H.; Libchaber, A. *Science.* **2002**, *298*, 1759.

9. Taylor, J. R.; Fang, M. M.; Nie, S. *Anal. Chem.* **2000**, *72*, 1979.

10. Duff, D. G.; Edwards, P. P. *J. Phys. Chem.* **1995**, *99*, 15934.

11. Chen, C. W.; Tano, D.; Akashi, M. *Colloid Polym. Sci.* **1999**, *277,* 488.

12. Dalmia, A.; Lineken, C.L.; Savinell, R.F. *J. Colloid Interface Sci.* **1998**, *205* 535.

13. Kumar, A.; Joshi, H.M.; Mandale, A.B.; Srivastava, R.; Adyanthaya, S.D.; Pasricha, R.; Sastry, M. *J. Chem. Sci.* **2004**, *116(5),* 293.

14. Yee, C.; Scotti, M.; Ulman, A.; White, H.; Rafailovich, M.; Sokolov, J. *Langmuir.* **1999**, *15*, 4314.

15. Ahmadi, T.S.; Wang, Z.L.; Green, T.C.; Henglein, A.; El-Sayed, M.A. *Science.* **1996**, *272*, 1924.

16. Joerger, T.K.; Joerger, R.; Olsson, E.; Granqvist, C.G. *Trends Biotechnol.* **2001**, *19*, 15.

17. Mukherjee, P.; Senapati, S.; Mandal, D.; Ahmad, A.; Khan, M.I.; Kumar, R.; Sastry, M. *ChemBioChem*. **2002**, *3*, 461.

18. Ahmad, A.; Mukherjee, P.; Senapati, S.; Mandal, D.; Khan, M.I.; Kumar, R.; Sastry, M. *Colloids Surf B Biointerfaces.* **2003**, *28*, 313.

19. Mukherjee, P.; Ahmad, A.; Mandal, D.; Senapati, S.; Sainkar, S.R.; Khan, M.I.; Ramani, R.; Parischa, R.; Ajayakumar, P.V.; Alam, M.; Sastry, M.; Kumar, R. *Angew Chem Int Ed.* **2001**, *40*, 3585.

20. Mukherjee, P.; Ahmad, A.; Mandal, D.; Senapati, S.; Sainkar, S.R.; Khan, M.I.; Pasricha, R.; Ajaykumar, P.V.; Alam, M.; Kumar, R.; Sastry, M. *Nano Lett.* **2001**, *1*, 515.

21. Shiying, He.; Guo, Z.; Zhang, Y.; Zhang, S.; Wang, J.; Gu, N. *Materials Letters.* **2007**, *61*, 3984.

22. Ahmad, A.; Senapati, S.; Khan, M.I.; Kumar, R.; Sastry, M.; *Langmuir.* **2003**, *19*, 3550.

23. Ahmad, A.; Senapati, S.; Khan, M.I.; Kumar, R.; Sastry, M. *J Biomed Nanotech.* **2005**, *1,* 47.

24. Shankar, S.S.; Ahmad, A.; Pasricha, R.; Sastry, M. *J. Mater. Chem.* **2003**, *13*, 1822.

25. Shankar, S.S.; Rai, A.; Ankamwar, B.; Singh, A.; Ahmad, A.; Sastry, M. *Nat. Mater.* **2004**, *3*, 482.

26. Bhattacharya, R.; Murkherjee, P. *Adv Drug Deliv Rev*. **2008**, *60*, 1289.

27. Gao, J.; Liang, G.; Zhang, B.; Kuang, Y.; Zhang, X.; Xu, B. *J Am Chem Soc.* **2007**, *129*, 1428.

28. Rashamuse, K.J.; Whiteley, C.G. *Appl Micro Biotech.* **2007**, *75*, 1429.

29. Riddin, T.L.; Gericke, M.; Whiteley, C.G. *Nanotechnology.* **2006**, *17*, 3482.

30. Song, J.Y.; Kwon, E.Y.; Kim, B.S. *Bioprocess Biosyst Eng.* **2010**, *33*, 159.

31. Govender, Y.; Riddin, T.; Gericke, M.; Whiteley, C.G. *Biotechnol Lett.* **2009**, *31*, 95.

32. Venu, R.; Ramulu, T.S.; Anandakumar, S.; Rani V.S.; Kim, C.G. *Colloids and Surfaces A: Physicochemical and Engineering Aspects.* **2011**, *384 (1-3)*, 733.

33. Mandal, S.; Selvakannan, P.R.; Roy,D.; Chaudhari, R. V.; Sastry, M. *Chem. Commun.* **2002**, 3002.

Chapter 3

Biological synthesis of quantum dots using fungus

Summary:

The growing demand for semiconductor (quantum dots) nanoparticles has fueled significant research in developing strategies for their synthesis and characterization. Quantum dots (Q dots) are extensively investigated by the chemical route; on the other hand, use of microbial sources for biosynthesis witnessed the highly stable, water dispersible nanoparticles formation. We report, for the first time, an efficient fungal-mediated synthesis of highly fluorescent CdTe quantum dots at ambient conditions by the fungus *Fusarium oxysporum* when reacted with a mixture of $CdCl_2$ and $TeCl_4$. Characterization of biosynthesized CdTe nanoparticles was carried out by different techniques such as Ultraviolet-visible (UV-Vis) spectroscopy, Photoluminescence (PL), X-ray Diffraction (XRD), X-ray Photoelectron Spectroscopy (XPS) and Transmission Electron Microscopy (TEM). Biosynthesized nanoparticles are capped by a protein layer which was confirmed by Fourier Transformed Infrared Spectroscopy (FTIR) analysis. CdTe nanoparticles showed significant antibacterial activity against Gram positive and Gram negative bacteria. Cell viability assay was carried out on NIH3T3 mouse embryonic fibroblast cell line. The fungal based fabrication provides an economical, green chemistry approach for the production of highly fluorescent CdTe quantum dots.

Introduction:

Semiconductor nanocrystals, also known as quantum dots (QDs), are nanosized particles composed of II-VI group or III-V main group elements. Q dots have gained a lot of attention for their unique electronic and optical properties resulting due to quantum confinement effects (1, 2). Over the past decades, efforts have been made to study different functionalities such as size, shape and chemical compositions (3-6). The semiconductors have been applied to various technological areas which include biological labels (7, 8), optoelectronics (9) and solar cells (10). Optical properties can be tuned by simply changing the size of nanoparticles and this also possesses potential application in cell labeling (11), cell tracking (12), in vivo imaging (13), diagnostics and DNA detection (14).

Cadmium telluride (CdTe), an important II-VI group semiconductor material with large exciton Bohr radius (7.3 nm) and narrow bulk band gap of 1.5 eV has shown significant potential for LED (energy), FRET (electronics), and biomedical applications (9, 15-17) due to their size dependent properties. CdTe quantum dots provide excellent photostability, narrow emission and high quantum yield in comparison with organic dyes, therefore explored in live cell bio-imaging (18). Organometallic method (3, 19, 20) and aqueous (water based) method (21-24) with thiols as capping agent are the two most useful protocols developed for the production of CdTe quantum dot nanoparticles. Moreover, these processes require high temperature and employ highly toxic chemicals, such as trioctylphosphane or tri-octylphosphane oxide. To address this concern, surface of the quantum dots need to be functionalized with proteins or biocompatible layers in order to decrease toxicity and then can be utilized in imaging and labeling (6, 25). Therefore, a novel, rational, cost effective and reproducible process is needed for the scalable synthesis of CdTe nanoparticles.

Biological routes have been employed to synthesize quantum dots with controlled sizes, shapes and other functionalities (25). Many organisms are reported for the synthesis of semiconductor nanoparticles, such as ZnS nanoparticles by sulfate-reducing bacteria, *Rhodobacter sphaeroides* (26). *Fusarium oxysporum* (27), *Schizosaccharomyces pombe* (28), *Rhodopseudomonas palustris* (29) and *Escherichia coli* (30), have been developed for synthesis of CdS nanoparticles. PbS nanoparticles have been synthesized by *Torulopsis* sp. (31). Holmes and co-workers have

demonstrated that the exposure of Cd^{2+} ions to the bacterium, *Klebsiella aerogenes* results in the intracellular formation of CdS nanoparticles in the size range of 20-200 nm (32). Dameron and coworkers reported that the yeasts such as *Schizosaccharomyces pombe* and *Candida glabrata* produced intracellular CdS nanoparticles when challenged with aqueous solution of cadmium salt (33). These biosynthesis processes occur at ambient conditions and are considered as environment friendly methods. Recently, CdSe nanoparticles have been synthesized intracellular by using yeast. For the isolation of intracellular nanoparticles, complicated procedures are required which include cell washing, cell disruption and removal of cell fragments for getting CdSe nanoparticles (34). In order to avoid the above complications Scientist started screening of extracellular inorganic nanomaterials using biological methods. Extracellular CdSe nanoparticle synthesis has been reported by the fungus *Fusarium oxysorum* (35). Very recently, lead sulfide nanoparticles were biosynthesized by lead resistant marine yeast *Rhodosporidium diobovatum* (36). To the best of our knowledge, this is the first demonstration of fungal-mediated approach for the synthesis of CdTe QDs.

Present work emphasizes on the use of fungus *Fusarium oxysporum* to biosynthesize CdTe (quantum dot) nanoparticles. The process utilizes Cd and Te precursors in a very dilute form and allows bottom up, one-step preparation of CdTe quantum dot nanoparticles. Different techniques were employed for their characterization such as SAED and XRD which confirmed the crystalline nature of biosynthesized CdTe nanoparticles. Biosynthesized CdTe nanoparticles are capped by proteins, secreted by the fungi in the reaction mixture, which makes CdTe nanoparticles water dispersible and provides stability in solution by preventing their agglomeration. These CdTe nanoparticles also showed antibacterial activity against Gram positive and Gram negative bacteria. Cell viability assay was carried out on NIH3T3 mouse embryonic fibroblast cell line. Fungus based approach provides a novel, rational and environment friendly synthesis protocol for nanomaterial synthesis.

Materials and Methods:

Materials:

Cadmium chloride ($CdCl_2$) and Tellurium tetrachloride ($TeCl_4$) were obtained from Sigma Aldrich. Malt extract, Yeast extract, Glucose and Peptone were obtained from HiMedia and used as-received.

Fungal growth and maintenance:

The fungus *Fusarium oxysporum* was maintained on Potato Dextrose Agar [PDA (potato 25% w/v, dextrose 2% w/v, and agar agar 2% w/v)] slants at 25^0C. Stock cultures were maintained by subculturing at monthly intervals. The fungus was grown at pH 7.0 and 25^0C for 5 days, the slants were preserved at 15^0C. From an actively growing stock culture, subcultures were made on fresh slants and after 5 days of incubation at pH 7.0 and 25^0C, were used as the starting material for synthesis of nanoparticles.

Extracellular biosynthesis of Cadmium telluride (CdTe) nanoparticles:

For the synthesis of quantum dot nanoparticles, the fungus was grown in 500 mL Erlenmeyer flasks each containing MGYP media (100 mL) composed of malt extract (0.3 %), glucose (1.0 %), yeast extract (0.3 %) and peptone (0.5 %) at $25\text{-}27^0$C under shaking condition at 200 rpm for 96 hr. After 96 hr of fermentation, mycelia were separated from the culture broth by centrifugation (5000 rpm) at 10^0C for 20 min and then the mycelia were washed thrice with sterile distilled water under sterile conditions. The harvested mycelial mass (20 g of wet mycelia) was then resuspended in 100 mL of aqueous solution of 1mM $CdCl_2$ and 1mM $TeCl_4$ solutions in 500 mL Erlenmeyer flasks and the same was put onto a shaker at $25\text{-}27^0$C (200 rpm). The reaction was carried out for a period of 96 hr and fungal biomass was separated by filterpaper to collect biomass and filtrate in sterile conditions. Periodically, aliquots of the reaction solution were removed and subjected to UV-Vis spectroscopy and fluorescence spectroscopy to check the formation of nanoparticles extracellularly.

Characterization of biosynthesized CdTe nanoparticles:

Various aliquots of the biosynthesized nanoparticles solution were collected during the course of reaction, by separating the fungal mycelia from the aqueous component by simple filtration. UV-Vis spectrophotometric measurements performed on a Shimadzu dual-beam spectrophotometer (model UV-1601 PC) operated at a

resolution of 1 nm. Fluorescence measurements were carried out using Perkin-Elmer LS 50B luminescence spectrophotometer. The diluted biosynthesized nanoparticles solution was drop cast on a carbon coated copper grid and analyzed using Transmission Electron Microscope-FEI Technai G2 system operated at an accelerating voltage of 80 kV at room temperature. The Selected Area Electron Diffraction (SAED) analysis was carried on the same grid. Thin films of the nanoparticles were drop casted on glass substrates and then subjected to X-ray diffraction analysis and data was recorded on Panalytical 'X' Pert PRO system, while X-ray photoelectron spectrum was recorded on VG MicroTech ESCA 3000 instrument. FTIR spectrum of biosynthesized nanoparticles solution was recorded on a Perkin Elmer Spectrum One B in diffuse reflectance (DRS) mode at a resolution of 2 cm^{-1}. Energy Dispersive Analysis of X-ray (EDAX) was carried out on a Leica Stereoscan-440 SEM equipped with a Phoenix EDX attachment. EDX spectrum was recorded in the spot-profile mode by focusing the electron beam onto a region on the surface coated with nanoparticles. Thermogravimetric analysis of nanoparticles was carried-out using the Q5000 V2.4 Build 223 instrument by TA Instruments at the scan rate 10^0C min^{-1} in N$_2$ environment.

Antibacterial activity:

The bacterial cultures *Staphylococcus aureus* NCIM 2079, *Bacillus subtilis* NCIM 2063, *Escherichia coli* NCIM 2065 and *Pseudomonas aeruginosa* NCIM 2200 used for the antibacterial activity were from our in-house culture collection unit, the National Collection of Industrial Microorganisms (NCIM), Pune, India. Evaluation of antibacterial activity of CdTe nanoparticles was carried out by filter paper bioassay (37). For antibacterial activity, bacterial culture were inoculated in nutrient broth and incubated at 37^0C for 24 hr. From the actively growing bacterial culture broth, 100 µl (0.1ml) of bacterial suspension (with a concentration of 10^5 CFU/ml) was mixed with half strength nutrient broth (0.9 ml) and was immediately overlaid on the surface of the sterile nutrient agar plates (90 mm diameter) and incubated at 37^0C for some time for initial growth. Sterile filter paper discs (Whatman No. 3: 10mm sq. cm) were placed on agar plates and then loaded with 50 µl suspension of CdTe nanoparticles of different concentrations. These plates were incubated for 24 hr. and visually monitored for the zone of inhibition. Filter paper disc on nutrient agar plate without

nanoparticles suspension was used as a control. After incubation, the zone of inhibition was measured in millimeter across the filter paper.

Cell Viability Assay:

The effect of nanoparticles on the proliferation of NIH3T3 mouse embryonic fibroblast cell line was assessed by MTT assay. Briefly, the cells (2×10^4 for NIH3T3) were grown in 96-well plates and were treated with varying concentrations of nanoparticles (0-500 µg/ml) for 24 hr at 37^0C. The cells were further incubated with MTT (0.5 mg/ml) at 37^0C for 3 hr followed by addition of 200 µl of isopropanol. The color intensity was measured at 570 nm using an enzyme linked immunosorbent assay (ELISA) reader. The experiments were performed in triplicates. The cell viability was plotted as percent of control (38).

Results and Discussions:

The fungus, *Fusarium oxysporum* when reacted with aqueous solution of $CdCl_2$ and $TeCl_4$ at room temperature for 96 hr under shaking condition on a rotary shaker (200 rpm) resulted in the formation of highly stable, water dispersible and fluorescent CdTe nanoparticles.

UV-Vis spectroscopy of CdTe nanoparticles:

The UV-Vis spectrum recorded for the biosynthesized CdTe nanoparticles solution, after the reaction with precursor solution is shown in Figure 1A, this showed notable feature around 400-450 nm for CdTe nanocrystals (39). The Tauc plot (Fig 1B) obtained from this data shows that the bandgap of CdTe nanoparticles is 2.61 eV. The inset of Fig 1 shows glass vials of the $CdCl_2$ and $TeCl_4$ reaction solution at the beginning (time t=0, glass vial on the left side) and after 96 hr of reaction (glass vial on the right side) with the fungus *Fusarium oxysporum*. The change in the color of the solution from colorless to dark yellow after reaction is due to the excitation of Surface Plasmon Resonance (SPR) of CdTe nanoparticles. Absorption between 270-280 nm suggests the presence of proteins in the reaction mixture (Fig 1). These secreted proteins capped the nanoparticles surface and made them water dispersible and stable.
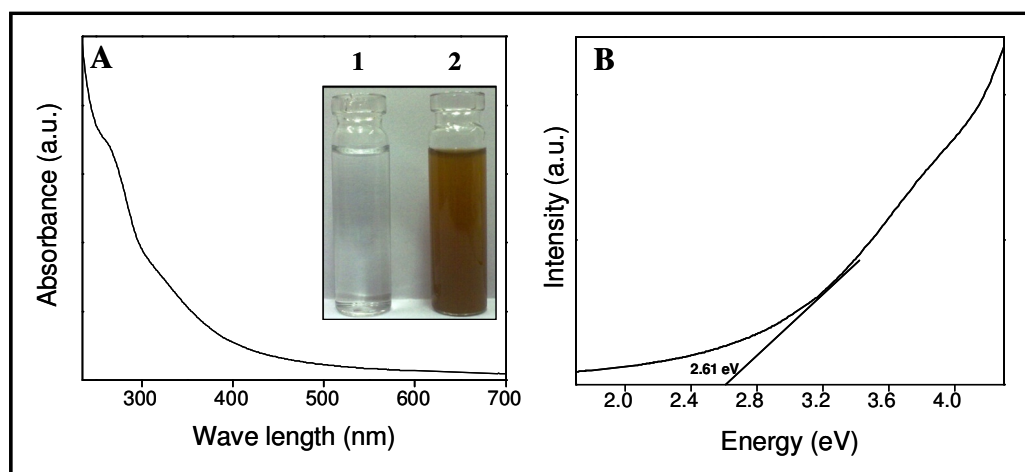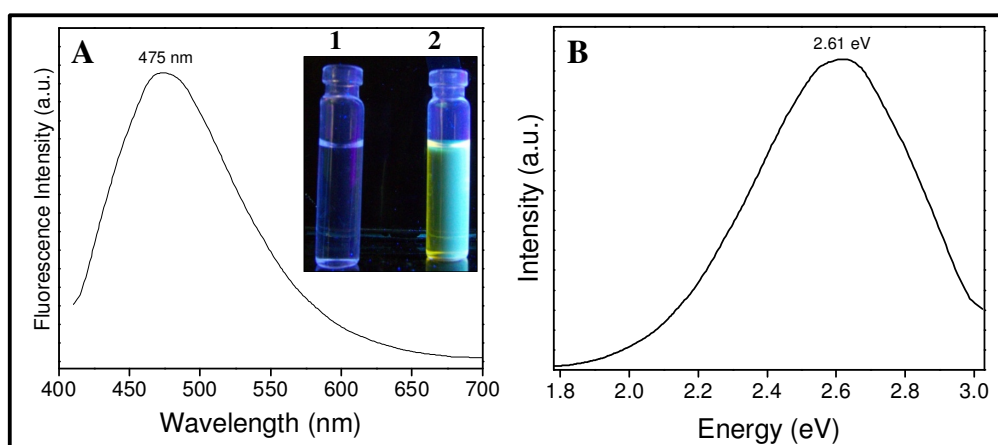

Fig 1: A) UV-Vis spectrum of extracellular CdTe nanoparticles, the inset shows glass vial containing $CdCl_2$ and $TeCl_4$ solution before (glass vial on the left side) and after reaction with the fungal biomass for 4 days (glass vial on the right side). B). Taucs plot for the CdTe quantum dot nanoparticles.

Fluorescence measurements of CdTe nanoparticles:

Fluorescence measurement of the biosynthesized CdTe nanoparticles was studied by exciting the reaction mixture at 400 nm. As shown in Fig. 2A, the biosynthesized QDs possess strong fluorescence emission band centered at 475 nm, which is in good agreement with nanoparticles synthesized by chemical methods. The inset of Fig 2 A shows glass vials containing $CdCl_2$ and $TeCl_4$ reaction solution at the beginning (time t=0, glass vial on the left side) and after 96 hr of reaction (glass vial on the right side). When the solution of nanoparticles was illuminated with a 365 nm lamp, an intense green luminescence was seen (the inset of Fig 2 A, glass vial on the right side). Green luminescence is significant for several applications and a subject of intense scientific research. The Tauc plot (Fig 2B) obtained from fluorescence data shows that the bandgap of nanoparticles is close to 2.6 eV.

Fig 2: A) Fluorescence emission spectrum of extracellular CdTe nanoparticles. The inset shows glass vial containing $CdCl_2$ and $TeCl_4$ solution before (glass vial on the left) and after reaction with the fungal biomass for 4 days (glass vial on the right) B). Tauc's plot derived from the fluorescence data.

Transmission Electron Microscopy of CdTe nanoparticles:

The TEM analysis of the CdTe nanoparticles showed that they are in the size range of 15-20 nm. The morphology of the nanoparticles was essentially spherical (Fig 3 A). Fig 3. B shows the Selected Area Electron Diffraction (SAED) pattern obtained from CdTe nanoparticles shown in Fig 3 A. The Scherrer ring pattern characteristic of face centered cubic (fcc), CdTe is clearly observed, showing that the structures seen in TEM images are nanocrystalline in nature.
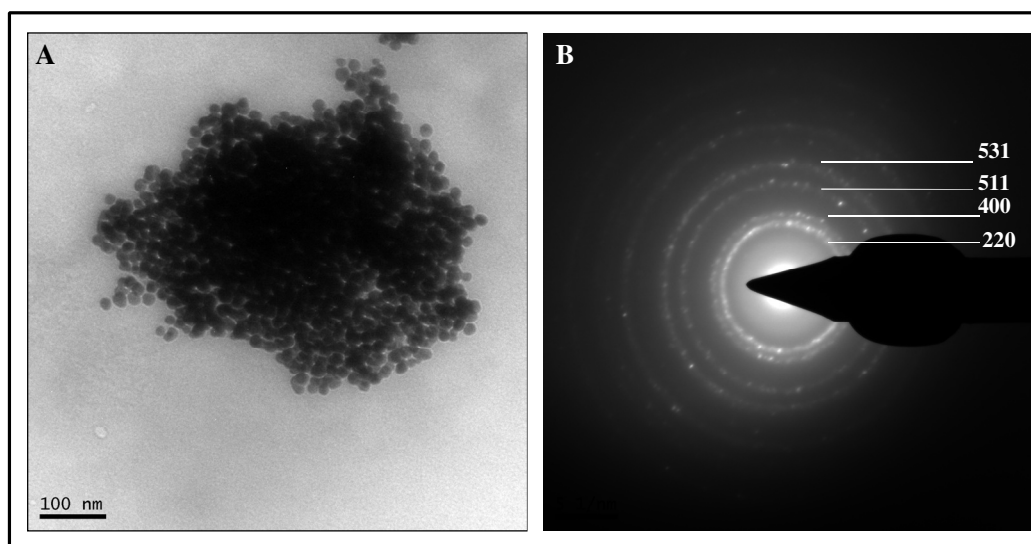
Fig 3: A) TEM micrograph of CdTe nanoparticles and B). SAED pattern recorded from extracellular CdTe nanoparticles shown in Fig 3 A.

X-ray Diffraction analysis of CdTe nanoparticles:

X-ray diffraction (XRD) analysis of these biosynthesized CdTe nanoparticles was carried out by depositing them as a thin film on a glass substrate (Fig 4) which showed intense peaks corresponding to (111), (220) and (311) planes in the 2 θ range of 15 θ-60 θ and agree with the standard diffraction pattern for CdTe nanocrystals (40). The broadening of Bragg's peaks indicates that the particles formed are in nanoscale dimensions.
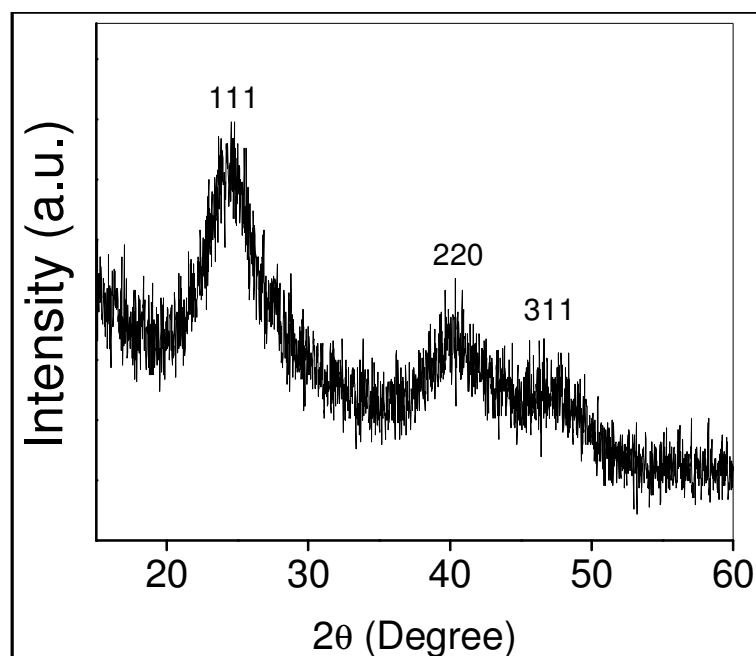
Fig 4: XRD pattern of extracellular CdTe nanoparticles.

X-ray photoelectron spectroscopy of CdTe nanoparticles:

The presence of CdTe nanoparticles was also confirmed by analyzing the sample by XPS as shown in Fig 5. The results showed the presence of Cd, Te, C, O, N as the prominent elements. In Figure 5, background corrected XPS was presented for the CdTe nanoparticles. Peaks correspond to chemically distinct C 1s core levels (Fig 5 A) originating from the α-carbon and –COOH groups present in the proteins with binding energies 285 and 286.5 eV respectively. The peak (in Fig 5B) corresponds to chemically distinct O 1s core level transition with binding energy 532 eV of proteins. The Cd 3d spectrum (Fig 5C) could be decomposed into two spin-orbit components 1 and 2 (spin-orbit splitting ~ 6.6 eV). The Cd $3d_{5/2}$ and $3d_{3/2}$ peaks occurred at binding energies of 406.6 eV and 413.2 eV respectively, which agrees with the core level binding energies and are characteristic of metallic Cd. Moreover, the binding energies of 573.19 eV and 585.2eV for Te 3d peak are comparable to the core level binding energies and are typical for metallic Te (Fig. 5D). The XPS data clearly indicates that all the Cd Te metal ions are fully reduced by the fungus *Fusarium oxysporum* and are in metallic form. These findings are comparable and in good agreement with the reported literature (41).
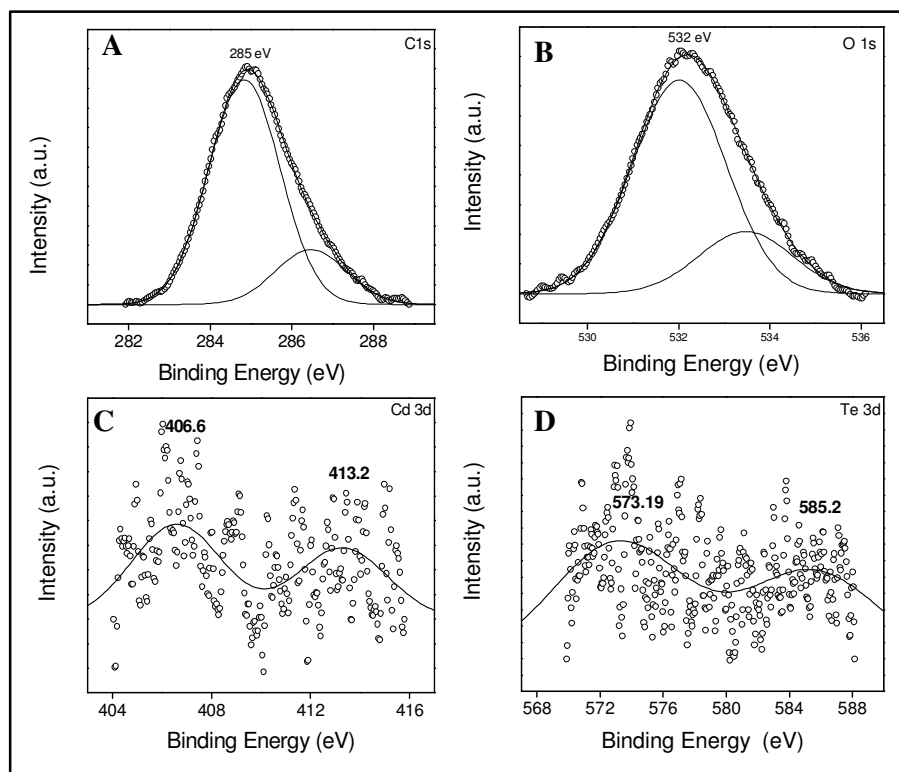
Fig 5: XPS analysis of extracellular CdTe nanoparticles.

Fourier transform infrared spectroscopy of CdTe nanoparticles:

FTIR analysis was performed to determine the nature of the present protein on the surface of nanoparticles. The presence of two bands in the region 1644 and 1530 cm^{-1} assigned to amide bands I and II respectively of proteins (Fig 6). Similar results were reported in our previous reports on the synthesis of CdS nanoparticles by *Fusarium oxysporum* (27). The data provide some insights on the nature of the capping layer of nanoparticles surface, which may be further utilized for biofunctionalization for different applications.
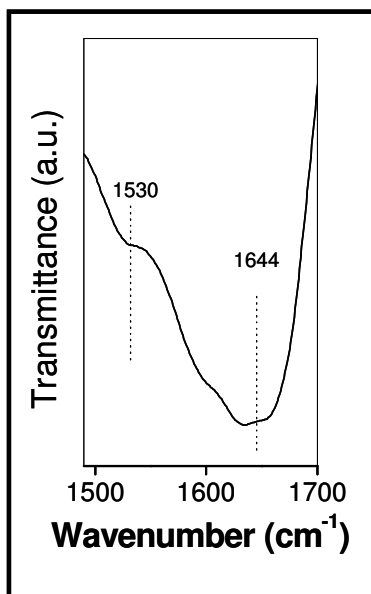
Fig 6: FTIR analysis of extracellular CdTe nanoparticles.

Energy Dispersive Analysis of X-ray (EDAX) of CdTe nanoparticles:

EDAX spectrum in Fig 7 shows the spot profile mode from one of the densely populated CdTe nanoparticle regions on the surface. Signals are observed from C, O, Cd and Te. The C and O signals are likely to be due to X-ray emission from proteins/ enzymes present on to the nanoparticles surface.
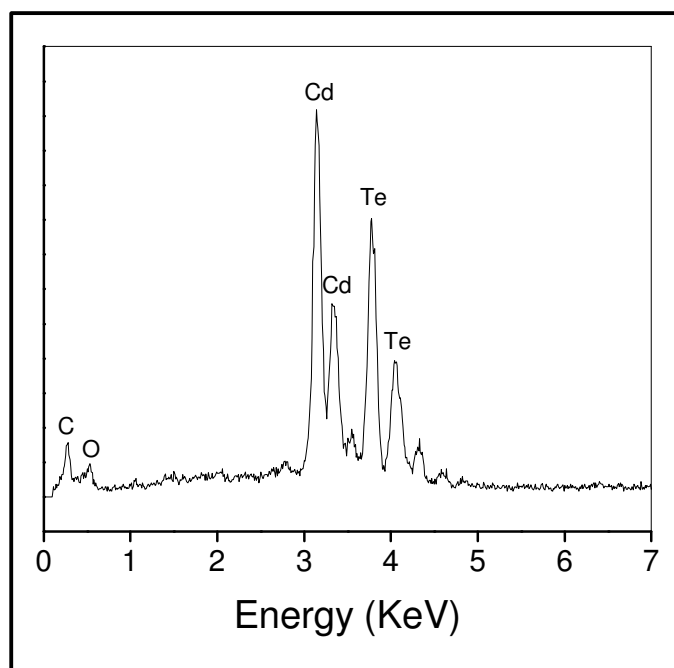

Fig 7: EDAX spectrum for extracellular CdTe nanoparticles.

Thermogravimetric analysis of CdTe nanoparticles:

As mentioned earlier, the nanoparticles synthesized by fungal based route are capped by protein layer that stabilize them against aggregation. To further estimate the amount of pure CdTe nanoparticles, thermogravimetric analysis (TGA) was performed. TGA plot from biosynthesized CdTe nanoparticles show weight loss (30%) in the range of 200-250^{0}C, corresponding to release of water vapour and some biomolecules which are loosely bound to the surface of nanoparticles. Therefore, a total of 30 % weight loss was recorded after heating up to 500^{0}C. Beyond 500^{0}C there was no indication for any weight loss for the nanoparticles, thus the rest 70% weight to be of pure CdTe nanoparticles.
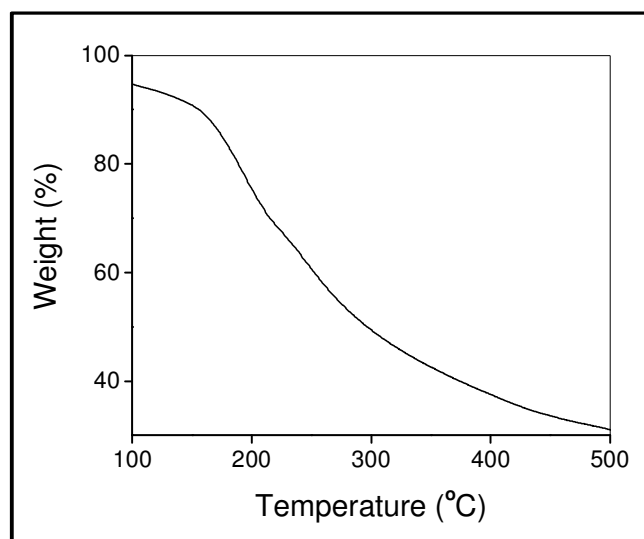

Fig 8: TGA analysis of extracellular CdTe nanoparticles.

Antibacterial activity of CdTe nanoparticles:

Antibacterial activity was performed against Gram positive (*Staphylococcus aureus* and *Bacillus subtilis*) and Gram negative bacteria (*Escherichia coli* and *Pseudomonas aeruginosa*) with different concentration of CdTe nanoparticles (100 µg, 500 µg and 1000 µg). CdTe nanoparticles showed growth inhibition against these bacteria (Fig 9 and Fig 10). The growth inhibition in terms of zone of inhibition was estimated and presented in table 1.
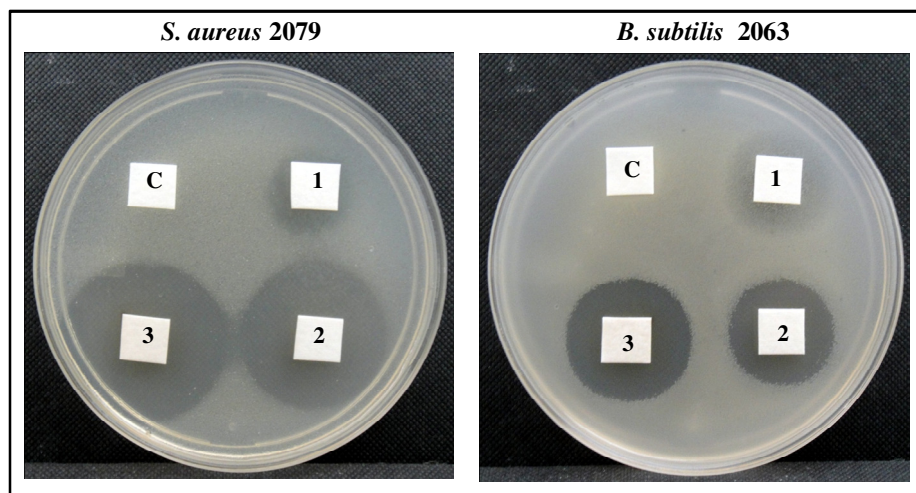
Fig 9: Antibacterial activity of CdTe nanoparticles against Gram positive bacteria (viz *Staphylococcus aureus* NCIM 2079 and *Bacillus subtilis* NCIM 2063) C: Control, Different concentrations (1: 100 µg, 2: 500 µg and 3: 1000 µg).
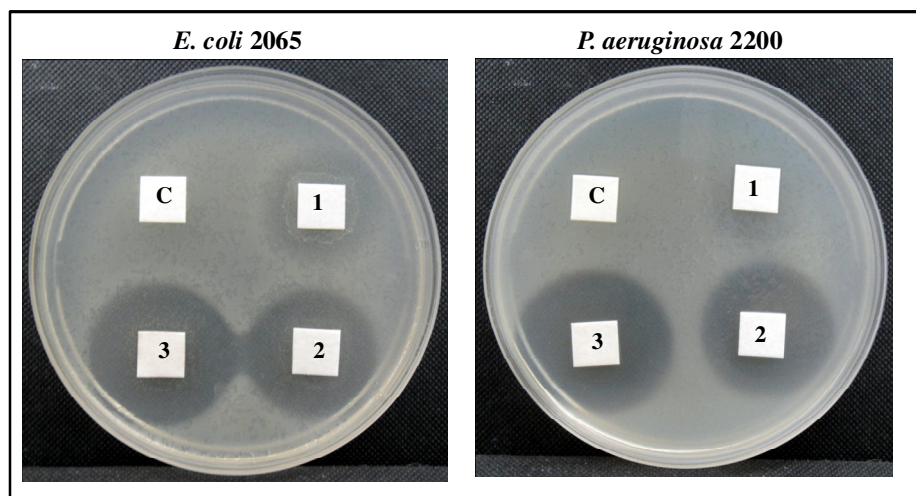

Fig 10: Antibacterial activity of CdTe nanoparticles against Gram negative bacteria (viz *Escherichia coli* NCIM 2065 and *Pseudomonas aeruginosa* NCIM 2200) C: Control, Different concentration (1:100 µg, 2: 500 µg and 3:1000 µg).

Table 1: Antibacterial activity in terms of zone of inhibition of CdTe nanoparticles against bacterial cultures was presented.

Organism	Concentrations/ Zone of Inhibition		
	100 µg	500 µg	1000 µg
Gram positive bacteria			
Staphylococcus aureus (NCIM 2079)	17 mm	30 mm	35 mm
Bacillus subtilis (NCIM 2063)	-	22 mm	26 mm
Gram negative bacteria			
Escherichia coli (NCIM 2065)	-	29 mm	33 mm
Pseudomonas aeruginosa (NCIM 2200)	-	27 mm	30 mm

Cell viability assay of CdTe nanoparticles:

The effect of CdTe nanoparticles on the cell viability of NIH3T3 mouse embryonic fibroblast cell line was checked by MTT assay. The cells were treated with varying concentrations of CdTe nanoparticles (50µg/ml, 250µg/ml and 5000 µg/ml) for 24 hr. The cell viability was reduced in a dose-dependent manner and the cytotoxicity of the nanoparticle was observed from concentrations of 50µg/ml. The cell viability was reduced by 37.57%, 59.18%, and 64.22% at 50µg/ml, 250µg/ml and 500 µg/ml concentrations respectively.
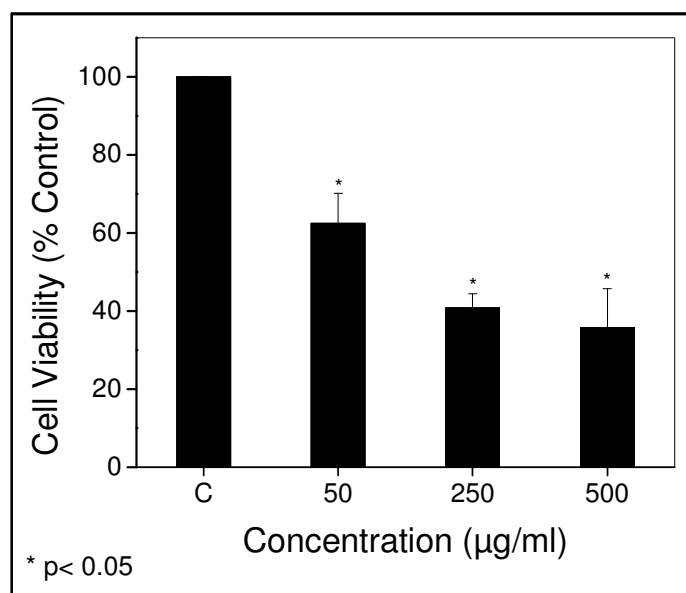

Fig 11: Cell viability assay of CdTe nanoparticles against NIH3T3 mouse embryonic fibroblast cell line. The data represented in the form of a bar graph and plotted using means + S.E. of triplicate determinations. The values were analyzed by Student's *t*-test ($p < 0.005$), statistical analysis, P values for significantly different means, *P < 0.005 and **P > 0.05 vs control.

We have established the extracellular biosynthesis of technologically important CdS semiconductor nanoparticles by the fungus *Fusarium oxysporum* by a purely enzymatic process (27). The fungus *Fusarium oxysporum* secretes some enzymes like sulfite reductase and capping proteins in the reaction mixture. The process has been discussed in greater details in our earlier reports. Purified enzymes from the same fungus *Fusarium oxysporum* viz. Sulfite reductase and Nitrate reductase was employed for the *in vitro* synthesis of gold and silver nanoparticles respectively (42, 43). We observe that the similar mechanism is also involved in the biosynthesis of CdTe nanoparticles but more research needs to be carried out to confirm the mechanism proposed above.

Conclusion:

In conclusion, the present investigation for the first time demonstrates a novel, rational, eco-friendly, efficient and most importantly an extracellular biosynthetic process for the synthesis of CdTe quantum dot nanoparticles. The synthesized nanoparticles are crystalline in nature and capped with a protein layer, that makes them water dispersible and stable toward aggregation. CdTe nanoparticles were characterized by different techniques such as UV-visible spectroscopy, fluorescence measurements, XRD, XPS, TEM, etc. These CdTe nanoparticles showed significant antibacterial activity against Gram positive and Gram negative bacteria. Cell viability assay also showed the reduction in the cell viability for these CdTe nanoparticles at different concentrations.

References:

1. Alivisatos, A.P. *J Phys Chem.* **1996**, *100*, 13226.

2. Alivisatos, A.P. *Science.* **1996**, *271*, 933.

3. Murray, C.B.; Norris, D.J.; Bawendi, M.G. *J Am Chem Soc.* **1993**, *115*, 8706.

4. Peng, X.G.; Manna, L.; Yang, W.D.; Wickham, J.; Scher, E.; Kadavanich, A.; Alivisatos, A.P. *Nature.* **2000**, *404*, 59.

5. Manna, L.; Scher, E.C.; Alivisatos, A.P. *J Cluster Sci.* **2002**, *13*, 521.

6. Zheng, Y.G.; Yang, Z.C.; Ying, J.Y. *Adv Mater.* **2007**, *19*, 1475.

7. Chen, C.; Peng, J; Xia, H.S.; Yang, G.F.; Wu, Q.S.; Chen, L.D.; Zeng, L.B.; Zhang, Z.L.; Pang, D.W.; Li, Y. *Biomaterials.* **2009**, *30*, 2912.

8. Idris, N.M.; Li, Z.; Ye, L.; Sim, E.K.W.; Mahendran, R.; Ho, P.C.L.; Zhang, Y. *Biomaterials.* **2009**, *30*, 5104.

9. Gaponik, N.P.; Talapin, D.V.; Rogach, A.L. *Phys Chem Chem Phys.* **1999**, *1*, 1787.

10. Huynh, W.U.; Dittmer, J.J.; Alivisatos, A.P. *Science.* **2002**, *295*, 2425.

11. Wu, X.; Liu, H.; Liu, J.; Haley, K. N.; Treadway, J. A.; Larson, J. P.; Ge, N.; Peale, F.; Bruchez, M. P. *Nature Biotechnol.* **2003**, *21*, 41.

12. Parak, W. J.; Boudreau, R.; Gros, M. L.; Gerion, D.; Zanchet, D.; Micheel, C. M.; Williams, S. C.; Alivisatos, A. P.; Larabell, C. *Adv. Mater.* **2002**, *14*, 882.

13. Dubertret, B.; Skourides, P.; Norris, D. J.; Noireaux, V.; Brivanlou, A. H.; Libchaber, A. *Science.* **2002**, *298*, 1759.

14. (a) Taylor, J. R.; Fang, M. M.; Nie, S. *Anal. Chem.* **2000**, *72*, 1979. (b) Xu, H.; Sha, M. Y.; Wong, E. Y.; Uphoff, J.; Xu,Y.; Treadway, J. A.; Truong, A.; O'Brien, E.; Asquith, S.; Stubbins, M.; Spurr, N. K.; Lai, E.; Mahoney, H. W. *Nucleic Acids Res.* **2003**, *31*, e 43.

15. Li, J.I.; Ha, K.S.; Yoo, H.S. *Acta Biomater.* **2008**, *4*, 791.

16. Li, R.; Li, C.M; Bao, H.F.; Bao, Q.L.; Lee, V.S. *Appl Phys Lett.* **2007**, *91,* 223901.

17. Yang, Y.J. ; Tao, X. ; Hou, Q. ; Chen, J.F. *Acta Biomater.* **2009**, *5,* 3488.

18. Pan, J.; Feng, S.S. *Biomaterials.* **2009**, *30*, 1176.

19. Peng, Z.A.; Peng, X.G. *J Am Chem Soc.* **2001**, *123*, 183.

20. Talapin, D.V.; Haubold, S.; Rogach, A.L.; Kornowski, A.; Haase, M.; Weller H. *J Phys Chem B.* **2001**, *105*, 2260.

21. Rogach, A.L.; Katsikas, L.; Kornowski, A.; Su, D.S.; Eychmuller, A.; Weller H. *Ber Bunsen-Ges Phys Chem.* **1996**, *100*, 1772.

22. Zhang, H.; Wang, L.P.; Xiong, H.M.; Hu, L.H.; Yang, B.; Li, W. *Adv Mater.* **2003**, *15*, 1712.

23. Bao, H.F.; Wang, E.K.; Dong, S.J. *Small.* **2006**, *2*, 476.

24. Bao, H.F.; Cui, X.Q.; Li, C.M.; Zang, J.F. *Nanotechnology.* **2007**, *18*, 455701.

25. Dahl, J.A.; Maddux, B.L.S.; Hutchison, J.E. *Chem Rev.* **2007**, *107*, 2228.

26. Bai, H.J.; Zhang, Z.M.; Gong, J. *Biotechnol Lett.* **2006**, *28*, 1135.

27. Ahmad, A.; Mukherjee, P.; Mandal, D.; Senapati, S.; Khan, M.I.; Kumar, R.; et al. *J Am Chem Soc.* **2002**, *124*, 12108.

28. Kowshik, M.; Deshmukh, N.; Vogel, W.; Urban, J.; Kulkarni, S.K.; Paknikar, K.M. *Biotechnol Bioeng.* **2002**, *78*, 583.

29. Bai, H.J.; Zhang, Z.M.; Guo, Y.; Yang, G.E. *Colloid Surfaces B Biointerfaces.* **2009**, *70*, 142.

30. Sweeney, R.Y.; Mao, C.B.; Gao, X.X.; Burt, J.L.; Belcher, A.M.; Georgiou, G.; et al. *Chem Biol.* **2004**, *11*, 1553.

31. Kowshik, M.; Vogel, W.; Urban, J.; Kulkarni, S.K.; Paknikar, K.M. *Adv Mater.* **2002**, *14*, 815.

32. (a) Holmes, J. D.; Smith, P. R.; Evans-Gowing, R.; Richardson, D. J.; Russell, D. A.; Sodeau, J. R. *Arch. Microbiol.* **1995**, *163*, 143. (b) Smith, P. R.; Holmes, J. D.; Richardson, D. J.; Russell, D. A.; Sodeau, J. R. *J. Chem. Soc. Faraday. Trans.* **1998**, *94*, 1235.

33. Dameron, C. T.; Reese, R. N.; Mehra, R. K.; Kortan, A. R.; Carroll, P. J.; Steigerwald, M. L.; Brus, L. E.; Winge, D. R. *Nature.* **1989**, *338*, 596.

34. Cui R et al. *Adv Funct Mater*, **2009**,*19*,2359.

35. Anil, S. Kumar.; Ansary, A. A.; Ahmad A.; Khan, M. I. *J. Biomed. Nanotechnol*, **2007**, *3*, 190.

36. Seshadri, S.; Saranya, K.; Kowshik, M. *Biotechnol Prog.* **2011**, DOI: 10.1002/btpr.651.

37. Bauer, A.W.; Kirby, W.M.; Sherris, J.C.; Turck, M. *Am J Clin Pathol.* **1965**. *45(4),* 493.

38. Philip, S.; Kundu, G.C. *J. Biol Chem.* **2003**, *278 (16)*, 14487.

39. Greene, Ivan. A.; Fanxin, Wu.; Zhang, Jin Z.; Shaowei, Chen. *J. Phys. Chem. B,* **2003**, *107,* 5733.

40. Gaponik, N. A.; Talapin, D. V.; Rogach, A. L.; Hoppe, K.; Shevchenko, E. V.; Kornowski, A.; Eychmuller, A.; Weller, H. *J. Phys. Chem. B.* **2002,** *106,* 7177.

41. Zhang, Hao.; Yang, Bai. *Thin Solid Films.* **2002**, *418,* 169.

42. Anil, S. Kumar.; Abyaneh, M. K.; Gosavi,S. W.; Kulkarni,S. K.; Ahmad, A.; Khan, M. I. *Biotechnol. Appl. Biochem.* **2007**, *47*, 191.

43. Anil, S. Kumar.; Abyaneh, M. K.; Gosavi, S. W.; Kulkarni, S. K.; Pasricha, R.; Ahmad, A.; Khan, M. I. *Biotechnol Lett.* **2007**, *29*, 439.

Chapter 4

Silicate nanoparticles by bioleaching of glass and modification of the glass surface

Summary:

Bioleaching is examined as a low temperature (50^0C), soft chemical approach to nanosynthesis and surface processing. We demonstrate that fungus based bioleaching of borosilicate glass enables synthesis of nearly monodispersed ultrafine (~5±0.5 nm) silicate nanoparticles. Using various techniques such as X-ray diffraction, X-ray photoelectron spectroscopy and FTIR, we compare the constitution and composition of the nanoparticles with that of the parent glass and establish the basic similarities between the two. The bioleaching process is shown to enhance the non-bridging oxygen component and correspondingly influence the Si–O–Si network. The root mean square roughness of glass surface is seen to increase from 1.27 nm for bare glass to 2.52 nm for 15 hr fungal processed case, this increase being equivalent to that for glass annealed at 500^0C.

Introduction:

Bioleaching is a well-known process in the context of metal extraction from minerals (1-7). However, its unique low temperature, soft processing green chemistry capabilities has hardly been exploited in the context of nanosynthesis and nanoscale surface processing. Indeed, biofluids generated by micro-organisms contain multiple organic acids capable of controlled slow leaching of elements and proteins which can dynamically cap and control the growth of molecular complexes, rendering the right conditions for the synthesis of capped ultrafine nanoparticles. Most importantly, this can be implemented at or near room temperature in an environment friendly manner.

In case of complex compounds such as multicomponent oxides, sulphides, carbonates etc. valence-controlled synthesis of stoichiometric nanosized particles is difficult because at low temperatures the proper phase may not form due to limitations of phase equilibria and at high temperatures the particle size can not be easily controlled within the nano-regime. In such cases, a promising approach is to start with a bulk source of the compound, either naturally extracted or synthesized by high temperature processing and subject it to stoichiometric extraction and nanosynthesis. Given the properties of biofluids described above, bioleaching and biotransformation clearly offer a viable top–down route to near room temperature nanosynthesis of such complex systems.

Glass is a complex functional material that is found in diversified applications ranging from window panes, optical gadgets, watches, contact lenses and goggles, bioactive glasses for tissue engineering, energy systems, chemical containers and microfluidic channels (8-10). It is therefore of great interest to synthesize nanoparticles of glass for potential use as filler or additive materials in composites, paints etc. or for biomedical applications. Glasses are of various types with varying chemical compositions and microstructural properties. It is of interest then to examine whether and to what degree a top-down nanosynthesis approach can transfer the composition and constitution from the bulk glass to the synthesized nanoparticles. In this work we have used borosilicate glass for bio-processing and have shown that the nanoparticles thus synthesized have a glassy state along with the desired inclusion of boron. Borosilicate glass is a heat resistant glass with a very low thermal expansion coefficient (one third of normal glass) and a low refractive index across the visible range. The corresponding nanoparticles may also find interesting applications exploiting these

unique properties. Finally, we have also examined the bio-processed glass surface for any modifications.

Since the present work concerns fungal processing of glass, a few remarks may be made about the available background knowledge related to bio-processing especially in the context of bioleaching (1-3, 5, 6). Although bioleaching is accomplished by several micro-organisms, its effectiveness varies for different organisms and ambient conditions. Bacteria and fungi have attracted particular attention in this regard. Several mechanisms such as acidolysis, complexolysis, redoxolysis and bioaccumulation are suggested to be involved in bioleaching. Compared to bacterial leaching, fungal leaching has advantages of the ability to grow under higher pH, thereby being more suitable in bioleaching of alkaline solids and rendering a relatively faster leaching. Acidolysis is shown to be the principal mechanism in bioleaching with *Aspergillus niger* (1, 11). The fungus has been reported to produce organic acids, which include citric, oxalic and gluconic acids during bioleaching. In bioleaching of sand, a two step process involving leaching of silica in the form of silicic acid followed by hydrolysis of silicate complexes has been suggested (12). In other studies, the mechanism of fungal bioleaching is suggested to be complex and not simply a direct chemical attack on the minerals. Indeed, the micro-organism is suggested to participate in the process actively (4). For example, as bioleaching proceeds and the chemical constitution of the ambient evolve, live bio-organism can dynamically change the battery of chemicals it can secrete. This has been suggested to be the case for bioleaching of minerals using *Aspergillus* sp. and *Penicillium* sp. (4).

Materials and Methods:

Materials:

Glass cover slip (commercially available borosilicate cover slips), malt extract, yeast extract, glucose and peptone were obtained from HiMedia and used as-received.

Extracellular bioleaching of glass cover slip by *Humicola lanuginosa*:

For the extracellular bioleaching of glass cover slips a novel alkalotolerant and thermophilic fungus, *Humicola lanuginosa* was isolated from self-heating compost from Pune district of Maharashtra, India. It was maintained on MGYP (malt extract, glucose, yeast extract, and peptone) agar slants. Stock cultures were maintained by sub culturing at monthly intervals. After growing the fungus at pH 9 and 50^0C for 4 days, the slants were preserved at a temperature of 15^0C. From an actively growing stock culture, subcultures were made on fresh slants and after 4 days of incubation at pH 9 and 50^0C, the same were used as the starting material for fermentation experiments. For the bioleaching of glass slides, the fungus was grown in 250 mL Erlenmeyer flasks containing 50 mL of MGYP medium which is composed of malt extract (0.3%), glucose (1%), yeast extract (0.3%), and peptone (0.5%). Sterile 10% sodium carbonate was used to adjust the pH of the medium to 9. After the pH of the medium was adjusted, the culture was grown with continuous shaking on a rotary shaker (200 rpm) at 50^0C for 96 h. After 96 h of fermentation, mycelia were separated from the culture broth by centrifugation (5000 rpm) at 20^0C for 20 min and then the mycelia were washed thrice with sterile distilled water under sterile conditions. The harvested mycelial mass (20 g of wet mycelia) was then resuspended in 100 mL of distilled water in 250 mL Erlenmeyer flasks at pH 9. Several glass slides (commercially available borosilicate cover slips) were then added to the solution and the same was put into a shaker at 50^0C (200 rpm) and maintained in the dark.

Characterization of bioleached nanoparticles:

The various fractions of the bioleached solution (used for the treatment of the glass cover slips) were collected during the course of reaction, by separating the fungal mycelia from the aqueous component by filtration. The diluted bioleached solution was drop cast on a carbon coated copper grid and analyzed using Transmission Electron Microscope JEOL model 1200 EX instrument operated at an accelerating voltage of 120 kV at room temperature. HRTEM images were also obtained using FEI

Technai G^2 system. FTIR spectra of all samples were recorded on Perkin Elmer spectrum one B in diffuse reflectance (DRS) mode. The AFM images were also recorded using Veeco multimode SPM Model-Nanoscope-IV to reveal and estimate the surface roughness changes due to fungal processing. X-ray diffraction data were recorded on Panalytical 'X' Pert PRO system, while X-ray photoelectron spectra were recorded on VG MicroTech ESCA 3000 instrument at a pressure $<1 \times 10^{-9}$ Torr.

Results and Discussions:

First, we analyzed the extracted solution for its contents. The corresponding transmission electron micrographs (Fig.1 and the insets) bring out the formation of very tiny ($\sim 5 \pm 0.5$ nm) and nearly monodispersed nanoparticles by the bioleaching process. The histogram shown in the top inset clearly brings out the extremely narrow nanoparticle size distribution. As stated earlier, in addition to organic acids, the biofluids also have a set of proteins which play the role of capping agents in the process. As the dissolved components get into the solution, they form reactive molecular complexes (that eventually lead to the inorganic nanoparticles) that are also dynamically capped by the proteins present. This arrests the growth of the complexes and hence that of the corresponding nanoparticles thus formed. Preliminary gel electrophoresis measurements indicate that the fungus secretion exhibits four distinct protein related bands, distinct with respect to their electro-mobility; the latter being a collective function of their molecular weights, mobility and other characteristics. One or more of such proteins may be the enzymes that act as the leaching agents as well as the capping agents for the extracted silicate nanoparticles (NPs). The presence of high concentration of such functionalizable proteins should explain the tiny size of the nanoparticles.
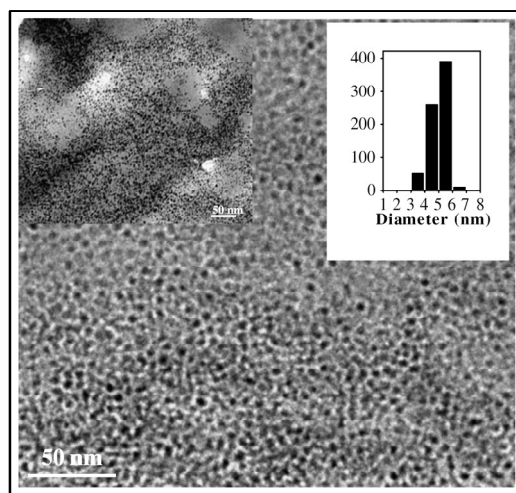

Fig.1. Transmission electron micrographs of the nanoparticles obtained by bioleaching of glass and biotransformation

In order to confirm the constitution of the nanoparticles, X-ray diffraction, FTIR and X-ray photoelectron spectroscopy (XPS) techniques were employed. The X-ray diffraction data shown in Fig. 2 compare the patterns for the parent glass (a), the as-extracted nanoparticles (b) and the nanoparticles sintered at $500^{0}C$ (c). The characteristics of the parent glass and those of as-extracted nanoparticles compare favourably, although there are small differences in details, which can be attributed to structural relaxations that can be expected in ultrafine nanoparticles (13). In particular, the primary lattice reflection is more weighted towards smaller 2θ or larger d-value. For the annealed NP sample a host of well-defined peak structures are seen to develop. These can be appropriately marked by various peaks corresponding to silica, silicate and boron oxide phases (JCPDS card PDF # 43-1300, 27-0784, 44-1085). This shows that the as-extracted nanoparticles do represent an amorphous glassy network phase comprising of various elements such as Si, Na, B and O resembling the parent glass and the same get decomposed upon annealing at high temperature. It is very interesting that most elements in the parent compound are extracted into the synthesized nanoparticles by the bioleaching process. This shows that the presence of multiple complex etchants in a biofluid have the collective ability to activate nearly stoichiometric extraction and biotransformation.
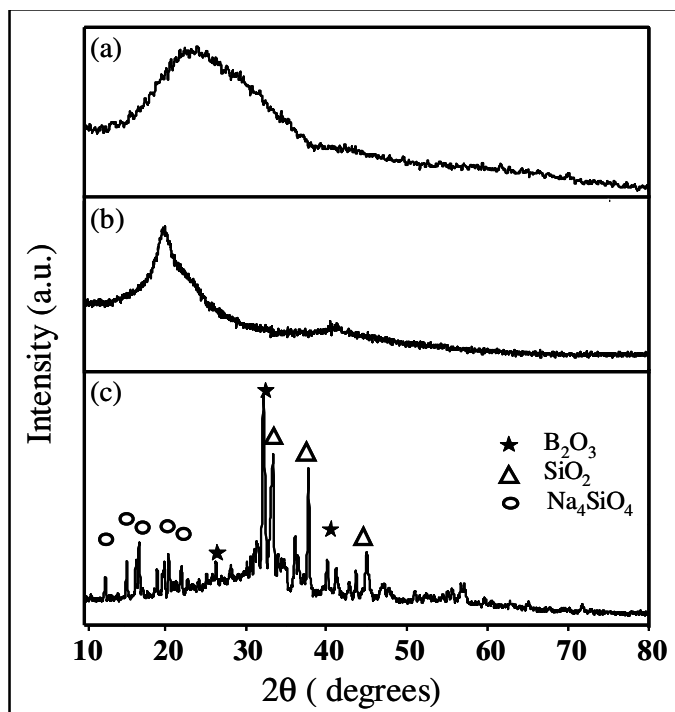

Fig.2. Comparison of X-ray diffraction patterns of (a) parent glass, (b) as-extracted nanoparticles and (c) nanoparticles sintered at $500\ ^{0}C$.

FTIR measurements were done to identify the specific bonding configurations in the samples. The specific interest was to examine whether boron related bonds are present in the NPs which could qualify it as a borosilicate rather than just silica (SiO_2) NPs. Thus, in Fig. 3(A) we compare the FTIR spectra in the cases of as-extracted (a) and 500^0C annealed (b) NPs. We also present in the same figure the FTIR data for pure silica (SiO_2) NPs (c) synthesized in our laboratory by chemical methods, and commercial B_2O_3 (d) for comparison. The various stretching and bending modes identified in the published literature have also been indicated (14-17). These data suggest presence of the signatures of v Si–O–Si, δ B–O–Si, v B–O–Si and v B–O bonds. This implies that the extracted nanoparticles are of borosilicate type. The presence of boron in the extracted nanoparticles was further confirmed by XPS. The corresponding data for the parent glass (a) and the drop cast film of extracted NPs (b) on the zirconia substrate are shown in Fig. 3(B). The signatures at 190.68 eV and 191.32 eV in the two cases correspond to boron (B 1s), albeit shifted due to small differences in the nature of bonding between the bulk and the nanoparticles (18, 19). Upon annealing, the peaks are seen to evolve and shift as expected and indicated by the four arrows. For instance, the signature indicated by "4" (which is better defined than that in curve "a") is close to but shifted with reference to the corresponding sharper signature in curve "c" for pure silica particles. Similarly signature "1" is close to that in B_2O_3 and "3" overlaps well with those in curves "c" and "d" for pure silica and B_2O_3. This is consistent with the evolution suggested by XRD upon annealing wherein phases of SiO_2 and B_2O_3 are seen to form.
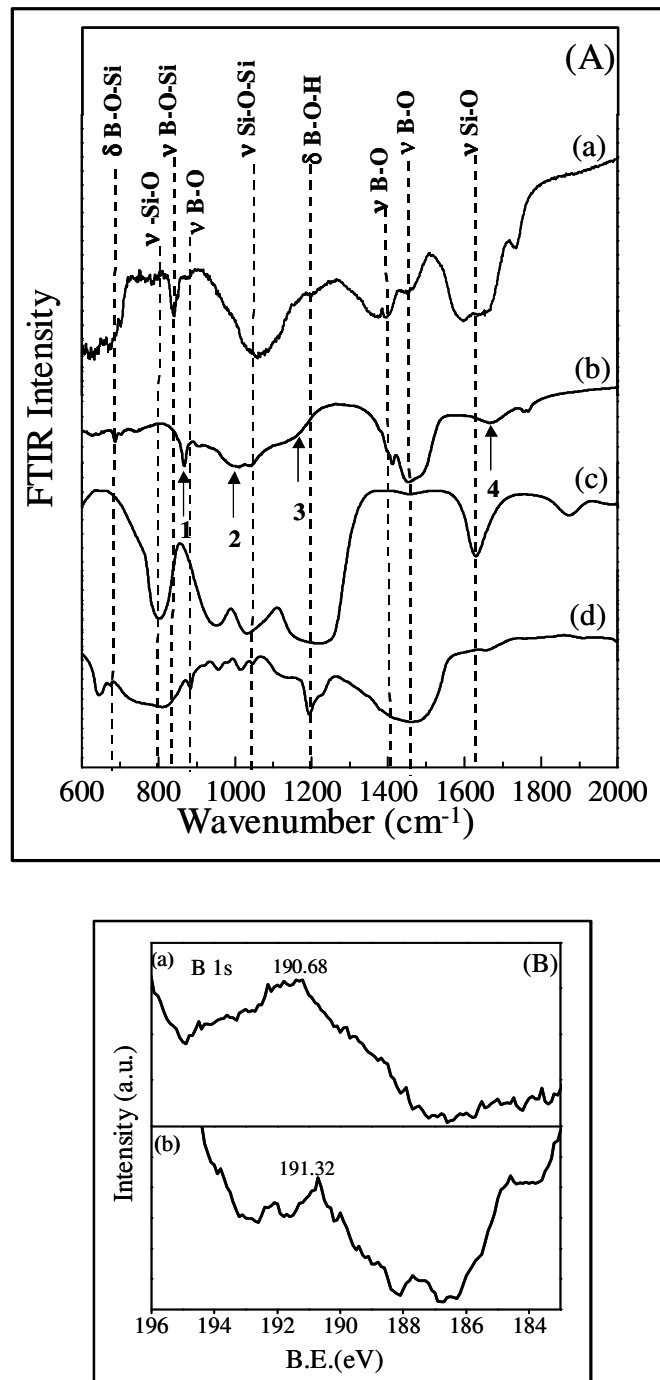
Fig 3. (A) Comparsion of FTIR data for (a) as-extracted silicate nanoparticles, (b) nanoparticles after annealing at 500^0C, (c) silica (SiO_2) nanoparticles (100 nm) prepared by Stober's method, and (d) commercial B_2O_3 powder; (B) X-ray photoelectron spectroscopy data for boron (B 1s) for (a) parent glass and (b) drop cast film of extracted nanoparticles on zirconia substrate.

In Fig. 4 we present the state of other elements seen in the XPS spectra of the parent glass, the extracted nanoparticles (drop cast film) and the bioleached glass surface. In the parent glass (a) case, characteristic Si 2p and O 1s peaks are observed at binding energy values of 103.2 eV and 532.64 eV, respectively, as expected. Interestingly, in the case of the drop cast NPs film (b) and the fungal processed glass surface (c) additional peaks appear on the lower binding energy side for both Si 2p and O 1s at 99.12 eV and 528.87 eV respectively. Moreover, shifts in the main peak positions toward lower energy are also observed, the shifts being slightly higher for the nanoparticles as expected due to relaxations. We also observed increase in the C 1s contribution toward its low energy side. But since it appears in the same region as that for adventitious carbon resulting from system hydrocarbon, it can simply be due to the enhanced adsorption area due to roughness as well as due to the extra proteins.
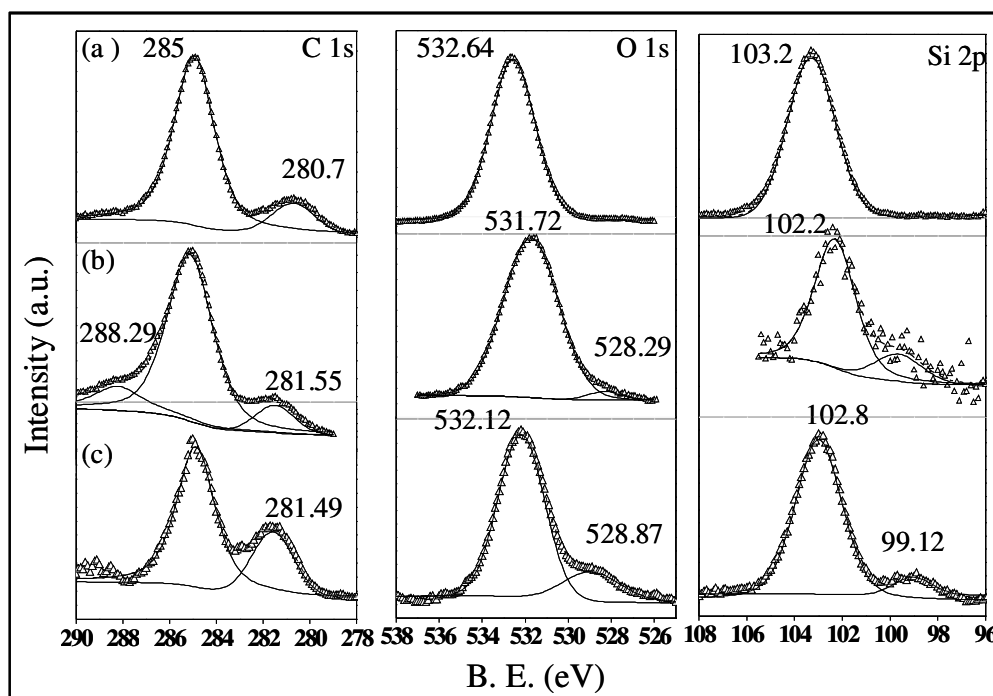

Fig. 4. X-ray photoelectron spectroscopy data for (a) parent glass, (b) the drop cast film of as-extracted nanoparticles on zirconia substrate, and (c) bioleached glass respectively; the triangles represent the experimental data and the solid lines represent the fits to the data.

Significant, compositionally dependent changes are known to occur in the O 1s spectra of glass samples. Previous studies have established that the larger binding energy peak ($\sim$532 eV) in the spectrum is due to bridging oxygen (BO) which is covalently bound to two silicon atoms (Si–O–Si) and the smaller binding energy peak ($\sim$529 eV) is due to non-bridging oxygen (NBO) which is covalently bound to one silicon and ionically bound to an alkali ion such as sodium (Si–O–Na) (20-23). Indeed, the intensities of the photoelectrons from these oxygen types bonded in different ways and the corresponding relative chemical shifts could be correlated with alkali and alkaline earth oxide contents and with the related cation field strengths. Moreover, the ionic binding character introduced into the glass networks by the alkali and alkaline earth ions is a non-localized effect as not only the NBO atoms but the BOs are influenced as well (25). With increasing alkali element fraction, the line positions are shifted to lower binding energy side (26). The intensity ratio of NBO/BO and their energy separation depends on the content of the silica network modifier introducing NBO. The XPS and FTIR data thus together imply that chemical modifications, especially the enhancements of NBO accompanies the bioleaching process and is present in the NPs as well as the processed glass surface.

Fig. 5 (A) compares the atomic force micrographs (AFM) for the parent [A (a)] and fungal processed (15 h) glass cover slips [A (b)]. The root mean square roughness was seen to increase from 1.27 nm for bare glass to 2.52 nm for 15 h processed case. It has been reported that root mean square (RMS) roughness of this order is generated on the glass surface by high temperature annealing at temperatures above 500^{0}C (24). It is very interesting that the same is generated by fungal processing at 50^{0}C. We also compared the FTIR spectra for the same two cases of interest [Fig. 5(B)]. When normalized at long wavelength, the spectra shows significant changes in the 500–1200 cm^{-1} region and small differences in the neighbourhood of 1800–2600 cm^{-1}. The spectral features in low frequency region are known to result from the Si–O–Si network (stretching mode in the range 1000–1300 cm^{-1}, Si–O–Si bending vibrations around 800 cm^{-1} etc.) (20, 25, 26). Thus, the network is clearly influenced by fungal processing and represents an important aspect of chemical modifications. We believe that the mild and controlled surface modification of glass by fungal processing may have applications in different fields.
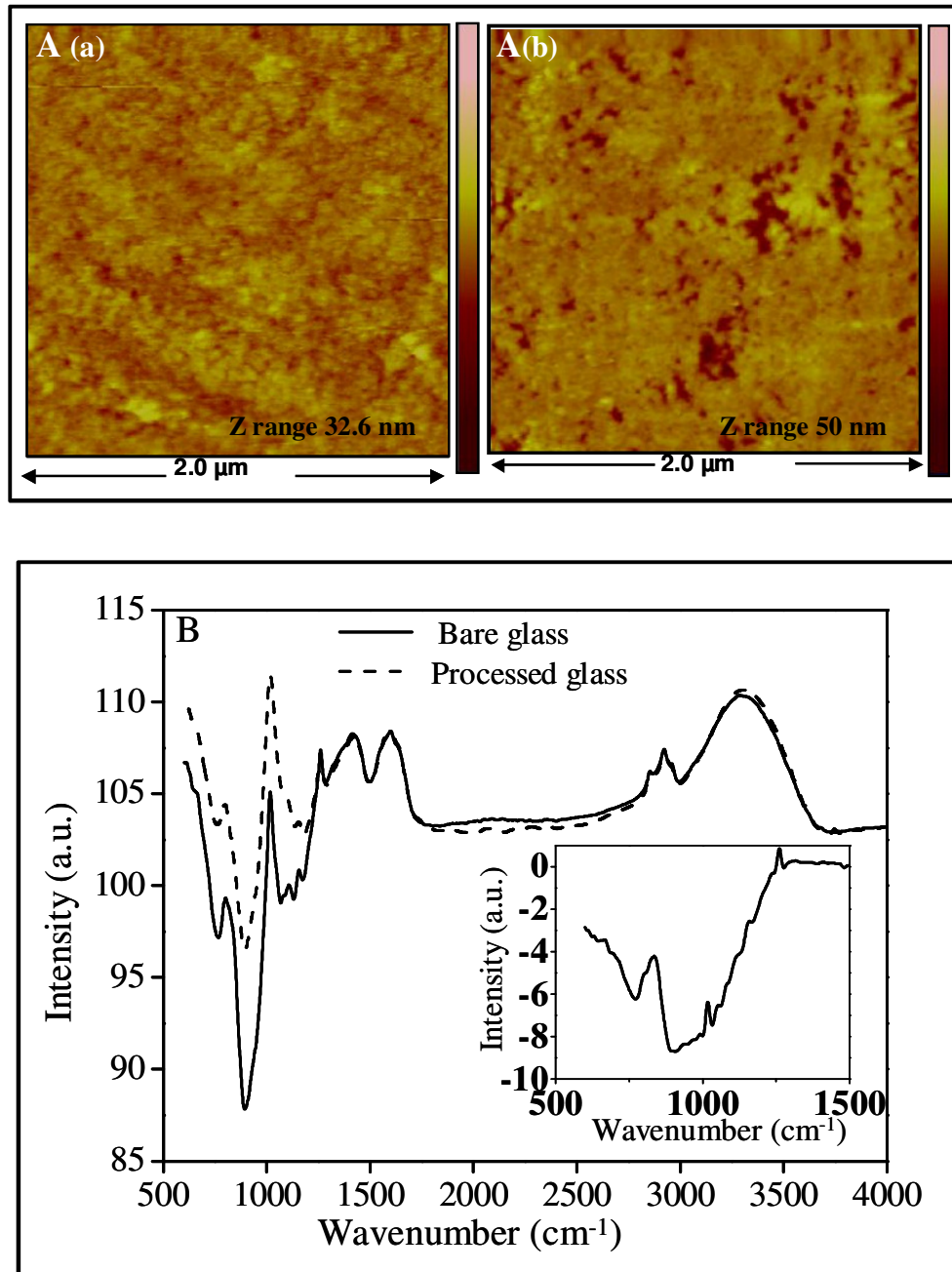
Fig.5. (A) Atomic Force micrographs (AFM) and (B) FTIR spectra, respectively, for (a) the parent glass and (b) fungal processed (15 hr) glass cover slips.

Conclusions:

In conclusion, we have demonstrated the use of fungus based bioleaching for the synthesis of water dispersible, nearly monodispersed ultrafine ($\sim 5 \pm 0.5$ nm) silicate nanoparticles coated with a naturally secreted protein and have shown that the processed glass surface also undergoes significant morpho-chemical modification. Various characterizations are used to demonstrate that fairly stoichiometric extraction and nanosynthesis are possible by bioleaching and biotransformation.

References:

1. Mulligan, C.N.; Kamali, M. *J. Chem. Technol. Biotechnol.* **2003**, *78*, 497.

2. Rawlings, D.E. *J. Ind. Microbiol. Biotechnol.* **1998**, *20*, 268.

3. Hung-Yee Wu.; Yen-Peng Ting, *Enzyme Microbial Technol.* **2006**, *38*, 839.

4. Valix, M.; Usai,F.; Malik, R. *Minerals Eng.* **2001**, *14*, 197.

5. Ehrlich, H.L.*Chem. Geol.* **1996**, *132*, 5.

6. Styriakova, I.; Styriak, I.; Nandakumar, M. P.; Mattiasson, B. *J. Microbiol. Biotechnol.* **2003**, *19*, 583.

7. Moira, E.K.; Henderson, K.; Duff, R.B. *J. Soil Sci.* **1963**, *14*, 236.

8. Boyd, D.C.; MacDowell, J.F. *Adv. Ceram.* **1986**, *18*, 157.

9. Duparré, A.; Flemming, M.; Steinert, R. J.; Fraunhofer, K. *IOF Annual Report*, **2001**, *38*.

10. Xynos, I.D.; Hukkanen, M.V.J.; Batten, J.J.; Buttery, L.D.; Hench, L.L.; Polak, J.M. *Calcified Tissue Int.* **2000**, *67*, 321.

11. Hall, N.; Tomsett, A.B. *Microbiology.* **2000**, *146*, 1399.

12. Bansal, V.; Sanyal, A.; Rautaray, D.; Ahmad, A.; Sastry, M. *Adv. Mater.* **2005**, *17*, 889.

13. Pe´ rez-Pariente, J.; Balas, F.; Vallet-Regi, M. *Chem. Mater.* **2000**, *12*, 750.

14. Canevali, C.; Scotti, R.; Vedda, A.; Mattoni, M.; Morazzoni, F.; Armelao, L.; Barreca, D.; Bottaro, G. *Chem. Mater.* **2004**, *16*, 315.

15. Soraru, G. D.; Dallabona, N.; Gervais, C.; Babonneau, F. *Chem. Mater.* **1999**, *11*, 910.

16. Moon, O.M.; Kamg, B.C.; Lee, S.B.; Boo, J.H. *Thin Solid Films.* **2004**, *464*, 64.

17. Yang, Q.; Sha, J.; Wang, L.; Zou,Yu.; Niu, J.; Cui, C.; Yang, D. *Physica E.* **2005**, *27*, 319.

18. Ennaceur, M.M.; Terreault, B. *J. Nucl. Mater.* **2000**, *280*, 33.

19. Belyansky,M.; Trenary, M. *Surf. Sci. Spectra.* **1995**, *3*, 147.

20. Mekki, A.; Holland, D.; MacConville; C.F. *J. Non-Cryst. Solids.* **1997**, *215*, 271.

21. Miura, Y.; Kusano, H.; Nanba, T.; Matsumoto, S. *J. Non-Cryst. Solids.* **2001**, *290*, 1.

22. Brückner, R.; Chun, H.U.; Goretzki, H.; Sammet, M. *J. Non-Cryst. Solids.* **1980**, *42*, 49.

23. Zemek, J.; Jiricek, P.; Gedeon, O.; Lesiak, B.; Jozwik, A. *J. Non-Cryst. Solids.* **2005**, *351*, 1665.

24. Jang, H.K.; Whangbo, S.W.; Choi, Y.K.; Jeong, K.; Whang, C.N.; Wang, C.H.; Choi Lee, D.J.S. *J. Non-Cryst. Solids.* **2001**, *296*, 182.

25. Serra, J.; Gonzalez, P.; Liste, S.; Serra, C.; Chiussi, S.; Leon, B.; Perez- Amor, M.; Ylanen Hupa, H.O.M. *J. Non-Cryst. Solids.* **2003**, *332*, 20.

26. Agarwal, A.; Tomozawa, M. *J. Non-Cryst. Solids.* **1997**, *209*,166.

Chapter 5

Physical manipulation of biological and chemical syntheses for nanoparticle shape and size control

Summary:

A nanosynthesis scheme is demonstrated which renders excellent control of nanoparticle shape, size and dispersity in a solution based synthesis process. The scheme termed as percolative microcavity synthesis, involves the use of a granular medium with percolative microcavities which facilitate nearly similar grain size/shape dependent reaction zones limiting intrinsic growth inhomogeneities and enabling particle size/shape control. The viability of the process is demonstrated for the synthesis of gold nanoparticles by a plant extract based biological method as well as a chemical method.

Introduction:

In view of the projected range of applications of nanomaterials, nanosynthesis has acquired great prominence recently (1-7). Although several approaches lead to nanoparticle (NP) formation, controlling their size, shape and dispersity concurrently is a persistent challenge. Here we propose and demonstrate a simple concept to achieve such control via percolative microcavity synthesis. The percolative network ensures fluid connectivity facilitating bulk synthesis while confining the reaction zone to a matrix of nearly identical tiny cells. Since the size and shape of the microcavities depend on the size and shape of the grains, the nanosynthesis can be expected to be controllably influenced in such cavities. Even in processes which already lead to monodispersity, the suggested process can lead to size control. We apply this concept to gold nanoparticle synthesis by a plant extract based method (8, 9) as well as a pure chemical synthesis method (10).

Figure 1 shows a sketch which compares the conventional route of direct chemical mixing with the suggested percolative multicavity synthesis (PMCS) process. In the direct chemical mixing, there is no limit on the molecular/radical flux accessible to any nucleated nanoparticle that could control its growth. Thus, unless the nucleation is rather abrupt and homogeneous in space, it is hard to expect monodispersity. On the other hand, the cellular division of the reaction zone as envisaged in a PMCS process can distribute the flow fluxes as well as the nuclei getting formed by these fluxes homogeneously without disconnecting them. This should ensure dispersity control. It is also to be expected that the size of the synthesized nanoparticles should depend on the dimensions of the cavity and the reactant concentrations. Another interesting natural consequence of the PMCS process is the nanoparticle growth on the surfaces of the granules, a case of heterogeneous nucleation of interest to several applications involving catalysis, creation of adherent and bioactive surfaces, functional composites, complex fluids, etc.
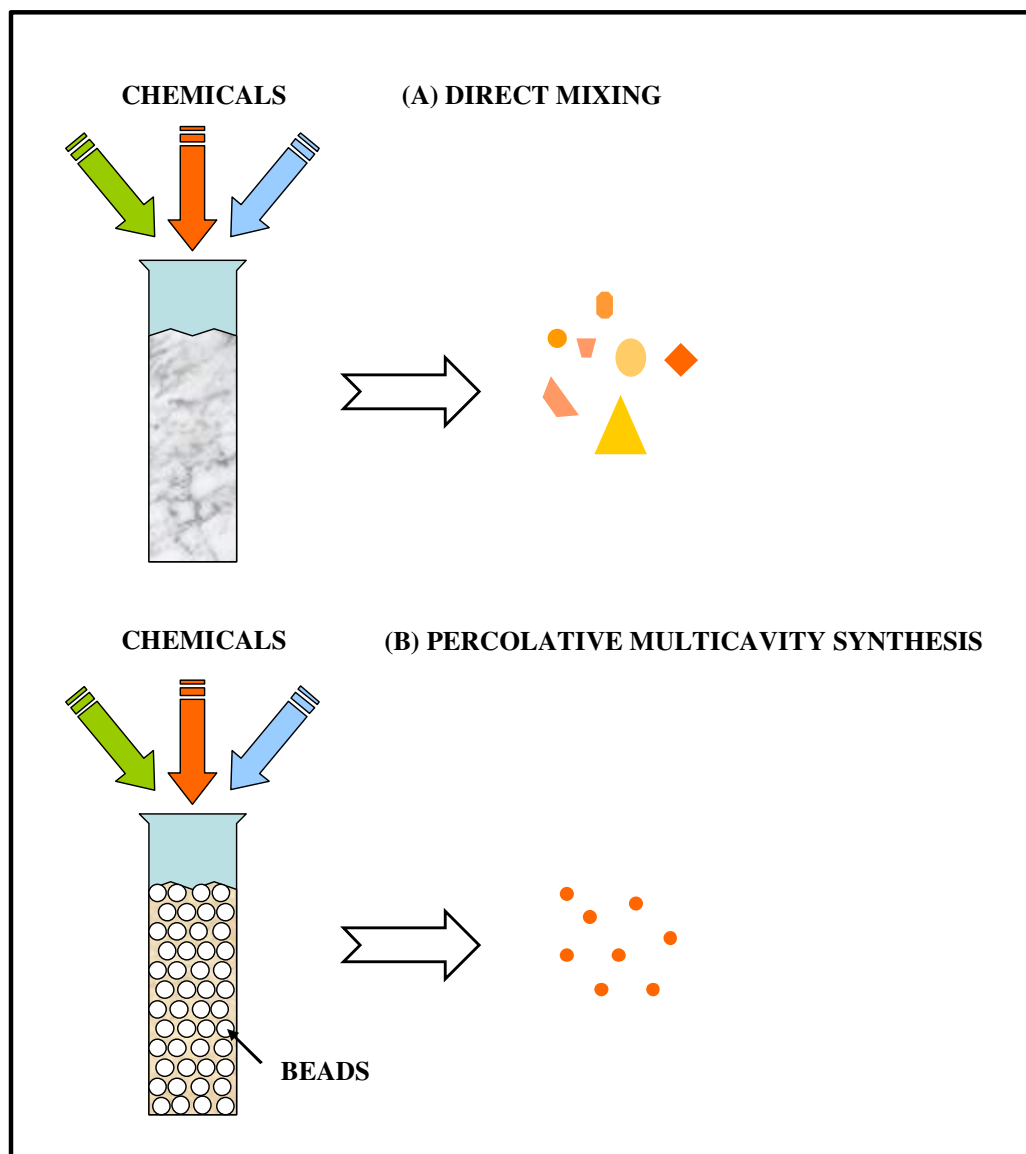
Fig 1:

Fig.1. Sketch comparing the suggested percolative multicavity synthesis (PMCS) process with the conventional route of direct chemical mixing

Materials and Methods:

Chemicals:

Chloroauric acid ($HAuCl_4$) and citric acid were obtained from Sigma Aldrich. Commercially available glass and ceramic beads.

Synthesis and characterization of gold nanoparticles by biological and chemical method:

The experimental aspects of the process and the solutions used are described elsewhere. Briefly, in the case of plant extract based synthesis, (8,9) 100 g of thoroughly washed and finely cut lemon grass leaves (*Cymbopogon flexuosus*) were boiled in 500 mL sterile distilled water for 5 min. After boiling, the solution was decanted and 1 ml of this broth was added in 10 mL of 10^{-3}M aqueous $HAuCl_4$ solution either directly (conventional method) or in different test tubes packed with glass or ceramic beads. Bioreduction of $AuCl_4$ was monitored by recording the UV-visible absorption spectra as a function of time of reaction of this mixture. In the chemical synthesis experiment (10), 10 mL of 10^{-3}M aqueous $HAuCl_4$ solution was diluted to 90 mL and was subsequently mixed with 10 mL of 10^{-2}M aqueous citric acid solution either directly or in different test tubes packed with glass beads. It was allowed to react for 12 hr. The TEM measurements were performed on a JEOL model 1200 EX instrument operated at an accelerating voltage of 80 kV.

Results and Discussions:

In Fig. 2(A) we show the TEM micrograph corresponding to the case of direct solution mixing, as followed normally. It is clear that this figure shows both size as well as shape dispersity. The shapes range from nearly spherical to triangular to multifaceted. In Figs. 2(B) 2(C), we show the TEM micrographs for the nanoparticles synthesized by the percolative multicavity synthesis process implemented with glass and ceramic beads, respectively. The diameter of the glass beads was ~500 μm while that of ceramic beads was about ~3 mm. It is remarkable to note that the PMCS process has changed the dispersity of the nanoparticles completely. The particles are nearly monodispersed both in size and shape. Equally important, the size of the nanoparticles is seen to change with the change in the size of the beads: $~7\pm2$ nm for the 500 μm glass bead case and 27 ± 2 nm for the ~3 mm ceramic bead case [please note the different scale bars on Figs. 2(B) 2(C)].
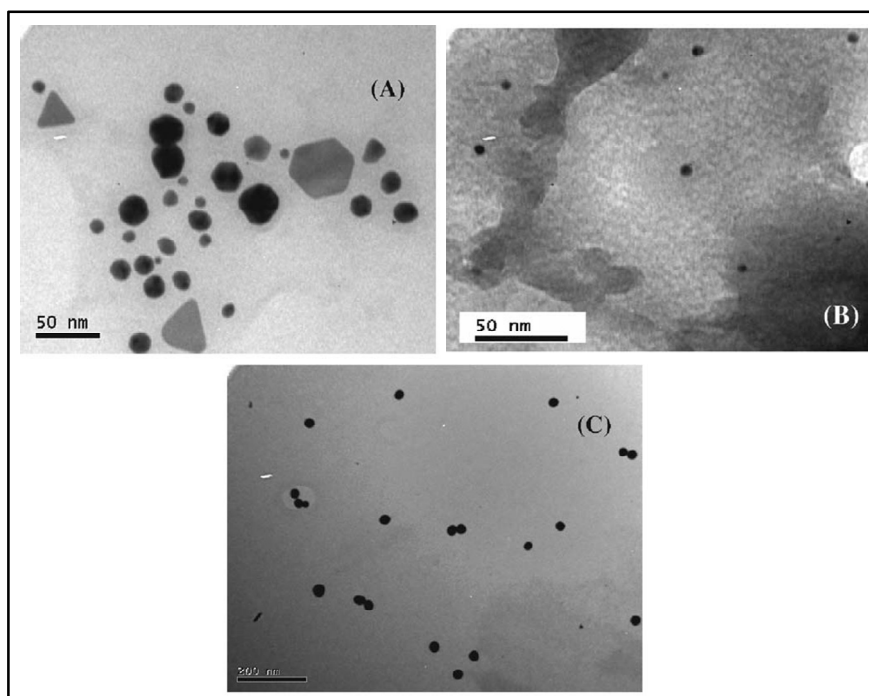

Fig. 2. Comparison of the TEM micrographs for the cases of direct solution mixing and percolative microcavity synthesis (PMCS) for lemon grass extract based synthesis: (A) corresponds to the direct mixing case while (B) and (C) show the results of nanosynthesis by the PMCS process implemented with glass (500 μm diameter) and ceramic beads (3 mm diameter), respectively. Note the different scale bars on (B) and (C).

Now we turn to the case of chemical synthesis. In Fig. 3(A) we show the TEM micrograph corresponding to the case of direct solution mixing. It is clear that this figure shows both size as well as shape dispersity. In Figs. 3(B) 3(C) we show the TEM micrographs for the nanoparticles synthesized by percolative multicavity synthesis process implemented with glass beads of diameters 2 mm and 85 µm, respectively. Once again, it is seen that the PMCS process has changed the dispersity of the nanoparticles completely. The particles are nearly monodispersed and the size of the nanoparticles is seen to be ~8±2 nm for the 85 µm glass bead case and 13.5±2 nm for the 2 mm bead case. The size differences between the plant based and chemical synthesis cases are interesting and could be traced to the differences in the nature of molecular chemistry and concentrations. We found that the beads displayed (not shown in figure) violet-type color (same as the color of gold nanoparticle solution) after the synthesis reactions, indicating their surface impregnation.
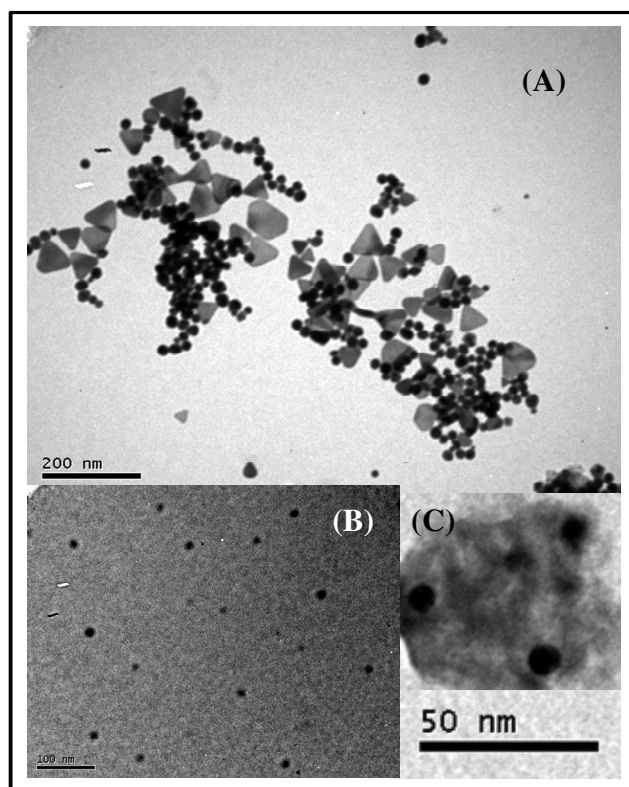

Fig.3. Comparison of the TEM micrographs for the cases of direct solution mixing and percolative microcavity synthesis (PMCS) for chemical synthesis: (A) corresponds to the direct mixing case while (B) and (C) show the results of nanosynthesis by the PMCS process implemented with glass beads with diameters of 2 mm and 85 µm, respectively. Note the different scale bars on (B) and (C).

Now it is useful to seek some insights into the possible reasons for the observed effects related to particle sizes and shapes. It is well known that these are primarily defined and controlled by the kinetic aspects of nucleation and growth, the latter involving both the diffusion of radicals in fluid media and their adsorption on the precursor particle surfaces along with the coarsening of tiny precursor particles. In order to explore how this complex evolutionary interplay changes when one uses a granular medium exemplified by the beads, we performed some analysis of the kinetics of nanoparticle formation. Basically the experiments with and without beads (3 mm case) were interrupted at different times and the state of nanoparticles was analyzed by optical and TEM measurements. The corresponding results are summarized in Fig. 4.
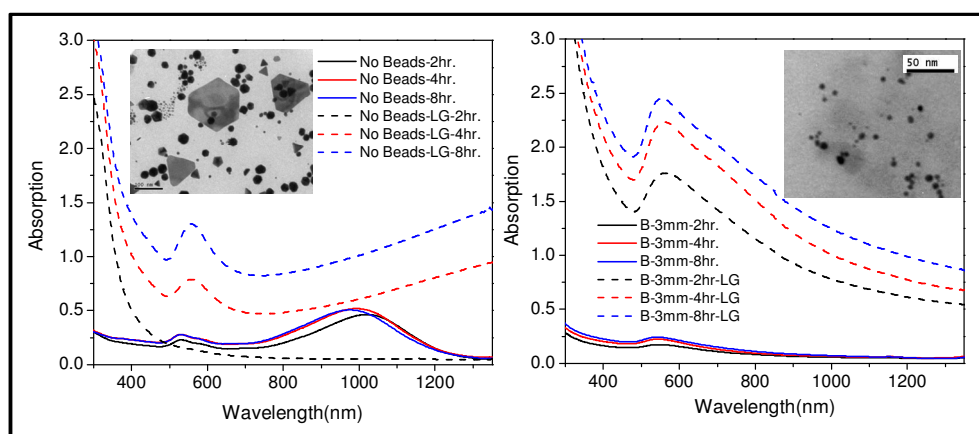

Fig. 4. Optical absorption data on interrupted nanosynthesis. The insets show transmission electron micrographs for the sample with no bead and 3 mm beads synthesized sample after 4 hr, for chemical synthesis.

The optical data reveal remarkable differences between the growths under no bead condition and with 3 mm beads. The primary difference is the existence of significant optical absorption weight in the infrared region under no bead condition for both the citrate and lemon grass synthesis cases and its near absence for the growth in the beads matrix (11). The spectral weight in the infrared region signifies considerable shape anisotropy of nanoparticles and its breadth reflects the size distribution (1-3, 8-13). The TEM data shown in the inset for 4 hr case compare and confirm the optically suggested difference for the no bead and with bead synthesis cases. The

plasmon contribution of gold nanoparticles seen to be near 530-560 nm is seen in both cases (no bead and with bead syntheses) as expected (1-3, 8-13). We will attempt a detailed analysis of the finer aspects of evolutionary optical data in a separate paper. It may suffice to note here in the context of the main point of this letter that the process of coarsening and sintering of the precursor particles leading to larger faceted particulates such as triangles which lead to infrared contribution is obstructed by the bead induced microcavity synthesis. Interestingly, the nucleation and early growth process is fairly brisk for both, with and without bead cases for citrate synthesis, but the process of coarsening/sintering picks pace right from the beginning only for the no bead case. Intriguingly, the nucleation process for the lemon grass synthesis is, in fact, quicker for the bead case than the no bead case, but once it occurs for the no bead case the coarsening/sintering process also picks pace and one gets infrared absorbance contribution, which continues to be absent for the with bead synthesis.

In Fig. 5, we show the mean Au NP size as a function of the confining bead size which shows a trend as reflected by a nominal exponential fit, though the number of data points is clearly insufficient to make quantitative analyses. In fact, it is also not clear whether a single function could fit the whole range once many more data points are added through controlled experiments (same bead types, precise temperature control, etc).
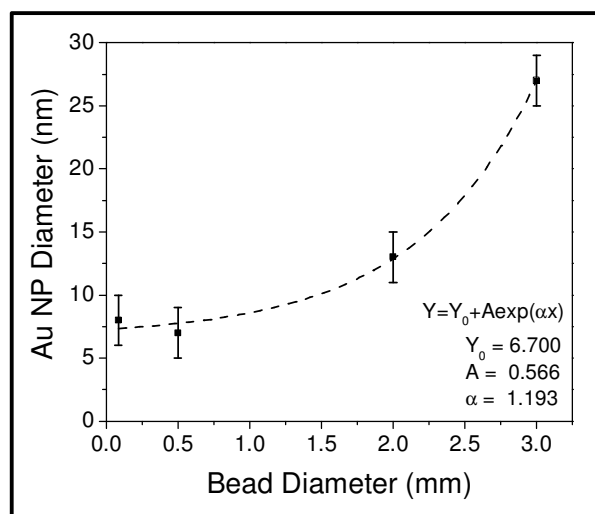

Fig.5. Dependence of Au NP size on the size of beads used for confinement. Nominal fit to exponential dependence is also shown

Burda *et. al.* (3) has discussed the key questions related to NP nucleation and growth in some details in relation to particle sizes and shapes. In typical solution growths, nucleation occurs under supersaturated condition and after formation of the critical nuclei, they grow via molecular addition, reliving the supersaturated step. When the concentration drops below the critical, nucleation stops but the particles continue to grow by the addition process until the equilibrium condition is reached. At this stage, the smaller particles grow more rapidly than the larger ones because the free energy driving force is larger for smaller sizes than for the larger ones if the particles are slightly larger than the critical size. This is a size focusing step. However, when the reactants are further depleted due to particle growth, Ostwald ripening or defocusing occur, where the larger particles continue to grow and the smaller ones get smaller and finally dissolve. This shows that the issue of particle sizes and shapes is defined by a complex interplay of many factors. The issue of confined synthesis has been addressed by Monnier *et. al.* (14) in the context of organic nanocrystal synthesis in silicate sol-gel matrices and narrow size distributions has been realized. Theoretical insights into nucleation in confined space have been provided by Andreazza *et. al.* (15) covering the full range of confinement length scale. They have argued that the stochastic process of nucleation needs higher threshold in confined regions and reflects some peculiar features including a maximum size limit on irreversibly growing clusters that are larger than the critical size in unconfined solutions and the same decreases with decreasing cavity size. As discussed by Monnier *et. al.* (14) higher nucleation threshold favors formation of single burst of nucleation, which when followed by slow but uniform diffusion-controlled growth and forbidden coalescence leads to improved dispersity. As pointed out by Andreazza *et. al.* (15) the size of nanocrystals formed in confined geometry is a nontrivial function of the cavity dimension, though the suggested trend is in the direction reflected by Fig 5.

Conclusions:

In summary, we have demonstrated a simple but interesting way to influence and control the size and dispersity of nanoparticles in a solution synthesis process by applying it to gold nanoparticle synthesis. It is clear that the concept has broader applicability to chemical, biological and physical syntheses. The suggested percolative multicavity synthesis is essentially a microfluidic reaction scheme that cellularizes the reaction zone.

References:

1. Daniel, M.C.; Astruc, D. *Chem. Rev*. (Washington, D.C.) **2004**, *104*, 293.

2. Rosi, N. L.; Mirkin, C. A. *Chem. Rev*. (Washington, D.C.) **2005**, *105*, 1547.

3. Burda, C.; Chen, X.; Narayanan, R.; El-Sayed, M. A. *Chem. Rev*. (Washington, D.C.) **2005**, *105*, 1025.

4. Niemeyer, C. M. *Angew. Chem.* **2001**, *40*, 4128.

5. Mohaddes-Ardabili, L.; Zheng, H.; Ogale, S. B.; Hannoyer, B.; Tian, W.; Wang, J.; Lofland, S. E.; Shinde, S. R.; Zhao,T.; Zia,Y.; Salmanca-Riba, L.; Schlom,D. G.; Wuttig, M.; Ramesh,R. *Nat. Mater.* **2004**, *3*, 533.

6. Zheng, H.; Wang, J.; Lofland, S. E.; Ma,Z.; Mohaddes-Ardabili, L.; Zhao,T.; Salmanca-Riba, L.; Shinde, S. R.; Ogale, S. B.; Bai,F.; Vieland, D.; Zia,Y.; Schlom,D. G.; Wuttig, M.; Roytburd, A.; Ramesh, R. *Science.* **2004**, *303*, 661.

7. Pankhurst, Q. A.; Connolly, J.; Jones, S. K.; Dobson, J. *J. Phys. D.* **2003**, *36*, R167.

8. Shankar, S.S.; Rai, A.; Ankamwar, B.; Singh, A.; Ahmad, A.; Sastry, M. *Nat. Mater.* **2004**, *3*, 482.

9. Shankar, S.S.; Rai, A.; Ahmad, A.; Sastry, M. *Chem. Mater.* **2005**, *17*, 566.

10. Shankar, S.S.; Bhargava, S.; Sastry, M. *J. Nanosci. Nanotechnol.* **2005**, *5*, 1721.

11. The absorption is much higher in the lemon grass case as compared to the chemical synthesis case because the chloroauric acid concentration used in the former case was an order of magnitude higher.

12. Link, S.; Mohamed, M. B.; El-Sayed, M. A. *J. Phys. Chem. B.* **1999**, *103*, 3073.

13. Shipway, A. N.; Lahav, M.; Gabai, R.; Willner, I. *Langmuir.* **2000**, *16*, 8789.

14. Monnier, V.; Sanz, N.; Botzung-Appert, E.; Bacia, M.; Ibanez, A. *J. Mater. Chem.* **2006**, *16*, 1401 and references therein.

15. Andreazza, P.; Lefaucheux, F.; Mutaftschiev, B. *J. Cryst. Growth.* **1988**, *92*, 415.

Chapter 6

General discussion and conclusions

General discussion:

Nanomaterials possess different novel properties as compared to their bulk counterparts. Nanomaterial synthesis represents a remarkable achievement in nanotechnology research. Nanosynthesis processes, in particular, bottom up approach, offers much more flexibility in terms of creating nanomaterials with desired features (controlled shape and size) by tuning the reaction conditions such as pH, temperature, reaction time, etc. Moreover, strategies to synthesize nanomaterials with desired features with reproducibility are vital for fundamental research and technological applications. Increase in the awareness toward biological process (green chemistry) has led to the development of an eco-friendly process for the synthesis of nanomaterials. Biological systems are environment friendly, effective, flexible and cheaper as compared to other (chemical and physical) methods. Microbial synthesis therefore emerged as an important branch in nanomaterial synthesizing technology. Microbes have their rich diversity and potential for the synthesis of nanomaterials and they could be regarded as potential nanofactories. Microbes are highly organized units in terms of morphology and metabolic pathways and are capable of synthesizing well defined size and structures with reproducibility. Furthermore, the biosynthesized nanomaterials exhibit water dispersible and biocompatible properties, which are crucial for many applications.

The present research work is focused on the biosynthesis of metals (such as gold, silver and platinum) and quantum dot (CdTe) nanoparticles. An attempt has been made to demonstrate bioleaching for the synthesis of silicate nanoparticles from glass cover slips. Size and shape controlled synthesis was also carried out by physical manipulation studies.

Introduction gives a brief idea about nanotechnology including various aspects. Different methods (chemical, physical and biological) and synthesis routes of nanomaterials are discussed with great interest in bio-based approaches. It also presents an account of different properties and applications of nanoparticles.

Biosynthesis of gold and silver nanoparticles from *Humicola lanuginosa* was demonstrated. The fungus was isolated and purified in the laboratory. The fungus was maintained on MGYP agar slants and grows at temperature 50^0C and pH 9. The fungus was identified by morphological studies and molecular tools in the laboratory and was identified as *Humicola lanuginosa* (*Thermomyces lanuginosus)*. The fungus was used for the first time for biosynthesis of metal nanoparticles. When the fungus

was exposed to chemical precursors such as $HAuCl_4$ and $AgNO_3$, it reduced the ions and formed gold and silver nanoparticles respectively in the solution. The change in the color of the respective solution indicates the formation of gold and silver nanoparticles. UV spectrum shows specific surface plasmon resonance for the gold and silver nanoparticles. TEM analyses were performed to analyze the size and shape of nanoparticles. The morphology of gold nanoparticles was found to be monodispersed while it was polydispersed in case of silver nanoparticles. XRD analyses showed crystalline nature of the nanoparticles. The produced nanoparticles are thus stabilized by the secreted protein in the reaction mixture. It was also supported by FTIR analyses. The biocompatibility and cytotoxicity of gold and silver nanoparticles was assessed by cell viability assay. These gold nanoparticles were further radiolabelled with Technetium-99m and injected into rat in order to see the biodistribution of gold nanoparticles. It was revealed that gold nanoparticles reached the liver, heart and kidneys and passed out through urine (within 45 minutes). Cardiotoxicity and renal toxicity occur due to doxorubicin. To avoid these complications, doxorubicin was conjugated with protein capped gold nanoparticles with the help of EDC coupling protocol and the conjugate was purified by HPLC.

Targeted therapy has a significant impact in the treatment of some types of cancer and is currently a very active area of research in order to provide a cheaper and effective drug delivery system which can reduce the current therapeutic intake of some of the costly drugs used in cancer therapy. Nanoparticles can be used in targeted drug delivery at the site of disease to improve the uptake of poorly soluble drugs, the targeting of drugs to a specific site and drug bio-availability. Nanomaterials such as polymeric nanoparticles, liposomes, dendrimers and inorganic nanoparticles as reported by several groups hold tremendous potential as carriers for drugs to target cancer cells. Among these, gold and magnetite nanoparticles synthesized by chemical routes are being used for targeted drug delivery. The lack of sufficient stability in water under strong electrolyte conditions and pH changes has impeded the application of these nanoparticles. There are so far no reports of conjugation of biologically synthesized, protein-capped, water-dispersible, inorganic nanoparticles to chemotherapeutic drugs for targeted drug delivery. In this context, we have synthesized a range of inorganic nanomaterials of different chemical compositions using fungi. These biologically synthesized nanoparticles can be used for drug

delivery and targeted drug delivery. Following the biosynthesis, conjugation of these nanoparticles with anti-cancer drug was also achieved. Cytotoxicity of these nanoparticles has been checked on NIH3T3 mouse embryonic fibroblast cell line and MDA-MB-231 human breast carcinoma cell line.

The fungus *Fusarium oxysporum* was exploited for the synthesis of various nanomaterials such as gold, silver, gold-silver alloy, CdS, CdSe, silica, titania, zirconia, magnetite, $CaCO_3$, barium titanate, etc. An attempt has been made for the production of platinum nanoparticles using the fungus *Fusarium oxysporum*. The fungus reduces the ions in the solution which are stabilized by the secreted proteins. The morphology of the nanoparticles was found to be spherical bearing in the dimensions of ~15 ± 5 nm.

Quantum dots were synthesized by chemical and physical routes but their increasing demand in bio-based approach due to their eco-friendly nature has witnessed the highly stable, water dispersible nanoparticle synthesis. In an extension to our previous work on the biosynthesis of quantum dot nanoparticles (CdS, CdSe) using the fungus *Fusarium oxysporum,* the fungus was reacted with a mixture of $CdCl_2$ and $TeCl_4$ resulting in the formation of stable and highly fluorescent CdTe nanoparticles. These particles are crystalline in nature which was supported by XRD data. FTIR analysis showed that these particles are capped by protein layer, which makes them water dispersible.

Laboratory methods for the synthesis of silica nanoparticles used chemical precursors (bottom up approach), which then extended to bioleaching approach (top-down approach) using naturally available materials (white sand, zircon sand) and agro-industrial by-products (rice husk). To follow up bioleaching work, the fungus was employed for the bioleaching of glass cover slips. The fungus leached out water dispersible and nearly monodispersed silicate nanoparticles with ~5 ± 0.5 nm size dimensions. These nanoparticles were capped with secreted proteins in the solution. Bioleaching by the fungus showed that glass surface also undergoes morpho-chemical modifications.

Synthesis of nanomaterials of different chemical compositions, sizes and shapes is an important developed area in nanotechnology. Although several synthesis methods are available for the nanomaterials, synthesis with desired features are still a constant challenge in nanotechnology. Percolative microcavity synthesis scheme was

developed for the size and shape controlled synthesis. Physical manipulation was performed for the solution based approach. The percolative cavity method ensures connectivity and formed a confined reaction zone for synthesis. Gold nanoparticles synthesized by biological and chemical methods are used to compare the percolative microcavity synthesis scheme. It represents a simple solution based process and is further exploited for synthesis of nanomaterials of different chemical compositions.

Future Prospects:

Microbial systems are found to associate with metals through metal-microbe interactions. Most of the microorganisms reduce the inorganic metals in solution. As compared to the other chemical and physical methods, biological methods attract greater attention and are regarded as the natural nano-factories. Although biosynthesis processes are emerging as a new and interesting field in nanotechnology, some crucial issues of concern have to be addressed. The major concern is that of the pathways leading to metal reduction and formation of nanomaterials. The identification of secreted biomolecules (enzymes) which reduce the metal ions and cap the nanomaterials as well as their nature and function has to be completely characterized. Surface chemistry also plays a pivotal role in different applications and therefore complete understanding about surface chemistry is also an equally important factor. Currently, the accessible ranges of chemical compositions of nanomaterials are confined to metals, sulfides, carbonates and oxides. Extension of these processes to enable reliable synthesis of multifunctional nanoparticles, physically and chemically hard to synthesize nanoparticles, etc. could make this process a commercially viable approach.

Some sort of questions related to the metal ion reduction reaction process in metabolism and the equally important possible role of the formed nanoparticles in cellular activity or these nanoparticles are formed as the by-products of the reduction process. Among the microbes, fungi are not normally exposed to the high concentrations of metal ions such as Cd^{2+}, $AuCl^{4-}$ and Ag^+. This stress induces cellular functions such as secretion of biomolecules (enzymes) when reacted, having the ability to reduce the metal ion and formation of respective nanoparticles which may help in the understanding of the process. Nanomaterials are being used for a variety of applications, especially in the field of medicine for drug delivery applications. It is very important to take care about the toxicity issues related to the

nanoparticles. Toxicological studies are needed for the nanomaterials (both *in vitro* and *in vivo*) for further applications. It is immature at present stage to talk about the various aspects of biosynthesized nanomaterials and more efforts are required to understand these issues. It is believed that the future research is of great interest and importance, because nanoparticles can be synthesized with the desirable features according to their applications that make an impact on different fields such as chemistry, physics, biology and medicine.

The nanoparticles which we have synthesized using fungi are capped with natural proteins making them water-dispersible and may bind to integrins or VEGFs (vascular endothelial growth factors). Therefore, targeting integrins and VEGFs is a novel anti-angiogenesis strategy for treating a wide range of solid tumors. Since these nanoparticles are capped by natural proteins, they may bind to various receptors such as LHRH, EGFR and EpCAM without targeting agent. Hence, these nanoparticles can be used directly as drugs in the future. They may fulfill the emerging need for cheaper drugs with no side effects.

Publications:

1. Ogale, S. B.; Ahmad, A.; Pasricha, R.; Dhas, V.V.; **Syed, A** (2006). Physical manipulation of biological and chemical for nanoparticle shape and size control. *Applied Physics Letters.* **89, 263105.**

2. Bansal, V.; **Syed**, **A.;** Bhargava, S. K.; Ahmad, A.; Sastry, M*(2007). Zirconia Enrichment in Zircon Sand by Selective Fungus-Mediated Bioleaching of Silica. *Langmuir.* **23, 4993-4998.**

3. Kulkarni, S.; **Syed, A.;** Singh, S.; Gaikwad, A.; Patil, K.; Vijayamohanan, K.; Ahmad, A*.; Ogale, S.B*. (2008). Silicate nanoparticles by bioleaching of glass and modification of the glass surface. *Journal of Non-Crystalline Solids*. **354, 3433-3437.**

4. Uddin, I.; Adyanthaya, S.; **Syed, A.;** Selvaraj, K.; Ahmad, A.;* Poddar, P*. (2008). Structure and Microbial Synthesis of Sub-10 nm Bi_2O_3. Nanocrystals. *Journal of Nanoscience and Nanotechnology.* **8, 3909-3913.**

5. Sreekanth, D.; **Syed, A.;** Sarkar, S.; Sarkar, D.; Santhakumari, B.; Ahmad, A.; Khan, M.I *(2009). Production, Purification, and Characterization of Taxol and 10-DABIII from a new Endophytic Fungus *Gliocladium* sp. Isolated from the Indian Yew Tree, *Taxus baccata*. *Journal of Microbiology & Biotechnology.* **19(11), 1342-1347.**

6. Bansal, V.; **Syed, A.;**Ahmad, A.;* Sastry M*. Visible light induced photocatalytic and broad-spectrum antimicrobial activity of N, C and F simultaneously doped biogenic TiO_2 nanoparticles. **(Under revision)**

7. Senapati, S.; **Syed, A.;** Khan, S. A.; Pasricha, R.; Kumar, R.;* Ahmad, A.;* Extracellular biosynthesis of metal sulfide nanoparticles using the fungus *Fusarium oxysporum.* **(Under revision)**

8. Sreekanth D.; Gupta,S. K.; **Syed**, **A.**; Khan,B. M.; Ahmad, A. Molecular and morphological studies of a Taxol producing endophytic fungus, *Gliocladium* sp. from *Taxus baccata*. **(Under revision)**

9. Sreekanth, D.; **Syed, A.;** Ahmad, A (2011). Transformation of taxol precursors 10 -Deacetyl baccatin III and side chain into biologically active taxane by fungus *Gliocladium* sp. **(Communicated)**

10. **Syed, A** and Ahmad, A*. (2011). Gold nanoparticles: Extracellular Biosynthesis, Characterization, biodistribution and conjugation with doxorubicin. (Manuscript under preparation).

11. **Syed, A** and Ahmad, A*. (2011). Bio-inspired silver nanoparticle synthesis using the fungus *Thermomyces lanuginosus*. (Manuscript under preparation).

12. **Syed, A** and Ahmad, A*. (2011). Fungus-mediated synthesis of metal (Platinum) and quantum dot (CdTe) nanoparticles. (Manuscript under preparation).